UNIVERSIDADE ESTADUAL DE CAMPINAS
Faculdade de Engenharia Mecânica

JORGE ALEJANDRO VIDOZA GUILLEN

Design and optimization of a floating power hub to energize oil production units aiming to reduce CO_2 emissions

Dimensionamento e otimização de ilha de potência para suprimento de eletricidade de unidades de produção de petróleo visando a redução de emissões de CO_2

CAMPINAS
2019

JORGE ALEJANDRO VIDOZA GUILLEN

Design and optimization of a floating power hub to energize oil production units aiming to reduce CO$_2$ emissions

Dimensionamento e otimização de ilha de potência para suprimento de eletricidade de unidades de produção de petróleo visando a redução de emissões de CO$_2$

Thesis presented to the School of Mechanical Engineering of the University of Campinas in partial fulfillment of the requirements for the degree of Doctor in Mechanical Engineering in the area of Fluids and Thermodynamics.

Tese apresentada à Faculdade de Engenharia Mecânica da Universidade Estadual de Campinas como parte dos requisitos exigidos para a obtenção do título de Doutor em Engenharia Mecânica, na Área de Térmica e Fluidos.

Orientador: Prof. Dr. Waldyr Luiz Ribeiro Gallo

ESTE EXEMPLAR CORRESPONDE À VERSÃO FINAL DA TESE DEFENDIDA PELO ALUNO JORGE ALEJANDRO VIDOZA GUILLEN E ORIENTADA PELO PROF. DR. WALDYR LUIZ RIBEIRO GALLO

CAMPINAS
2019

UNIVERSIDADE ESTADUAL DE CAMPINAS

FACULDADE DE ENGENHARIA MECANICA

COMISSÃO DE POS-GRADUAÇÃO EM ENGENHARIA MECÂNICA

DEPARTAMENTO DE ENERGIA

TESE DE DOUTORADO ACADEMICO

Design and optimization of a floating power hub to energize oil production units aiming to reduce CO₂ emissions

Dimensionamento e otimização de ilha de potência para suprimento de eletricidade de unidades de produção de petróleo visando a redução de emissões de CO₂

Autor: Jorge Alejandro Vidoza Guillen
Orientador: Waldyr Luiz Ribeiro Gallo

A Banca Examinadora composta pelos membros abaixo aprovou esta Tese:

Prof. Dr. Waldyr Luiz Ribeiro Gallo
Faculdade de Engenharia Mecânica, Universidade Estadual de Campinas

Prof. Dr. Silvio de Oliveira Junior
Departamento de Engenharia Mecânica, Universidade de São Paulo

Prof. Dr. Arnaldo Cesar da Silva Walter
Faculdade de Engenharia Mecânica, Universidade Estadual de Campinas

Prof. Dr. Jose Antonio Perrella Balestieri
Faculdade de Engenharia, Universidade Estadual Paulista

Prof. Dr. Waldir Antonio Bizzo
Faculdade de Engenharia Mecânica, Universidade Estadual de Campinas

A Ata da defesa com as respectivas assinaturas dos membros encontra-se no processo de vida acadêmica do aluno.

Campinas, 27 de fevereiro de 2019

Agradecimentos

Resumo

Este trabalho de doutorado foi inspirado nas tendências atuais do setor de exploração de petróleo de gás em diminuir o impacto ambiental nas atividades de exploração e produção. Empresas deste ramo tem investido em pesquisas para diminuir a emissão de gases de efeito estufa. Neste sentido, esta tese propõe uma configuração inovadora de suprimento de energia para unidades de extração de petróleo offshore. Uma plataforma flutuante dedicada à geração de energia substitui às turbinas individuais em pelo menos três plataformas convencionais de produção de petróleo. Para desenhar e otimizar essa "ilha de potência" foi necessário simular blocos de ciclos combinados, conformados por turbinas a gás, turbinas a vapor, caldeiras de recuperação de calor, condensadores e bombas, principalmente. Cada equipamento foi projetado e integrado a uma otimização de algoritmos genéticos. Foram analisados diversos casos: Caldeiras de um e dois níveis de pressão; turbinas a gás convencionais e customizadas, e configurações isoladas da ilha de potência e conexão com a rede em terra.

Igualmente, foram realizadas otimizações de objetivo simples e multi-objetivo para entender as diferenças e benefícios de cada solução, otimizando em primeiro lugar objetivos simples como eficiência em plena carga, peso e custo. Para depois realizar uma otimização considerando as variações de carga ao longo do tempo de vida do campo petrolífero, utilizado simulações fora de condições de projeto do ciclo combinado, estabelecendo os objetivos de eficiência média, relação peso/potência e valor presente líquido.

Os resultados apontam que a aplicação de uma ilha de potência teria uma potencial diminuição de emissões de CO_2 na ordem de 13,1 e 23,4% com respeito ao cenário base. Em detrimento do desempenho econômico, precisando de uma taxa de carbono de 61 a 122 USD por tonelada para ser economicamente viável. A opção de enviar energia à terra possui ganhos econômicos, resultando em valores presentes líquidos maiores a zero, porém com incremento das emissões em até 68%.

Palavras chave: *Ciclo combinado flutuante, redução de emissões, eficiência energética*

Abstract

This PhD thesis was inspired by the current trends of oil and gas industry in reducing the environmental impact on its exploration and production activities. Companies in this field have invested in research to reduce the emission of greenhouse gases. In this sense, this thesis proposes an innovative configuration of energy supply for offshore oil extraction units. A floating platform dedicated to power generation replaces individual turbines on, at least, three conventional oil production platforms. To design and optimize this "power island" or "power hub" it was necessary to simulate combined cycle blocks, composed by gas turbines, steam turbines, heat recovery steam generators, condensers and pumps, mainly. Each equipment was designed and integrated within a genetic algorithm optimization. Several scenarios were analyzed, the scenarios considered: one and two pressure level heat recovery units, conventional and customized gas turbines, and two connection configurations, isolated grid a connection to shore.

Likewise, simple and multi-objective optimizations were performed to understand the differences and benefits of each solution, optimizing at first objectives at full load, namely: weight, costs and efficiency. After analyzing combined cycle design points, simulations of the combined cycle off-design performance were elaborated, in order to perform optimizations considering the load variations over the oilfield lifetime, establishing objectives of: average efficiency, weight-to-power ratio and net present value.

The results indicate that the application of a power island would have a potential decrease of CO_2 emissions in the order of 13.1% and 23.4% with respect to the base scenario, with penalties in economic performance. A carbon trading market, with carbon certificate prices around 61 to 122 USD/ton could make this type of offshore grid more viable, when considering most optimistic layouts regarding efficiency and economic performance. The option of exporting electricity to land has economic gains, resulting in net present values higher than zero, but with an increase in emissions of up to 68%.

Keywords: *Floating combined cycle, emission reductions, energy efficiency*

Figure Index

Table Index

Nomenclature

Variables

Letter	Meaning
Afo	Fin surface area
Apo	Prime surface area
BAU	Business-as-Usual or Base case
C	Costs
d	Diameter
E	Fin Efficiency
f	Friction Factor
h1	Inlet Enthalpy
h2	Outlet Enthalpy
HTA	Heat transfer area
HXI	Heat Exchanger Quantity Integer
J	Colburn Factor
k	Thermal conductivity
Lf	Tube length
lf	Fin length
m	Mass flow
M	Weight
nf	number of fins
Nr	Number of tube rows
Nt	Number of tubes per row
NTR	Number of Gas Turbines
Nu	Nusselt
p	Pressure
PEC	Purchase Equipment Cost
Pl	Longitudinal pitch
PP	Pinch Point
Pr	Prandtl
Pt	Transversal pitch
Q	Heat
r	Gas turbine pressure ratio
Re	Reynolds
T	Gas/Air temperatures
t	Water/Steam temperatures
TIT	Turbine inlet temperature
Uo	Overall heat transfer coefficient
W	Power
Wt	Casing width
η	Efficiency

Subscripts

Letter	Meaning
1,2,3,4,5	Gas Turbine States
air	Air inlet stream
cc	Combined Cycle
cb	Combustor
co	Compressor
cond	Condenser
ct	Compressor Turbine
e	Effective
ec	Economizer
ev	Evaporator
fuel	Fuel stream
gas	Exhaust gases
GT	Gas Turbine
HP	High Pressure
i	Inside
LP	Low Pressure
m	Mechanical
o	Outside
pm	Pump
pt	Power Turbine
sh	Super Heater
ST	Steam Turbine
w	Wall

Index

1 INTRODUCTION

Brazilian offshore oil and gas activities have recently focused on the exploitation of the Pre-salt basin. Brazilian energy-related organizations are expecting a substantial increase in oil and gas production due to the current investments. There are several ongoing projects that aim to develop technology for those activities, with interventions of public and private sector. One of the most important projects is the construction of a series of similar ships, responsible to carry out the production and storage of oil and gas along the different fields in the Pre-salt basin. The ships are called FPSO's (Floating Production Storage and Offloading), they are designed to cover a wide range of situations and scenarios. Several equipment modules compose the FPSO's, which perform different activities, such as separation, processing and compression of the fluids coming from the wells.

All FPSO main base characteristics and Business-as-Usual (BAU) parameters explained in this chapter are based on Gallo et al. (2017), unless stated otherwise. Power generation modules are located in the FPSO to energize all activities regarding oil production and processing, and to cover power demands of the accommodation facilities. Power generation modules are fixed and non-modifiable all along the FPSO lifetime, which is approximately of 20 to 25 years. Four gas turbines compose the module; three will be operative and one will remain as back up. As it is common in most offshore oil platforms, power generation units are over-dimensioned, due to the critical aspects of maritime operations, that is, in case of any peak demand there must be available back up to cover energy needs. All Brazilian Pre-salt FPSO's will have the same power units, the maximum capacity is supposed to cover all demand scenarios.

However, it is reasonably expected, that not all oil fields behave on the same manner regarding crude oil, water and associated gas compositions and mass flows. In this sense, some compression and separation modules can be bypassed, according to the actual needs of the specific well, arising considerable energy consumption differences in the FPSO's. In order to analyze this different behavior, operational cases were established. Forecasts of energy consumption in these cases show that loads on the power generation units can vary from a minimum of 30% to a maximum of 98%. If gas turbines on the power generation unit run for long periods in low loads, it would result in very inefficient operations with increased specific fuel consumption. This is a common scenario among offshore oil and gas platforms,

mainly in the last lifetime years when energy intensity becomes greater, and fluid outputs become lower.

Nevertheless, during recent years, the concerns of energy efficiency and CO_2 emissions have led the path for research and development of alternatives for energy supply in the offshore oil and gas industry. Even though industrialized countries aim to become less dependent of fossil fuels, crude oil and derivatives are still crucial for the development of emerging economies. In order to cope with the emission targets, and to reduce fuel consumption, it is necessary for oil producers to implement energy efficient processes.

The profitability of gas associated with oil production has always been a subject of debate. Decades ago, strong legislation against flaring of associated gas pushed companies to diminish the waste of this resource. In offshore operations, the transport and handle of natural gas can be problematic, as the low density and gaseous state of natural gas makes it costly to transport. Gas-to-Power applications try to internalize this aspect, by converting the natural gas into a more useful or easy-to-handle resource, such as electricity. This is particularly interesting for isolated production places or to offshore industry. Applying Gas-to-Power to Brazilian FPSO's would be a chance to reduce fuel consumption, by centralizing power generation through a large-scale offshore power plant, instead of smaller inefficient power generation. Usually, onshore power plants are designed to operate at maximum efficiency; however, in offshore oil and gas industry, loads and power demand vary considerably over time. Flexible arrangements that operate more efficiently at diverse load levels are a critical objective for innovative offshore operation.

1.1 State of the art and motivation

Several researchers have devoted to build technological scenarios to improve oil and gas industry environmental impact. Nguyen et al. (2014a, 2013) determined improvement opportunities for the oil treatment process, along with thermal, environmental and economic optimization procedures for bottoming cycles. Kaviri et al. (2012) designed a combined cycle using optimization algorithms for exergy efficiency and costs. These studies focused on exergy analysis, however other critical aspects for offshore systems such as equipment weight and space are not explored among the objectives.

Pierobon et al. (2016; 2013, 2014a, 2014b; 2014) established procedures for the optimum selection of the waste heat technology, and focused on the dynamic operation of a combined Organic Rankine Cycle (ORC). A comparative analysis with knowledge-based and optimized solutions for offshore Rankine bottoming cycles along with off design simulations are presented by Nord et al. (2013; 2014) and Walnum et al. (2013). As those were case studies related to already operating platforms, the gas turbine was taken as a black box, properties such as turbine exhaust temperature and mass flow were known. In new systems optimum points could be achieved by varying the gas turbine in terms of its design parameters, which is not addressed in those references.

Energetic and exergetic analyses of offshore facilities for the Brazilian case are found various studies; De Oliveira et al. (1997) established preliminary bases for exergy balances in Brazilian offshore oil production units. Carranza et al. (2015) proposed a CO_2 capture system and Barrera et al. (2015) analyzed a bottoming Organic Rankine Cycle, both studies proposed alternatives for CO_2 emissions reduction in Brazilian FPSO units in design conditions. Nevertheless, off-design analyses are convenient to determine efficiencies in part load production periods, this aspect was not documented in such studies.

A distinct approach was given by Korpås (2012), Marvik (2013) and Orlandini (2016). In those cases, the oil platform was not an isolated energy producer/consumer, but it was connected to offshore wind farms, creating a small grid of renewable and non-renewable sources. Even though, for the Brazilian case, including wind energy may pose uncertainties due to the region's scarce wind potential and water depths, the concept of creating an offshore grid could be profitable. In this sense, Hetland et al. (2009) introduced the power hub concept as a floating combined cycle power plant, this study focused in the integration of a carbon capture scheme on the floating power hub. Additionally, Windén et al. (2013) studied the cost-effectiveness of such alternative for Australian oil platforms. Both latest studies were based on on-land combined cycles installed offshore. Nevertheless, offshore energy demand is extremely project dependent, it is a function of the well fluids and environment properties which change over time. Therefore, a land-based combined cycle design may not be optimum for offshore applications.

Most of the alternatives are based on the fact that energy equipment in offshore facilities are operated with low efficiency rates, because they are designed for a specific point of the lifetime production forecast. Brazilian Pre-salt basin exploitation is going through an expansion process in which there are improvements opportunities to cope in a future with tight energy efficiency and GHG emission reduction requirements. Offshore grids have

been pointed as important means of energy trading to further develop in upcoming years (GORENSTEIN; HAKVOORT, 2016; JAY; TOONEN, 2015; PIERRI et al., 2017) . However, studies regarding floating power hubs like the ones presented by Hetland et al. and Windén et al. (HETLAND et al., 2009; WINDÉN et al., 2014) are scarce. In order to introduce a convenient design for a power hub, it is necessary to consider aspects that are often left behind when designing land-based power plants. Space and weight are critical characteristics for maritime power plants, as robust arrangements may be detrimental for the total capital costs. Additionally, the flexibility of operation its quite important as, opposed to most land-based combined cycle power plants, they need to operate at different loads over time.

This thesis addresses two important aspects which have not been covered in previous literature. First, as exposed previously, the power hub concept has been analyzed along with commercial land-based combined cycles. This thesis aims to propose optimized arrangement, tailored to the specific needs of the Brazilian case. In the proposed scenario, the power hub would supply energy for three Floating Production Storage and Offloading (FPSO) units. The integration of power demand reduces equipment redundancy in the FPSO and avoids the operations at extremely low loads, which are more energy intensive.

The second aspect concerns the gas turbine in combined cycle designs, either for maritime or land-based cases, a special attention is often given to the waste heat recovery unit. In the literature, authors in references (AHMADI; DINCER; ROSEN, 2013; MANASSALDI et al., 2016; MEHRGOO; AMIDPOUR, 2017; ROVIRA et al., 2011; VALDÉS; RAPÚN, 2001) proposed optimized parameters for different pressure levels HRSGs in land-based systems. The gas turbine is often considered to be of a specific model, or to have fixed output parameters. To deepen in the particularity of offshore power system design, this study integrates the gas turbine layouts and properties in the combined cycle calculation through the optimization of main design parameters. This integration on offshore systems was not addressed by previous literature.

The previous state-of-the art revision allowed orienting this work according to the following preliminary aspects:

- Most studies regarding offshore power generation in oil platforms relate to already operating or built facilities, which limits the options regarding efficiency to adaptations and refurbishments.

- There are few studies regarding offshore power generation hubs based on associated gas extraction and are limited to fixed commercial equipment sets.
- Gas turbines in combined cycle optimizations are generally taken as black boxes. Gathering gas turbine parameters and options to the optimization could broaden and improve the set of feasible options.

In this sense, it is meaningful to propose an adequate combined cycle for an offshore power hub, which integrates aspects regarding thermodynamics, volume limitations and off design parameters into one optimization procedure, so all equipment composing the power plant fits the trade-off between thermal efficiency and space constraints. The main scope of this work is to present a tailored arrangement to satisfy Brazilian Pre-salt basin specific needs, by executing an in-detail analysis of the components design and off design performance of an offshore power hub. However, the methodology followed could be applied to any situation concerning variable loads and power-space trade-offs.

1.2 Objectives and Thesis structure

The main objective of this thesis is to "propose optimized Combined Cycle arrangements for a Floating Power Hub in Brazilian Pre-salt Basin, in order to supply electricity to three FPSOs increasing efficiency and reducing carbon dioxide emissions". It is expected to reach the main objective through a set of smaller milestones, such as:

- Elaborate a Combined Cycle thermodynamic model that integrates most important equipment, namely, Gas Turbine, Steam Turbine, Heat Recovery Steam Generator and Condenser.
- Determine the off-design Combined Cycle performance to analyze efficiency, fuel consumption and emissions.
- Create a model that allows estimating the power hub components dimensions, namely weight and volume, and integrate the impact of the components size in the overall analysis.
- Select critical optimization parameters, in order to assess the tradeoff among costs, efficiency and size.

- Evaluate different electric grid layouts, for example, an isolated offshore grid and a connection to national grid, to determine most convenient economical scenarios.

The main objective and milestones are achievements along with their correspondent analyses and theoretical bases are structured in the thesis as follows. The first chapter introduced the motivations and objectives. The second chapter aims to give a background of Brazilian Offshore Oil Industry, to understand the context in which the thesis was developed. The third chapter deepens in the particularity of energy consumption in Offshore Oil Platforms. The fourth chapter offers thermodynamic general references for such applications. The methodology followed can be found in the fifth chapter. Results are shown in the sixth chapter. Finally, the conclusions and final remarks are in the seventh chapter.

2   BRAZILIAN OFFSHORE INDUSTRY BACKGROUND

2.1   Oil production and consumption forecasts

In recent years, emerging economies and developing countries have gained more importance in geopolitics. Southeast Asia, Africa and Latin America are regions expecting to become more prosperous regarding economic growth. Particularly in developing countries, this economic improvement carries out and inherent increase in energy and primary resources consumption. As industry sector grows bigger and more people moves from low-income to middle-high-income classes, energy becomes a crucial mean to accomplish a stable economic development.

Energy sector has suffered important changes, as renewable energies increased their share within total energy production. However, fossil resources are still needed for economic and social development particularly in emerging economies. Among this group, fossil fuel consumption is expected to increase. OPEC (2017) has forecasted an increase in oil demand in approximately 12,5% in the following next 10 years, and 20% in for 20 years (with respect of 2014 demand values). Converting percentages, actual production increase rises up to 11,3 million barrels per day for 2025 and 18 million barrels per day for 2035. In this context, Brazilian oilfields, and especially the Pre-salt basin, will be a key for domestic development in near future. According to the International Energy Agency, Brazil can become the second country with highest production grow outside OPEC. The exploitation of new maritime fields could raise Brazilian oil production to 3 million barrels per day for 2019 (IEA, 2018).

2.2   Brazilian oil and gas production

Nowadays, worldwide offshore oil production is passing through a considerable increase. Estimations show that roughly 12% of conventional oil resources are found in oceanic basins (AIE, 2014). In 2013, a share of 6% of total world oil production

corresponded to liquid reserves in deep water fields. In Brazil, there is an important historic background of offshore oil production, mainly in the Campos Basin and the Santos Basin, which localization on Brazilian territory is seen in Figure 1. The latter one comprises a region of oceanic continental shelf of approximately 350 thousand square kilometers, that extend from Cabo Frio in the State of Rio de Janeiro (bordering with Campos basin to the north), to Florianopolis in Santa Catarina (bordering with Pelotas field to the south).
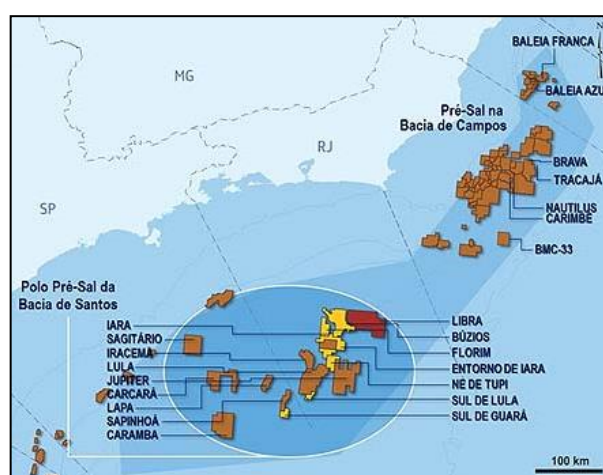
Source: (PETROBRAS, 2014)   Source: (PETROBRAS, 2014)

Figure 1 Santos Basin Localization and Fields

Santos basin exploitation started in the 1970's decade, with the beginning of several geological and seismic studies to verify the availability of fossil resources. The basin actual production potential was confirmed in the following decades through advanced studies. The presence of light hydrocarbons in a geological segment called Pre-salt was confirmed in 2006. The Pre-salt is a group of sedimentary geologic formations in the deep-water southern Atlantic Ocean subsoil, created with the separation of the African and American continents. Organic materials were accumulated in this new available space. The whole organic matter was exposed to thermal and physic phenomena that transformed it in hydrocarbons, specifically oil and associated natural gas (PETROBRAS, 2014)

A remarkable milestone for Brazilian oil industry was the discovering of Tupí oilfield (latter renamed Lula) also in 2006, when the official proved reserves where increased and the commercial exploitation of the Pre-salt started. It is estimated that Tupí oilfield by itself holds 5 to 8 billion commercial barrels of oil (PETROBRAS, 2014).

The Pre-salt region has numerous fields, some of them are still in study and analysis of actual production potential. Fields neighboring Lula are among the most

important; Iara, Carioca, Guará and Iracema (latter renamed Cernambí). Petrobrás, forecast an increase of their production up to 3,2 million of barrels per day, of which 52% will be from Pre-salt basin. In order to achieve this objective, at least 26 production units will be installed in Campos Basin. The behavior of Brazilian oil production can be seen in Figure 2 based on SEEG (2017), the older Campos Basin offshore platform production is starting to decay, and the additional offshore fields production is in rise. One of the greatest challenges of including these new production units is the application of technologies that reduce costs and maintain the viability of Pre-salt production, due to the unstable and fluctuant oil prices.
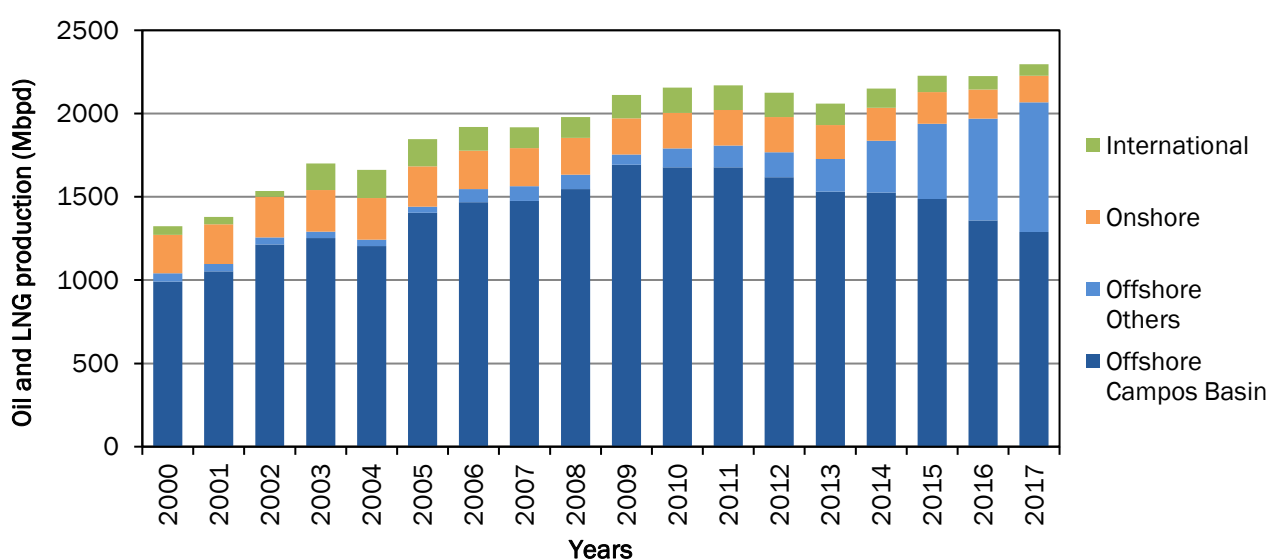
Figure 2 Brazilian onshore and offshore oil production
Source: SEEG (2017)

Another key factor of Pre-salt region future is the production of associated natural gas. This important resource for energy generation and petrochemical industry constituted 13,7% of 2015 Brazilian energy matrix. Total Brazilian average natural gas production for the same year reached 96,24 MMm^3/day, which means an increase or 10,14% with respect to 2014. Offshore natural gas production accounted for 76,1% of the overall production. According to EPE (2018), potential supply of natural gas could reach 131,5 MMm^3/day in 2022, not considering imports, while total demand may reach 180,4 MMm^3/day, of which approximately 80% would be consumed by thermal power plants.

Pre-salt natural gas production in 2015 was approximately one third of overall natural gas production (34 MMm^3/day). Pre-salt natural gas is rich in CO_2, therefore its profitability is restricted, as no other alternatives have been constructed, and most of the obtained gas (approximately 60 to 70%) is currently being reinjected. The commissioning of

new platforms and production units is expected to increase the profitable quantity of natural gas in this region to 115 MMm^3/day in an optimistic scenario. Produced natural gas is expected to be transported to land by using three submarine gas ducts reaching an approximate capacity of 51 MMm^3/day. However, even in less optimistic gas production forecasts, planned and installed gas ducts will not be able to handle the whole natural gas production. Alternatives to cover these transportations demands could be the installation of additional gas ducts, or the implementation of LNG technology, careful assessment should be done to evaluate the profitability of such alternatives.

2.3   Greenhouse gasses emissions

As a common worldwide trend, last decades have been marked by a growing concern about climate change and resources depletion. Scientist and researchers all over the world have devoted to study causes, consequences and mitigation aspects for the increasing CO_2 levels in the atmosphere. This critical situation has encouraged some powerful economies to develop economical mechanisms that lead the path for new alternative energy sources and diminish the quantity of greenhouse gases emissions. The carbon tax has been successfully applied in several European countries. Public and private companies have started to produce alternatives that cope with emission targets and lower the quantity of taxes paid. Energy generation is a key sector when talking about reduction of anthropogenic greenhouse gases, as it accounts for the largest share in overall emissions.

In Latin American countries, greenhouse gasses scenario is slightly different, as most of them rely in cleaner energy matrices, due to the large hydraulic capacity. However, thermal-based generation is still responsible for an important part of greenhouse gases emissions in these countries. The relatively recent discovery and exploitation of the Pre-salt fields in Brazil, have raised worries about the future of Brazilian energy matrix and sustainability. Traditionally, Brazil has supplied energy through a hydrothermal system, and more recently it has successfully applied economic strategies to promote alternative energy sources, such as sugar cane products (ethanol and bagasse), wind power in the northeastern and southern region, solar heating, and solar photovoltaic power generation,

waste-to-energy plants, among others. Notwithstanding, exploration of Pre-salt basin may open the opportunities for investments in potentially energy intensive activities.
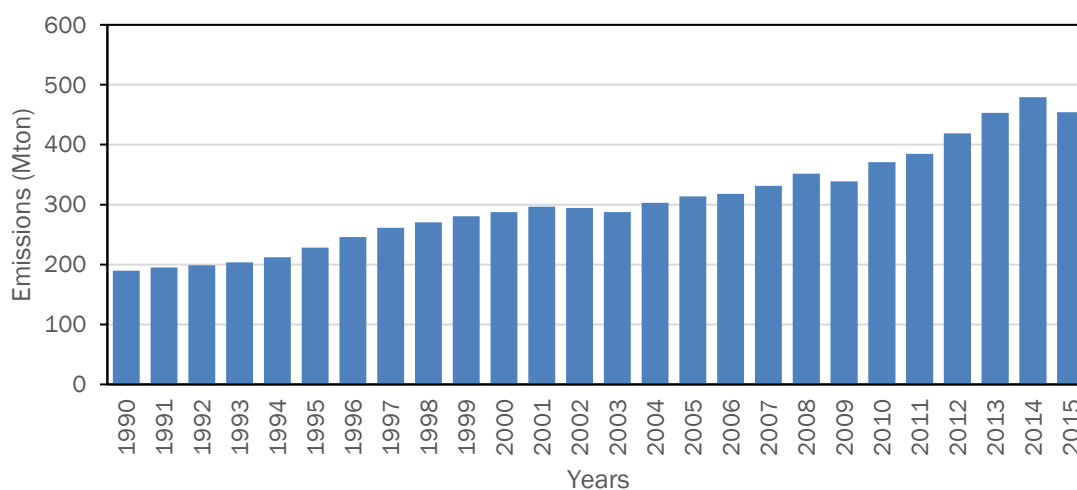
Figure 3 Brazilian energy related Emissions
Source: SEEG (2017)

According to the System Study Greenhouse Gas Emission Estimates (SEEG), Brazilian CO_2 emissions have a non-constant trend, with peaks on years 1995 and 2004. This is mainly due to the fact that Brazilian emissions are driven by land use and agriculture, which varies from year to year. Nevertheless, a consistent trend can be traced in energy-related emissions. These kinds of emissions have increased from 189 Mt in 1990 to 454 Mt in 2015, as seen in Figure 3. The northeastern region emissions were driven essentially by agriculture and land-use back in the 1990's decade. Emission profile in this region changed drastically, as energy share increased in the majority of Northeastern states, with exception of Bahia, Piauí and Maranhão, in which emissions are still dominated by land use. This may be linked with the reduction of poverty and the investments on energy intensive industries on this region in the last decades. On the other hand, southeastern region emissions have been more linked to energy and industrial processes since 1990. In 2015 energetic emissions in the four southeastern states accounted for 44% of their total emissions, and 57% of the total energy related emissions in Brazil.

As there will still be a need of exploiting fossil fuels for several years, there must be continuous improvements in research and development regarding less pollutant technologies. In the last decade it has been promoted the use of natural gas instead of heavier fossil fuels. Another alternative is synthesis gas, which can be obtained from heavier

fuels but penalizing in the conversion efficiency. Natural gas is less pollutant and has a lower carbon quantity which results in lower emissions. The implementation of efficient generation technologies, which reduces both the resources application and CO_2 emissions, is a key for a more sustainable use of natural gas.

Brazil, as many other growing economies is going through an expansion process, in which life quality and expectance is increasing. Wealth increase is related to more energy consumption, even with a decaying population grow rate. Brazilian emissions origins are diverse, most of the efforts have been given to reduce deforestation grow rate, and implement policies that limit the uncontrolled expansion agriculture and livestock industries (ROVERE; GROTTERA; WILLS, 2018). Accomplishing future goals in reducing emissions depends on a complex set of aspects related to a sustainable introduction of renewable energies, and sustainable agricultural industry growth.

Brazilian electricity generation matrix is changing in recent years. The limitation of hydropower storage, the climate change, and the introduction of intermittent energy sources such as wind and solar, is driving the system to look for more flexibility. As a short-term option, thermal power plants seem to offer some flexibility, when considering start-stops and open cycle technologies. A growing energy demand and the needs for complementing intermittent sources may support a growth for thermal based system (DRANKA; FERREIRA, 2018), deriving in more energy related greenhouse gases emissions.

3   ENERGY CONSUMPTION IN OFFSHORE OIL INDUSTRY

3.1   Brazilian FPSO Pre-salt project

3.1.1   Definitions and Operation

FPSOs are specialized ships, usually refurbished oil tankers prepared to perform a wide variety of activities regarding offshore oil processes. This type of unit is interesting when dealing with ultra-deep-water oil production. Mostly all treatment and separations processes are located in the ship. FPSOs operation is divided in modules or small groups of equipment performing a specific function, modules are separated and designed in order to ease and reduce the cost of FPSOs construction. Each module has a specific location in the FPSOs deck; modules can be skipped or not depending on the production case.

Source: TALCYON (2018)   Source: SEVAN (2018)

Figure 4 Examples of FPSO units, ship and round FPSO shapes

The following explanation refers to Pre-salt FPSOs replicant project. At first, fluids coming from the well are collected in production manifolds. These fluids pass through different separation processes. Main separation occurs in a three-phase separation unit followed by two additional two-phase separators, which include electrostatic treatment. Gas extracted from the additional separation suffers a condensate and vapor extraction process,

to then join the main gas stream from the first three-phase separator. The water stream obtained from the well fluids is treated and either reused or rejected to the sea. Extracted oil is dehydrated, remaining water is linked to the cooling water system and the dry oil is stored in tanks within the ship.

A key aspect when switching operational cases is the composition and quantity of gas coming from the wells, as an example, three possible options are depicted in Figure 5. Obtained gases from the well are sent to a main compression hub, where an initial main compression is realized, this system is energized by an electrical motor. Afterwards, the gas mixture passes through two treatment processes, composed by a dehydration process through molecular sieves, and a dew point control treatment. If the treated gas is rich in methane it can be, optionally, passed through a membrane to separate carbon dioxide, as seen in the (a) path in Figure 5.
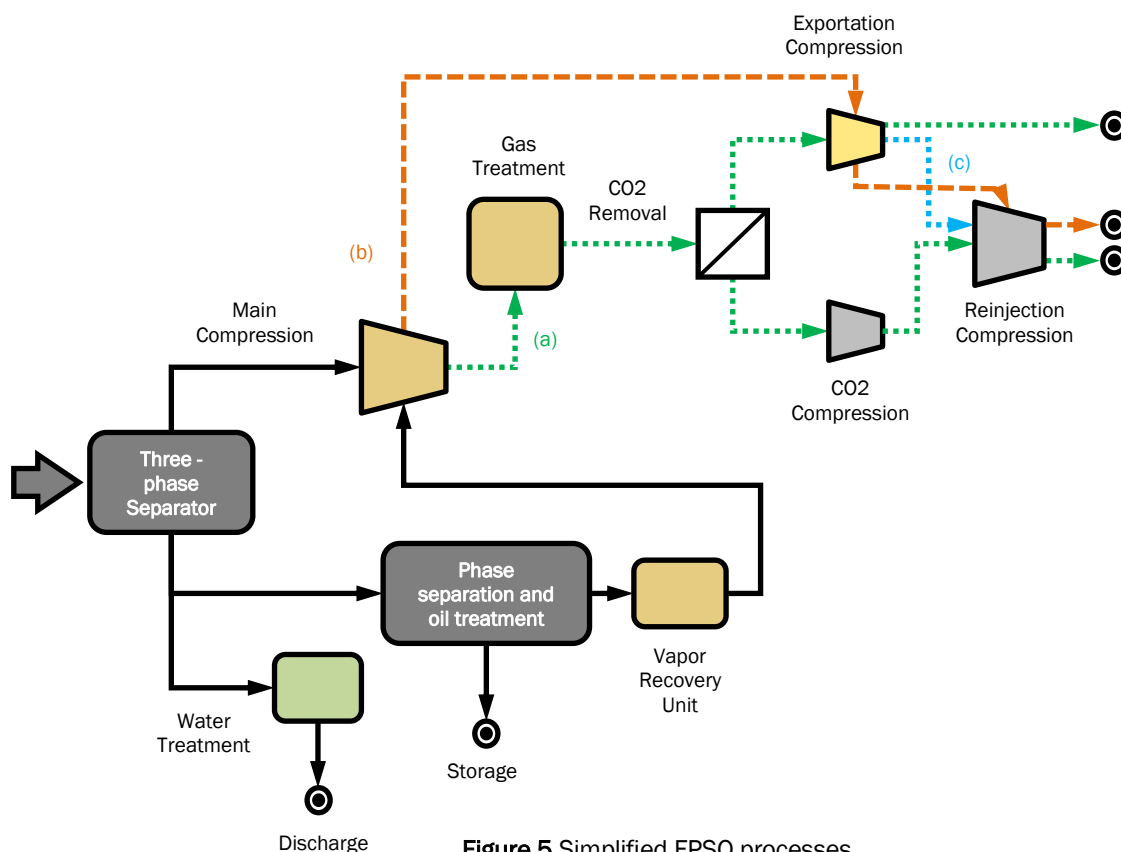
Figure 5 Simplified FPSO processes
Source: Petrobrás

The separation membrane reduces the quantity of CO_2 acid gas and other pollutants such as hydrogen sulfide. The remaining stream of CO_2 from this separation process goes through a first CO_2 booster compression, composed by two compression trains, which are not linked to electrical power supply; they are energized directly by dedicated gas turbines

of 23 MW installed capacity. Resultant associated natural gas can be either exported, through the exportation compression train, used for gas lift, or sent to the reinjection compression train in path (c). A crucial application of the obtained gas after the exportation compression is feeding the gas turbines on the platform. Nevertheless, gas production forecasts may vary substantially; therefore, it is possible that fuel gas is imported from submarine piping, or even diesel could be imported from land, in case gas coming from the wells is not sufficient.

This situation is most likely if obtained gas is not rich in useful hydrocarbons. In this case obtained gases skip the separation membrane and are directly reinjected, following the (b) path on Figure 5. Gases would flow into the booster exportation compressor, and then follow to the injection compressor.

3.1.2   Heat and Power requirements

As it has been previously addressed in several studies regarding offshore oil platforms, usually, the largest irreversibilities occur in burning gases for energy generation. Irreversibilities and exergy destruction are caused by inefficient processes. Hence, efforts must be focused in energy generation design or retrofits, in order to observe considerable efficiency improvements. In most cases, offshore platforms must be auto-sufficient, and must generate all energy needed to carry out their diverse processes.
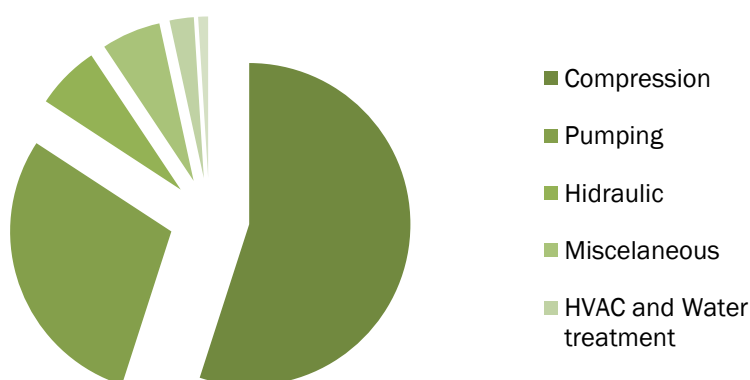
Figure 6 Main Power demand groups in FPSO
Source: Petrobrás

In the Brazilian case, as studied in previous sections, there is a large energy demand related to compression of gases and pumping injection water. Three of the four compression processes rely on electrical power supply, the remaining CO_2 compression system is energized directly by gas turbines. Main compression system increases gases pressure from 2MPa to 25MPa, while pressure at injection compression outlet reaches 50 MPa. An analogous situation occurs in the energy needed for the water pumps to carry out water injection. Those large pressure gradients are inherently related to energy intensive processes.

Table 1 Demand shares according to Final Use

Final Use	kW	%
Compression	40.391	54,96
Main Gas Compressor	17.668	
Exportation Gas Compressor	14.993	
Injection Gas Compressor	5.597	
Other Compression	2.133	
Pumping	21.494	29,25
Main Injection Water Pump	11.081	
Sulphate Removal Pump	3.833	
Sea Water Lift Pump	1.706	
Cooling Water Pump	893	
Other Pumping	3.980	
Hydraulic	4.723	6,42
Miscellaneous	4.362	5,94
HVAC and Water treatment	1.783	2,43
Electrical Losses	728	1
Total	73.480	100

Source: Author, based on Petrobrás

This effect can be observed in approximate power consumption balances for the FPSOs unit, as seen in Table 1 and Figure 6. Those values are based on demands for a hypothetical operational case in which the gas treatment is bypassed. In this case, compression and pumping demand shares account for 84% of the total. In general, off-shore oil industry is related with critical and high-risk operations, therefore the equipment must be able to manage a broad range of situations. Over-sized equipment working at low loads, and anti-surge operations are very energy demanding. Even though it is out of the scope of this study, important achievements could be obtained if the Compression processes were

designed for attain high efficiency levels while also dealing with a broad range of mass flow rates.

FPSO project is conceived for a broad range of situations, besides presented operational cases "a", "b" and "c", further sub-cases are established depending on the fluid components and mass flow rates, in "1", "2", "3", etc. Specifications about flow rates and components in such cases are not accessible, since they are property of the FPSO project developers. However, these details are not relevant to this study as the focus is given to the final demand and installed capacity. In previous researches it was determined that loads among analyzed sub-cases can vary from approximately 31 MW to 74 MW, as observed in Table 2 .

Table 2 Comparison among compression processes power demand [MW]

Sub-case	Max. Oil & Gas	50% BSW	Max. Water
Total Power Demand	73	33	31
Total Compression Demand	51	12	18
Main Compressor	21	6	6
Exportation Compressor	20	5	7
Injection Compressor	10	1	5
Compression Demand Share (%)	71	37	59

Source: Author, based on Petrobrás

Brazilian Pre-salt operations are expected to demand a considerable amount of heating energy, as seen in Table 3. Heat will be transmitted through a closed pressurized water loop, which heat source is the exhaust gases coming from the gas turbines. Water temperature rises up to 130°C in the heat exchangers coupled to the gas turbines and continues to dehydration process plant, fuel gas treatment and separation processes.

In the dehydration plant, hot water releases vapors contained in natural gas, as a further separation process besides of the previous phase separators. Gases for power generation in gas turbines come in relatively low temperature, in order to be effectively injected. Its temperature is raised by the hot water system, which also allows further vapors separation. The largest share of heat is consumed in the first two separation stages, where temperature gradients in oil from the well are between 30 K and 90 K (depending on the operational case) to ease phase separation. Table 3 summarizes power and heat demand for three different cases.

Table 3 Heat and Power Demand Summarized

Sub-case	Max. Oil & Gas	50% BSW	Max. Water
Electric Demand [MW]	73	33	31
GT operating	3	2	2
GT Load [%]	99	45	64
Heat Demand [MW]	47	46	33

Source: Gallo (2017)

Power supply in FPSO's is realized by four GE LM2500 gas turbines located on the deck. This aeroderivative gas turbine model is frequently used in maritime applications. It can be coupled directly for shaft power or used as a Turbine-Generator set for power supply, as seen in Figure 7. Each turbine has a nominal capacity of 30 MW in ISO conditions. The average output for this type of turbines, corresponding with the actual environmental characteristics, is around 25 MW per unit. One of the turbines remains in standby, which results in a total installed capacity of 75 MW. This model also offers the possibility of installing a cogeneration set, which is crucial to supply the heat demand on the FPSOs.
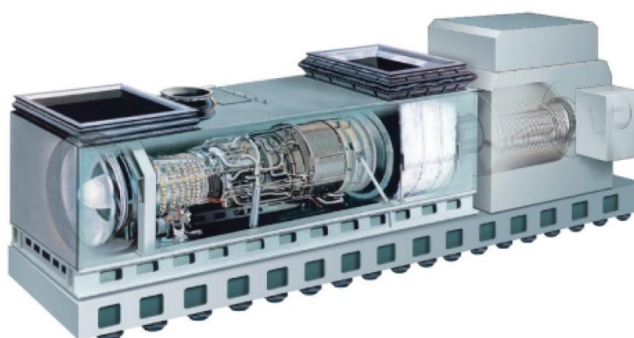
Figure 7 LM2500 Turbine-Generator Set
Source: GE LM2500 Fact Sheet

3.2 Alternatives for energy supply in oil production platforms

This section is dedicated to review latest advances in efficiency assessment and alternatives in offshore platforms. Even though current trends establish efficiency enhancement as an important part of technology development, most offshore platforms

were installed decades ago, with less caring about energy savings or greenhouse gases emissions. For that reason, some studies apply, at first, an overall diagnostic of actual systems to determine which processes are most critical, in order to propose improvement opportunities. Most alternatives are highly dependent on specific environments and resources available in each situation. Energy efficiency measures should adapt to each case and conditions, for them to deliver significant advantages.

3.2.1 Energy and Exergy balances

Offshore oil platforms are composed of complex processes in which multiple mass and energy fluxes interact. In general, energy and exergy balances are applied as a first step to evaluate efficiency performance in such complex plants. Exergy analysis allows detecting specific thermodynamic processes with large irreversibilities. Specifically, in offshore oil industry it has been used to evaluate and compare efficiency performances. On Northern sea platforms, Nguyen et al. (2014a, 2013) and Voldsund et al. (2014) conducted studies emphasizing in the processing plants. In the Brazilian case, De Oliveira et al. (1997) performed initial exergy and efficiency assessments for a typical Brazilian FPSO, Carranza et al. (2015) emphasizes in a platform operating in the Pre-salt, also adding a hypothetical CO_2 capture system.

Generic studies regarding exergy analysis in oil platforms points large exergy destruction in the utility system. The utility system is mainly composed by the electricity generation system and heating water processes. Exergy is lost mainly in the rejection of high temperature gases in the cogeneration system, and in burning and venting gases from the well. Commonly, a platform is designed for a specific gas/oil or water/oil ratio, based on production projections and well behavior forecasts. However, aging wells tend to increase their gas/oil and water/oil ratios. If an original platform is not designed for such situations, irreversibilities would increase through time, as pointed by Ortiz (2015).

3.2.2 Bottoming Cycles

Some alternatives to improve efficiency and thermodynamic performance can be evaluated after realizing initial exergy assessments. One of the most promising alternatives is coupling a bottoming cycle to the regular gas turbine open cycles located in offshore platforms. This is not too frequent mainly due to the increased weight of additional equipment in platforms, and to the high cost of the retrofitting.

In the literature, Pierobon et al (2014a) compared three different bottoming cycles for a specific given oil platform; Compressed air cycle, Rankine cycle and Organic Rankine cycle, while Walnum et al (2013) modeled CO_2 bottoming cycles, also for offshore applications. Among those studies, Rankine cycles gave better results. These cycles have been broadly studied for such applications. Particularly Organic Rankine cycles (ORC) are very interesting for maritime operations due to its compactness and use of low heat resources. For the Brazilian case, Barrera et al (2015) evaluated the performance and improvements of conceptually installing an ORC to a Pre-salt projected platform.

The following off-shore combined cycle cases were explained in Følgesvold (2015), which states that by now, refurbishing to combined cycle has been performed in only three oil platforms in the world. Those platforms are located in Norwegian shelf and possess interesting and diverse characteristics. Oseberg-D platform is part of an interconnected small system of three platforms known as Oseberg Field Center. The other platforms are Oseberg-A and Oseberg-B, which are accessible by elevated bridges. Oseberg- D has two LM2500 turbines coupled to two exportation compressors. Heat recovery was installed for those two turbines in order to reduce the energy needed from main generation units. An important aspect of this refurbishing is that steam produced through heat recovery must travel 400 m to the steam turbine.

Another case is platform Eldfisk 2/7-E, this is a water injection platform in which two heat recovery units were installed. One of them is coupled to two GE LM1600 gas turbines driving water injection pumps. The other is coupled to one GE LM2500, employed for gas compression. This platform is independent and all power supply relies on the electric system within the platform facilities. The installation of a steam turbine, also allowed extracting steam for processes heating if needed.

Finally, the Snorre B platform has one heat recovery unit connected to two GE LM2500+ gas turbines. This is also a cogeneration arrangement, able to supply heat for processes. There is a tradeoff between steam for heating and power purposes, which varies depending on the current needs of the platform. In order to maintain a constant efficiency, the combined cycle is always running at full load. Snorre B is connected by a 10 km subsea

wire to another platform Snorre TLP, this connection grants a surplus energy from the combined cycle to Snorre TLP in case it is needed.

The two first mentioned platforms Oseberg-D and Eldfisk 2/7-E were further refurbished to change the initial waste heat recovery technology of the combined cycle. HRSG were replaced to OTSG type heat exchangers. The application of a combined cycle in all mentioned systems produced total approximate savings of 98 Mm³ per year and reduced 222.000 t of CO_2 per year. It must be pointed that Norway has strong legislation regarding CO_2 emissions, and a CO_2 carbon tax, which improves the viability and economical results of such technology applications. However, reduction of greenhouse gases and efficiency improvements are every time more important factors when establishing energy production technologies, even in Brazil, where there's not yet a carbon tax, the application of such efficiency techniques can lead to better performance of operations, and economical revenues due to the reduction of consumed fuel.

3.2.3 Power Plant Design and Analysis

Reviewed literature in the last section focused on improvements on case studies based on the Northern Sea. However, some tools and methodologies to be implemented can be adapted to any power plant regardless of its location. The authors and studies presented in this section followed a similar reasoning for designing and establishing optimum operational parameters. The analysis and evaluation of their results is crucial to determine the best approach to design a floating power plant, which mixes both characteristics of scale-economy of on-land installations, with the compactness and versatility of offshore power units.

Over the past years *cost-effectiveness* has been assessed in several ways to include not just the capital investments and operational costs, but also considering the thermodynamic characteristic of the system. These are known as thermo-economic analysis and *exergo-economic* analysis. This method was used by Casarosa et al. (2004), in which the exergy losses are minimized to obtain high efficiency operational parameters for a HRSG. Thermo-economic relationships were also used by Godoy et al. (2011, 2013; 2010) by using alternative optimization algorithms to evaluate long-term performance of combined cycles.

Manassaldi et al. (2011) applied *single objective optimization* methods to establish HRSG dimensions and steam cycle power output. Authors in this study also assessed important *sizing magnitudes* such as weight and volume of the HRSG. This case was based on an onshore power plant, considering fixed exhaust gas properties of the gas turbines. On the other hand, Rovira et al (2011) modeled a set of Spanish thermal power plants, in order to propose operational parameters that optimize the integrated system, in this case, *off-design performance* was considered in costs. Results allowed comparing traditional costs calculation based on correction factors instead on off-design parameters.

Also, for onshore facilities, Toffolo et al. (2002) gave a different approach by using *multi-objective optimization* evolutionary algorithms. This work evaluated simultaneously the trade-off among several characteristics, including exergy efficiency and cost-effectiveness. A remarkable aspect in this case, is that gas turbines are included in the optimization to find optimum pressure ratios and turbine inlet temperatures. In some cases, commercial gas turbines are considered instead, in order to give a more realistic approach to the results and methodology. This is the case of Nord et al. (2014) in a study focused in off-shore power plant parameters. GT Pro of Thermoflow ® (2017) is used to perform thermodynamic calculations for gas turbines, followed by multi-optimization algorithms to determine optimum parameters, according to the weight and power output objectives. Off-design parameters were also taken into account in this study. A comparison of the obtained Pareto front and the knowledge-based selection was carried out, in order to understand what improvements could be done to traditional power plant selection for offshore oil platforms.

These references gave a broad idea of what are the main aspects being considered and the tools being implemented when dealing with combined cycle analysis. The integration of those several aspects derive in more reliable results. Figure 8 is depicts such considerations.

Figure 8 Main aspects considered for power plant analysis
Source: Elaborated by author

3.2.4 Offshore Power Grids

Wind Power

Integrating renewable energies to the traditional fossil-fuel based generation in offshore operations would be the best way to reduce greenhouse gases emissions. However, safety and continuous availability are critical in oil and gas operations and renewable energies lack of a continuous nature. Therefore, those cases must be carefully studied in order to produce feasible results, that cope with oil and gas industry needs. Northern Sea oil platforms profit the proximity a high wind power density area. This situation has raised the interest in mixing resources, with the purpose of energizing platforms and even feed onshore power demands.

Korpas et al. (2012) analyses two cases of mixing energy from a wind farm with two gas turbines operating on an oil platform, the authors remark the importance of operational strategy, in order to produce a technically and economically stable performance. Orlandini

et al. (2016) also evaluates stability and operational restrictions on a more complex grid, besides wind power, it integrates three gas turbines each one of them coupled to an Organic Rankine Cycle.

A relevant study regarding offshore winds in Brazil was carried out by Pimenta et al. (2008), results show that best offshore wind power density is located in southern shelf close to Santa Marta in the state of Santa Catarina. Northern coast of São Paulo and Rio de Janeiro states, that correspond with Campos basin, has less wind power density, as seen in Figure 9. This figure illustrates average wind velocities for the Brazilian southern shelf. Offshore region from Curitiba to São Paulo has lower wind velocities and thus less wind power exploitation potential, when compared to Rio Grande do Sul offshore region and even Offshore Espiritu Santo.
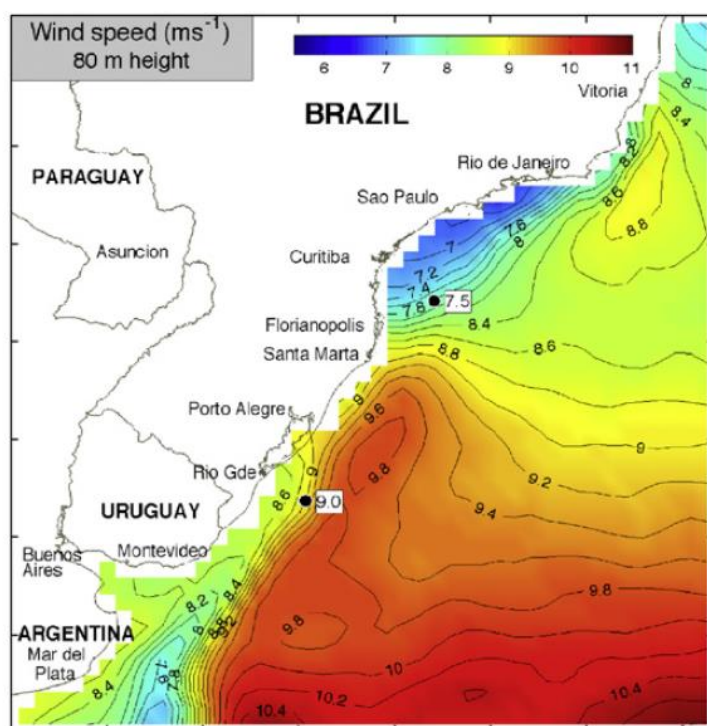
Figure 9 Average wind velocities in Brazilian southern shelf at 80m
Source: Pimenta et al. (2008)

This work proposes a grid linking wind farms, oil platforms and the mainland through a High Voltage Direct Current (HVDC) transformation hub, in order to minimize losses in long distance wiring, and to increase transmission efficiency. An example scheme can be seen in Figure 10. Even though there are restrictions regarding wind power, a hub linking offshore units with the onshore system would add important flexibility of operations in Campos basin.

Offshore units would not be restricted to the capacity installed, and its energy needs could be feed externally.

In contrast with other mature regions such as Northern Sea and Mexico's Gulf Brazilian, Pre-salt has not been completely explored yet, allowing the development of useful and innovative alternatives of energy supply. Energy systems can be adapted since the beginning of its operation to be more efficient, without the need to refurbish or to adapt old equipment.
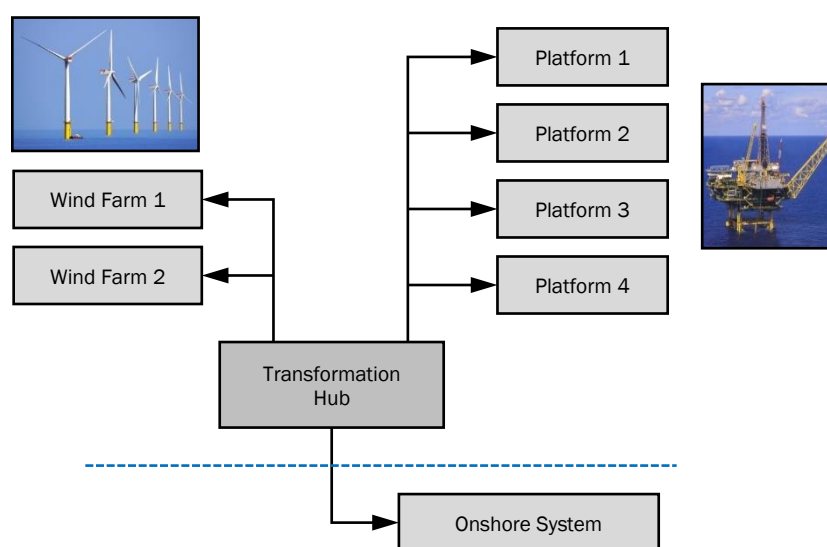
Figure 10 Wind Farm and Oil Platforms Offshore Grid
Source: Reproduced from Marvik et al (2013)

Gas-to-Power technology and Power Island Concept

In the literature, some authors introduced the concept of a floating power hub; Hetland et al. (2009) presented an arrangement that gathered a Siemens commercial combined cycle and a cylindrical offshore platform by Sevan. This commercial multi-purpose system combines several useful processes, like regasifiying natural gas and capturing and reinjecting CO_2 to reduce emissions. A whole ship dedicated to auxiliary and power systems allows constructing more efficient equipment offshore. Sevan Floating Power Plant has various configurations; one is based in four blocks consisting in two Siemens SGT-800 gas turbines, two heat recovery steam generators and a SST-700 steam turbine, or, two blocks

comprising five Siemens SGT-800 gas turbines and one SST-900 steam turbine. Das Norske Veritas (DNV) has also launched a similar concept named OPera.

The implementation of a floating power hub can be very interesting to increase efficiency and take advantage of offshore gas production. However, offshore oil unit design is very project-specific, which means that the particular aspects of Brazilian Pre-salt should be integrated in an appropriate design in order to analyze the economic and thermodynamic performance. In this field Windén et al. (2014) analyzed Sevan's configuration through an economical and cost-effective perspective. In this case, the authors performed a case-study for Australian offshore gas production and compared the cost-effectiveness of installing a power-hub against installing submarine gas ducts to transport extracted gas to shore. Profiting gas onsite in this type of applications is often called Gas-To-Wire, sometimes long distances or places on rough locations may profit of generating electricity directly from gas production, instead of constructing a gas duct grid to transport it to main power plants.

Grid Connections

Energy supply is mostly dictated by a similar scheme all over the world; energy is produced in large concentrated centers and is consumed in a complex set of users. Energy produced must travel from generation centers to end users in populated conglomerations or industrial regions. Electricity transportation is usually divided in transmission and distribution. The transmission concerns the transportation of high voltage current exiting generation power plants. Distribution regards the lower voltage and more stratified supply of energy to end users.

This division is important to understand the technical needs of each step for delivering energy properly and efficiently. The transmission step of energy supply extends along long distances. In last decades, with the liberalization of energy markets and globalization trends, energy grids have become larger. High Voltage Alternate Current (HVAC) transmission has proven to be less efficient in long distances, because of energy losses due to reactive power. High Voltage Direct Current (HVDC) transmission allows reduce costs in wiring and reduces losses in long distances. This has been an option for transnational transmission lines and isolated hydropower generation. In this case, instead of transporting power through alternate current, conversers are used to rectify energy and transform it to

direct current. As stated by Pierri et al. (2017), there are two main converting technologies, Line Current Source Converters (CSC) and Voltage Sourced Converters (VSC). CSC has a stable technology and has been traditionally used since the beginning of HVDC use, while, VSC are still in constant development and are particularly of interest in Offshore Wind applications. Its profitability in offshore industry relies on several performance characteristics above CSC, among them: - VSC are capable of control active and reactive power. - CSC are more restricted regarding input current characteristics, while VSC are more flexible to operate. – VSC control methods result in significant reduction of harmonic production, (ENTSO-E, 2011).

Generation plants and demands centers must be connected by submarine wires in offshore cases. Wiring is a very important aspect when concerning offshore installations as they represent a large share of total capital costs, both options HVDC and HVAC have been already used for such applications. However, there are a considerable amount of construction plans or projects for HVDC connections over the world. Wire composition for both types of currents is not too different from each other, both contain a core and a set of insulation covers. The capacity of holding higher current densities makes HVDC wires to need smaller cross sections, thus, reducing material costs (ENTSO-E, 2011).

4 THERMODYNAMIC BASES

4.1 Combined Cycle

Turbines have prevailed in large scale power plants ever since first innovations in electricity generation. At first coal fired steam turbines were used for electricity generation. More flexibility in operations was added when gas fired turbines were introduced to the market. Nowadays, mixing both cycles in a combined system is one of the most efficient ways in producing electricity, reaching up to 60% of thermal efficiency as compared in Figure 11. Combined cycles share of total installed capacity worldwide reached 20%, compared to 5% ten years ago (KEHLHOFER et al., 2009). Gas capacity additions in 2015 accounted for 46 GW, from which about three-quarters were combined cycle (INTERNATIONAL ENERGY AGENCY, 2017).
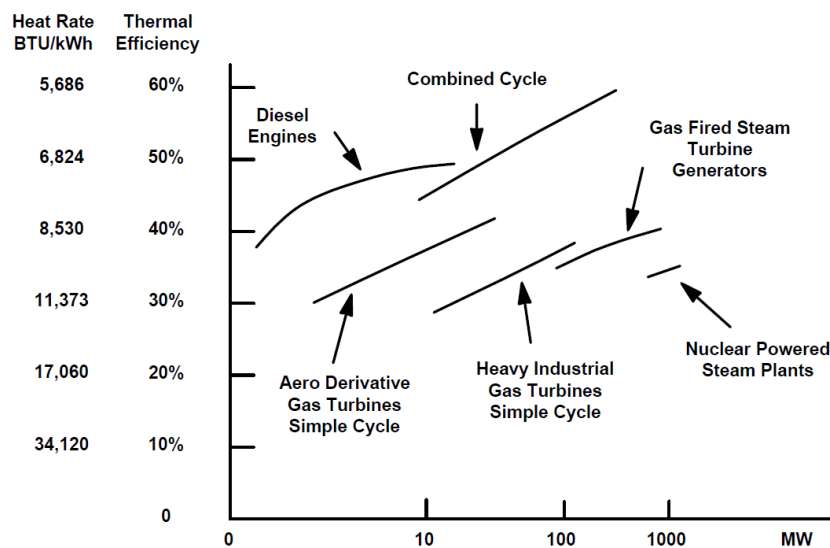
Figure 11 Thermal Efficiency of various technologies
Source: Kehlhofer et al (2009)

Nonetheless, combined cycles in marine applications are relatively a new field. In this case, operations of a combined cycle should adapt to offshore restrictions, the whole system should be compact and have a quick response to highly variable power demands, when installed in offshore platforms. An average Temperature - Entropy diagram of a combined cycle can be seen in Figure 12, where the gas turbine Brayton Cycle diagram is on top and the Rankine Cycle diagram is on the bottom.
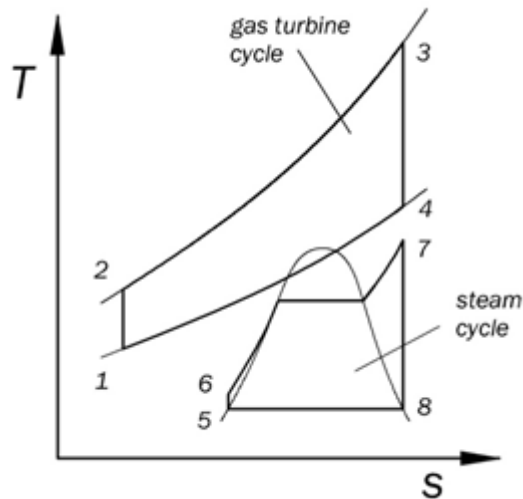
Figure 12 T-s diagram of a combined cycle
Source: Elaborated by author

Design and operation of combined cycles is mostly dependent on the gas turbine. The bottoming cycle maximum power is proportional to the exergy of the gas turbine exhaust gases. Methodologies to calculate the design and off- design characteristics of a combined cycle are based on the analysis of such properties. Next sections are dedicated to present most important theory and characteristic of combined cycle components.

4.1.1   Gas turbine (Brayton Cycle)

A gas turbine is a combustion engine in which hot compressed gases flow into an expander, generating shaft power. Since its first models developed in the 30's decade, they have been used in a large variety of applications from jet propulsion to energy generation. Gas turbines for offshore applications usually range from 1 to 50 MW, and may be modified aero-engines or industrial turbines. Traditionally, a gas turbine consists of three main sections, a compressor, a combustion chamber, and a power turbine or expander. This arrangement may vary substantially depending on the application and manufacturer of the equipment. A simple scheme and T-s diagram are plotted in Figure 13, along with the usual irreversibilities in each process of the cyle. Ambient air enters the compressor at (1), it suffers an ideal isentropic compression (1-2). Then, it enters the combustor where fuel and air are mixed and heat is added to the process at constant pressure (2-3). Shaft power is generated in (3-4) where the combusted air mixture is expanded in an isentropic process. Main components of a gas turbine cycle can be seen in this same figure; however, real

turbines are equipped with multiple stages of compression and expansion, and additional auxiliary equipment.

Source: Elaborated by author   Source: Elaborated by author
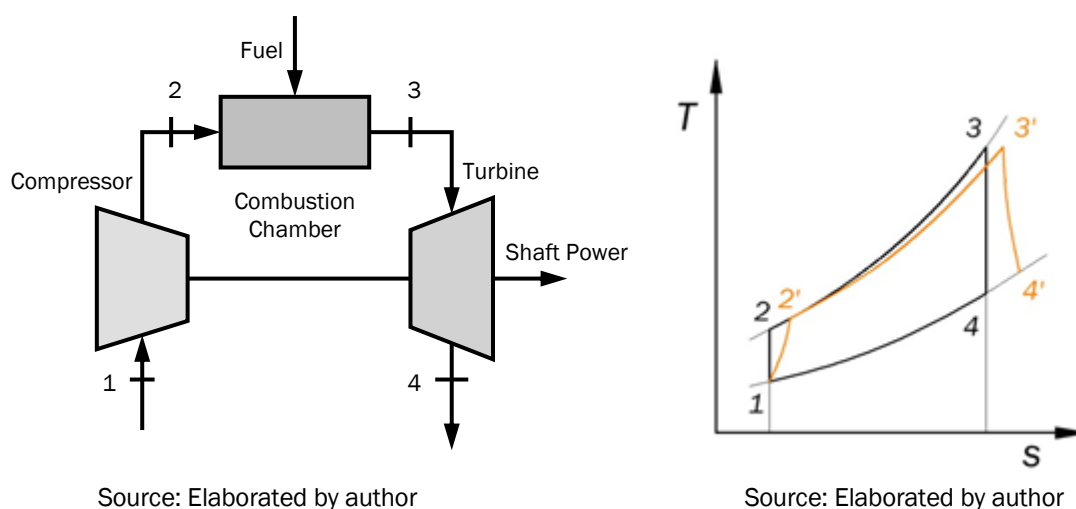
Figure 13 Simplified scheme of gas turbine (left) Temperature - Entropy diagram Brayton cycle (right)

Gas turbines are complex equipment involving a large quantity of variables. The pressure ratio between the intake of the compressor and the inlet of the combustion chamber is taken as one of gas turbines main characteristics. It is considered as an indicator of the overall gas turbine performance and the driver of the turbine's efficiency; the higher-pressure ratio, higher will be the turbine efficiency. For every turbine inlet temperature (TIT) and efficiencies (compressor, turbine) there is a single optimum pressure ratio, and when thermodynamic efficiency increases, so does the pressure ration, turbine inlet temperature and isentropic efficiencies as seen in Figure 14, Figure 15 and Figure 16. Figure 14 curves represent a sensitivity analysis for the compressor-turbine efficiencies, whilst Figure 15 and 16 show curves with fixed efficiencies and varying the turbine inlet temperature. The TIT is an important variable that indicates the maximum temperature achieved in the cycle.
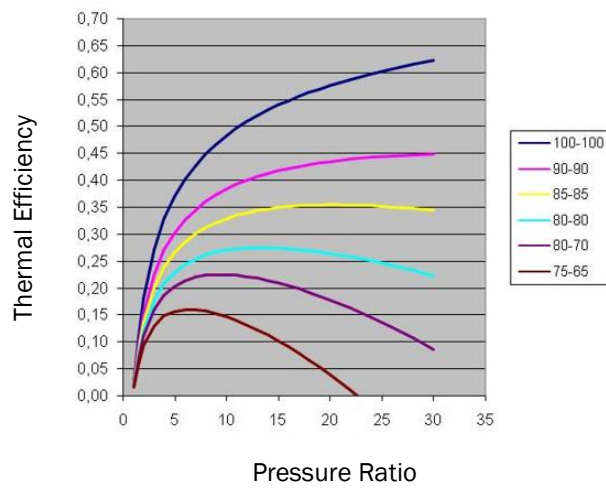
Figure 14 Irreversibilities Effect Constant Temperature Ratio
Source: Gallo (2018)
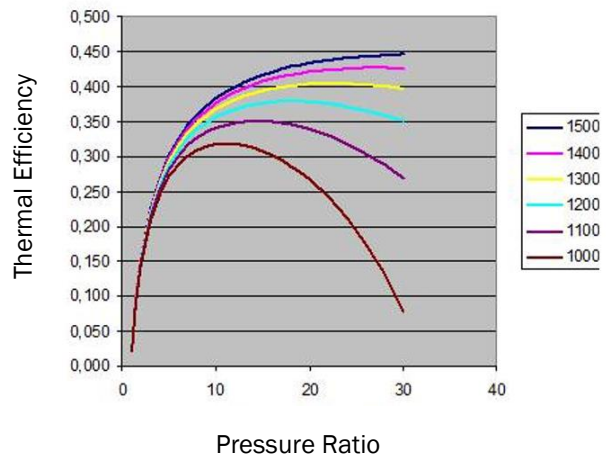
Figure 15 Irreversibilities Effect Constant Efficiencies 0,9
Source: Gallo (2018)
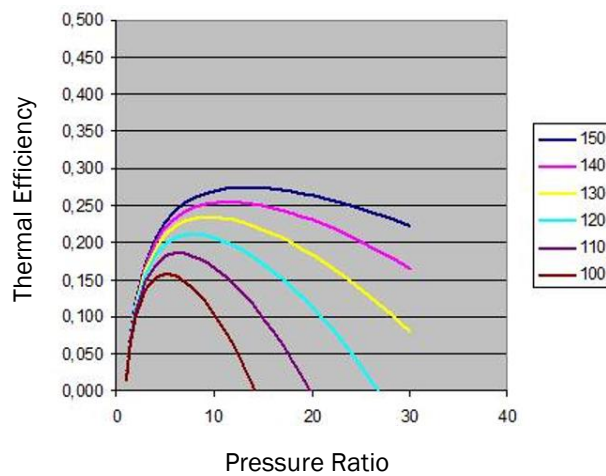
Figure 16 Irreversibilities Effect Constant Efficiencies 0,8
Source: Gallo (2018)

The power output and size of the plant depends on both pressure ratio and turbine inlet temperature (SARAVANAMUTTOO et al., 2009). This is usually a main restriction for design due to the material characteristics in the burner and in the turbine first stages. Such components may deteriorate on extremely high temperatures. Recent innovations have achieved values of 1600°C for TIT. To avoid damaging, blades and nozzles are usually cooled with compressed air or even steam of the combined cycle

Aeroderivative and Industrial Gas Turbines

Gas turbines may be classified by several aspects, such as, shaft quantity, rating, and flow direction, among others. An important parameter to classify gas turbines is by their application, dividing them in aeroderivative and industrial gas turbines, an initial overview is given in Table 4. Aeroderivative models were first designed for flying aircraft propulsion; therefore, their main characteristics are high reliability and lightweight. Aeroderivative turbines are also characterized by fast start-up and response to load changes, easy handling, and shorter downtime maintenances.

Table 4 Comparison Overview

Areoderivatives	Industrial
- Adapted to work at several pressure at temperature levels.	- Designed to operate at constant loads for longer time periods.
- Higher operational flexibility.	- Heavier and larger sizing, usually achieve larger generation capacities.
- More compact and less heavy equipment.	
- Shorter maintenance downtimes	- Maintenance periods are extended and with careful planning.

Industrial and Heavy-Duty gas turbines usually cover a larger range of capacities, from 5 MW up to 400 MW, they are oriented to on-land applications, and hence, weight and footprint are less restricted. In contrast with Aeroderivative turbines, industrial turbines are not focused on work at different loads and shaft speeds. More efficient performances and fewer emissions are emphasized aspects in industrial gas turbines. This type of turbines is

also more prepared to work with a different range of liquid and gaseous fuels, on the other hand, Areoderivatives were, at first, ignited by specialized liquid fuels. Even though at the beginnings both types of turbines were designed with different purposes, nowadays advances in technologies have made them much closer in performance and flexibility. Turbines illustrations are shown in Figure 17.
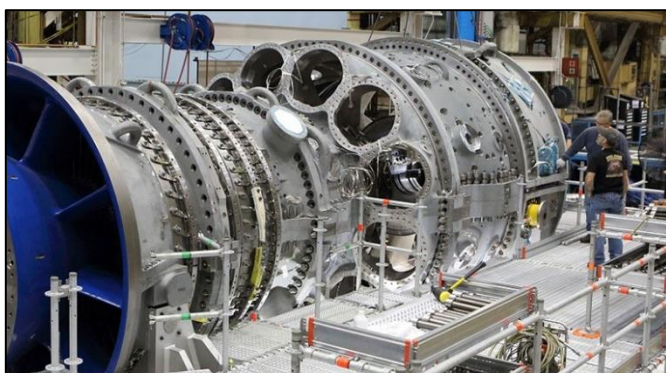
Source: GE (2016)   Source: Siemens (2017)

Figure 17 Aeroderivative (right) and Industrial gas turbines (left).

4.1.2 *Waste Heat Recovery Units*

The link between both Rankine and Brayton cycle in combined cycles is made through a heat recovery unit. Its main purpose is to extract the residual energy from the exhaust gases of the gas turbine. Waste heat recovery units (WHRU) are designed to meet specific needs of the plant. They can be adapted to generate steam for production processes or to produce power in a steam turbine, as in a combined cycle. These units vary in forms, shapes and sizes. They can have horizontal or vertical arrangements with natural of forced circulation. WHRU selection depends on the specific case, among important aspects: interacting fluids and properties, space availability, costs, environment, etc. In offshore applications an important characteristic of waste heat recovery units is their compactness, a compact and efficient unit must be proposed due to the space constraints.

Basic Heat Recovery Steam Generators

Heat recovery steam generators (HRSG) are specialized heat exchangers used in combined cycles. HRSGs consist in a group of staggered or in-line tubes, usually finned to increase the heat transfer area. Exhaust gas pass through these tubes in which internal side flows the inside fluid to the Rankine cycle. The set of tubes are usually divided in sections depending on the phase properties of the inside fluid, basic sections are; economizer (liquid to saturated liquid), evaporator (saturated liquid to saturated vapor), and super heater (saturated vapor to superheated steam). An important characteristic of HRSGs is the presence of steam drums to maintain an equal pressure of the system. HRSGs may count with different pressure levels or reheating which add more complex sections. Most common multiple pressure configurations are two and three pressures, divided in low and high pressure or low, intermediate and high pressures. These pressure levels in the HRSG are connected with the steam turbine different pressures. In a HRSG design there is a relevant tradeoff regarding steam mass flow and pressure, both characteristics define ST power output. When saturation pressure arises, so does the saturation temperature, thus, a larger part of the thermal energy contained in the exhaust gas will be used in the evaporation process, resulting a in lower steam production.

One of the main approaches to design and study HRSG is through pinch point analysis. The pinch point is known as the minimum temperature difference between hot and cold stream, in a HRSG it is the difference between the temperature of gas stream leaving the evaporator and the saturation temperature of the water stream. Ganapathy (2003) presented a method for an initial assessment of HRSGs without dimensional data, through a thermodynamics analysis and Pinch Point information.

This value is an important indicator of the overall HRSG performance and efficiency. Systems with low pinch points produce larger quantities of steam, therefore, higher combined cycle power outputs. Larger pinch points result in smaller and less efficient HRSGs, with higher stack temperatures, thus, less energy being recovered, as illustrated in Figure 18 for a single pressure HRSG.
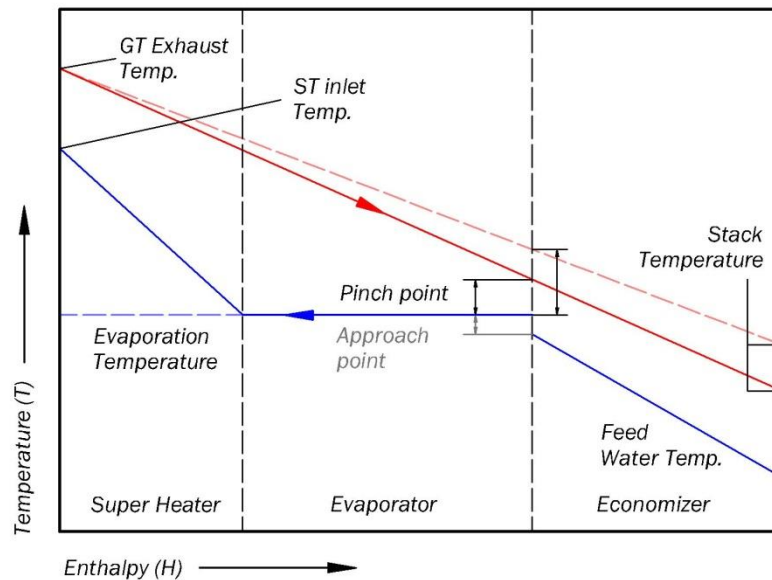
Figure 18 HRSG diagram with pinch point
Source: Elaborated by author

Another important concept is the approach temperature, which is the difference between the saturation temperature, and the economizer water stream outlet temperature. The implementation of an approach point is a measure taken to avoid evaporation in the economizer section. Such situation could result in damages and increased corrosion of the economizer.

Advanced Heat Recovery Steam Generators

Reviewing the single pressure steam generator allows to establish important concepts of combined cycle heat exchange. However, for more efficient applications, there are several additional arrangements; for example, more thermal energy from the exhaust gases can be obtained if different pressure levels are installed. As seen in Figure 19, the area between hot and cold streams becomes smaller, which indicates a reduction of irreversibilities in the HRSG. The addition of a second or third pressure level impact on the whole HRSG and steam turbine design as more steam drums need to be constructed. The steam coming from the HRSG at different pressures must be injected in the steam turbine at the right level; the steam turbine must count with the right steam inlets at different pressures.
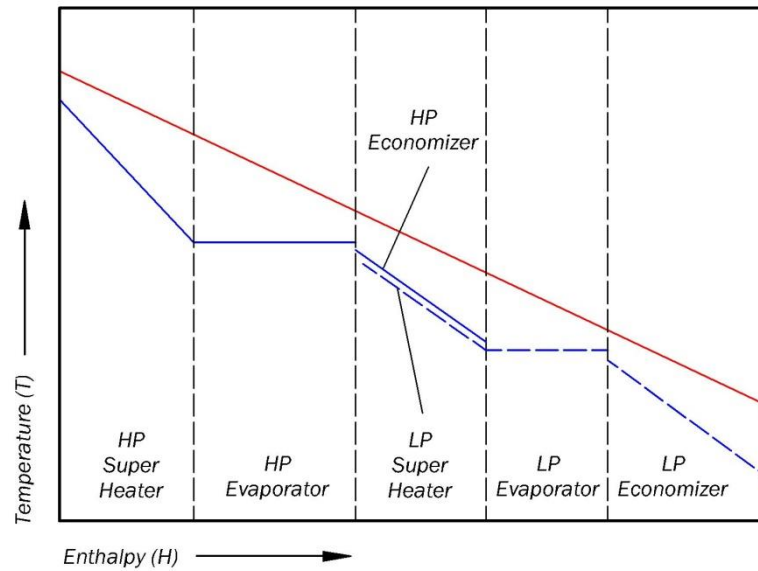
Figure 19 Example of Temperature - Heat diagram with two pressure levels
Source: Elaborated by author

In addition to the quantity of pressure levels in the HRSG, an additional combustion of exhaust gases could be used to further increase their temperature, this is known as supplementary firing. This method introduces more thermal energy to the HRSG, which results in increased steam output and hence increased power output. An increased consumption of fuel increases operational costs of the power plant and considerably reduces its efficiency. The expense of reducing the efficiency must be assessed according to the fuel and electricity prices of the region in which the combined cycle is installed. Supplementary firing is done through duct burners in the inlet duct of the HRSG, as highlighted in Figure 20
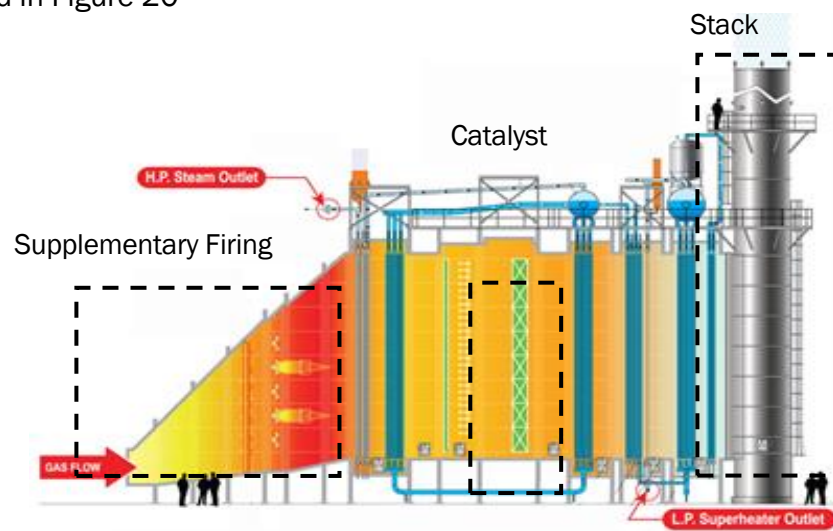
Figure 20 HRSG with duct burners and catalyst controls
Source: Victory Energy (2017)

Once Through Steam Generators

This type of heat exchanger has gained more interest among maritime applications, due to its compactness and flexibility of operation in high pressures. Once through steam generators (OTSG) are simplified equipment when compared to HRSG. An approximate physical comparison is shown in Figure 21.
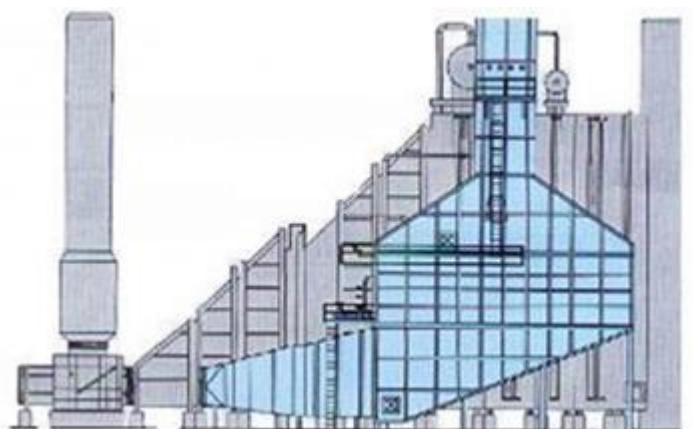
Figure 21 Comparison between HRSG and OTSG
Source: IST Company

In OTSG water flows through tubes, which arrangement can be vertical or horizontal, in this case there is no section distinction: economizing, evaporation and superheating processes happen in the same set of pipes. Even though pumps, drums and bypass stacks are retired from this steam generator, prices are balanced due to the high material costs. Costs of materials rise by virtue of the specialized steels that must resist operations without bypassing flue gases, (FØLGESVOLD, 2015).

4.1.3 Steam cycle

Steam turbines are based on the Rankine cycle, one of the first cycles used for electricity generation back in the 19th century. Rankine cycle energy is produced by expanding steam from a boiler, which can have different heat sources: fossil fuel based,

such as coal, diesel or heavy oil, or biomass based, such as sugarcane bagasse, wood pellets, etc. Over time Rankine cycles alone have been substituted by more efficient and cleaner gas cycles, depending on the available resources. However, modern coal plants and biomass plants rely on steam turbines to produce electricity and hot streams for processes or house heating.

In a steam Rankine cycle water is pumped to a high pressure (5-6). After this pressurizing process the water is heated at constant pressure in a boiler (6-7), until superheated steam phase. subsequently, the high-pressure steam is expanded on a turbine to produce shaft power (7-7a,7b-8). The resulting saturated steam returns to liquid phase by dismissing the remaining heating energy in a condenser (8-5). The fluid coming from the condenser starts the loop again. The condenser unit selection depends on the characteristics of the cooling fluid and its availability.

Real steam turbines are usually modified from the original cycle to be more efficient, Figure 22, depicts a cycle arrangement (left) and a T-s diagram (right) of a reheat Rankine cycle, in which the expansion is done in two stages, after the first expansion the steam is reheated to enter on a second expansion. Another common arrangement is the regenerated Steam Rankine cycle. In this case, steam is extracted at some point of the expansion to preheat feedwater. The heat exchange can be realized in open or closed heat exchangers.
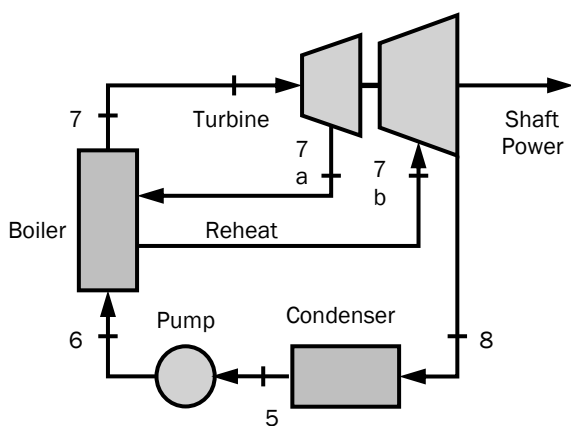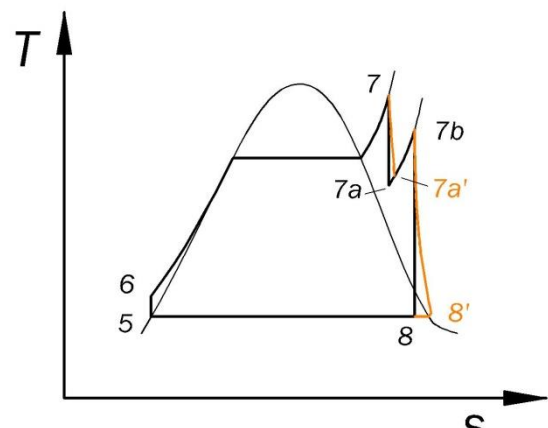
Source: Elaborated by author   Source: Elaborated by author

Figure 22 Simplified scheme of steam turbine with reheat (left)
Temperature - Entropy diagram Carnot cycle (right)

Condensing and Backpressure steam turbines

Steam produced in Rankine cycles has diverse applications such as heating, process steam or power generation. It is possible to combine various applications in one facility by installing diverse arrangements. If the steam turbine is intended to full power generation it is common to have all steam produced in the boiler passing through the expander. As all energy contained in the steam is desired to convert in shaft power, stream exiting the turbine must be close to saturation.

In other applications where, other energy sources are needed or power generation is not the main scope, steam may be removed of the turbine to other processes. A possible way to accomplish this, is extracting steam along the expanding process. This is called an Extraction Steam Turbine Cycle, in this case a fraction of steam is removed through inter-stage valves or through the turbine casing, the remaining steam is expanded until being close to saturated condition. Detriment of power generation occurs by reducing the mass flow passing through the expander.

Another possibility is to maintain a constant mass flow over the steam turbine stages, removing the steam at the turbine exit with enough latent heat to feed other processes. This is a Backpressure Steam Turbine Cycle, in which power generation is also affected by diminishing the enthalpy drop. Nevertheless, in this case, heat rejection of steam is better used in processes, instead of being wasted in a condenser.

4.1.4 Overview of control strategies and off-design performance

The following section is dedicated to review a set of concepts for modeling part-load and off-design conditions of the main components of a combined cycle. This modeling is crucial to determine the fuel consumption and the efficiency performance on   proposed systems and compare with current power units' arrangement.

Gas Turbines Cycle

In common onshore power plants, gas turbines are mostly selected to run at constant loads to supply power in peak demand periods. In contrast with onshore installed gas turbines, offshore and maritime gas turbines must be prepared for sudden changes in loads and operate most of the time below their design point. Hence, off-design analysis of a more efficient power plant for offshore applications is a critical issue that needs to be covered in this study.

In a combined cycle, the gas turbine is the main commander of the whole power plant load as the downstream equipment mainly depends on the heat produced in the exhaust gases. Gas turbine load may be controlled by different techniques. Control techniques have been improved to fit several propulsion and energy generation applications. The simplest way to control power output in a gas turbine is by modifying the amount of fuel in the combustion chamber, nevertheless, a drop in fuel flow maintaining a constant air mass flow reduces the Turbine Inlet Temperature, and hence the Turbine Exhaust Temperature (TET), which is undesirable for combined cycle applications, and reduces overall efficiency. For aeroderivative gas turbines is it possible to operate at part-load by changing the velocity of the gas turbine while keeping constant the velocity coupled to the generator.

Other operation parameters may be modified to reduce power output with fewer penalties in efficiency. Controlling and varying the shaft speed is among the most efficient ways in operating at part-load, however, this technique is specially restricted in single-shaft units and operations needing constant speeds, such as power generation. In order to perform shaft speed modifications a digital power controller would be needed.

A common and commercial part-load control of gas turbines is by restricting the pass of air flow rate through the compressor or turbine. Most heavy-duty modern gas turbines have variable guide vanes (VGVs) on their compressors. Mass flow restriction allows reducing load without drastically reducing the exhaust temperature. This same approach is applicable on a double shaft gas turbine, in which variable area nozzles (VANs) are installed on the power turbine. These devices restrict the pass of gases into the power turbine, reducing the load and maintaining a considerably high exhaust temperature.

The broad quantity of configurations and the nature of phenomena having place in gas turbines make part-load performance estimation usually a though work. Theoretical

bases are demonstrated in by authors such as Saravanamuttoo (2009), Kehlhofer et al. (2009) and Kurzke (1996).

Steam Cycle

Off-design operations of the whole set: HRSG, pump, steam turbine and condenser is based on the fluctuations of steam mass flow production in the HRSG. These fluctuations are clearly depended of the gas turbine part-load performance. The steam turbine is particularly sensitive to changes in flow characteristics, as it suffers drastic expansion changes along each stage. Controlling the steam turbine power output and the heat exchangers performances is mainly based in pressure regulation of the steam flow. Pressure can be regulated in several ways and in different part of the cycle. Controlling methods relevant to this work are sliding and constant pressure.

Constant pressure operation is achieved by throttling valves before the live steam inlet. Its main drawback is the sudden pressure change having place in the first stage of the steam turbine, which could cause a considerable increase in the vapor quality in the latter stages of the steam turbine. This reduction in the enthalpy directly affects efficiency performance of the steam turbine operated at constant pressures for part-loads, (GUARINELO, 2012). On the other hand, most modern combined cycle power plants use the sliding pressure mode. This method is based on the simultaneous regulation of pressure valves in the HRSG and the main pump to control the pressure and steam mass flow rate.

Two important variants of this controlling method are addressed. A pure sliding pressure control would gradually reduce the operation pressure according to the steam flow production. Both pressure and steam mass flow decrease linearly from 0% to 100% load. In a different manner, partial sliding pressure consist in a mixed method, in which pressure decreases linearly with respect to the steam generation until approximately 50% of the load, from then on, the pressure is maintained constant for lower loads, as seen in Figure 23.
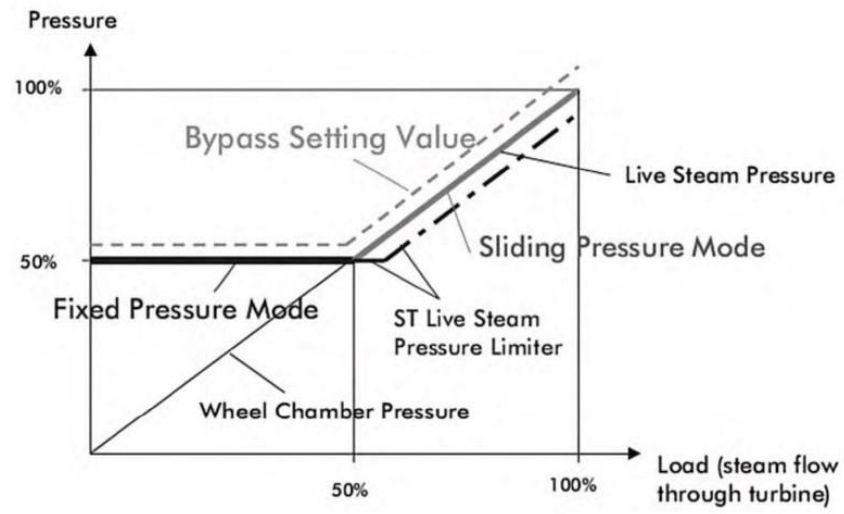
Figure 23 Sliding Pressure operation scheme
Source: Kehlhofer et al (2009)

5 METHODOLOGY

Procedures and calculations performed to accomplish objectives are presented in this chapter. The methodology applied in this study is based on combined cycle analysis aspects studied in the literature review. Those aspects regard thermodynamic, economic and physical design and optimization. This floating facility would consist in blocks of combined cycles (CC), as seen in Windén et al. (2014) and Hetland et al. (2009). CC blocks are conformed by one or more of the following components: gas turbine (GT), heat recovery steam generator (HRSG), steam turbine (ST), condensate pump and a condenser.

Two main optimization approaches are considered in order to establish the quantity and design of CC groups: single-objective optimization and multi-objective optimization. The overall methodology can be considered as top down because most important thermodynamic outputs are calculated first, followed by detailed dimensional and economic calculations. Thermodynamic, economic and dimensional models simulating the combined cycle system are established, so they can fit the optimization algorithms. Two set of variables are separated, the design variables and the dependent variables. The first set consist in important decision parameters for the design of the CC components, the second set are related to calculations and processing of the first set.

After the optimized variables are obtained, the economic and environmental performance of each result is analyzed to perform comparisons regarding the best conceptual scenario in order to apply the power hub alternative. This chapter is devoted to explain the construction of the mathematical models and tools utilized to obtain main design parameters, including the optimization procedures, and economic considerations, which are also detailed.

Power hub arrangements could be interesting for oil production basins with several operative offshore units, the methodology could be used also for other off-shore applications for which similar trade-off analysis needs to be addressed. Application restrictions need to be thoroughly studied for each case, some restriction examples could be: scarce fuel gas production, unavailability of infrastructure to sell surplus gas and operational aspects regarding heat demand. Benefits would also differ depending on the selected case, for example, in Brazil, benefits may rely in surplus gas opportunity cost, for the Norwegian case,

less fuel consumption implies paying less carbon taxes, alternatively, when there is a link to shore benefits may be related to selling electricity to main grid.

For this thesis, Brazilian pre-salt basin and Replicant FPSOs are taken as case study, power and heat demands are known and are based on expected production conditions. It is assumed that surplus gas could be sold and delivered by submarine gas ducts, link to shore is also considered. As mentioned, these boundary conditions and considerations could be modified depending of the application region.

5.1 FPSOs Bases

One of the projects related to production and exploitation of the Pre-salt region consists in the construction of multiple FPSO units featuring a similar general design. This design replication implies that equipment to be installed in those FPSOs were devised with similar characteristics, even though they will operate in diverse exploration blocks and oilfields. Thus, installed equipment must deal with a wide range of operating conditions, to match all the possibilities that could arise in the diverse production areas. For this reason, most of the equipment could be constrained to operate at part-load for a considerable amount of their expected lifetimes.

As stated in the Introduction Chapter, Pre-salt "replicant FPSOs" are equipped with an energy module, consisting in four GE LM2500 gas turbines. Under the specific temperature, pressure and humidity conditions of the Brazilian Pre-salt basin, the energy module total capacity reaches approximately 75 MW. Production forecasts indicate the possibility of obtaining an associated gas with a high percentage of CO_2, along with the oil and water mixture. Diverse compression modules impulse the obtained gas through treatment, injection or exportation processes. FPSOs production scenarios contemplate several operation situations. Depending on the CO_2 quantity of the associated gas, it can either be exported through pipelines, or reinjected in the reservoir. The CO_2 may be removed from the gas stream in some cases, through a separation module. The obtained stream rich CO_2 is handled by a module comprising two turbo-compressors. The particularity of CO_2 compressors is that they are isolated from the power module. Two additional GE LM2000 turbines provide mechanical drive for this compression section. A more specific overview of

Pre-salt FPSOs operation scenarios can be detailed in Gallo et al (2017). Combining both demands from the main power module and the CO_2 compression module, total electric demand in a Replicant Pre-salt FPSO may reach up to 80 MW.

The proposed floating power hub would gather electricity demand for three FPSOs, aiming to concentrate supply in a power plant as seen in Figure 24. Natural gas being produced and treated in the vessels is sent to the power hub, and in turn, it sends electricity via submersible cables to each vessel. FPSOs needs a heat source to perform treatment and separation processes, therefore, at least one cogeneration turbine must be left locally in each FPSO to supply such requirements. The remaining three turbines could be hypothetically removed and the turbines used to energize CO_2 compressors could be replaced by electrical drive. Total demand of three FPSOs would sum up 240 MW, considering that at least 25 MW must be left in each vessel, it is estimated that the minimum installed capacity to be supplied by the power hub is 165 MW, considering the respective reserve margin.
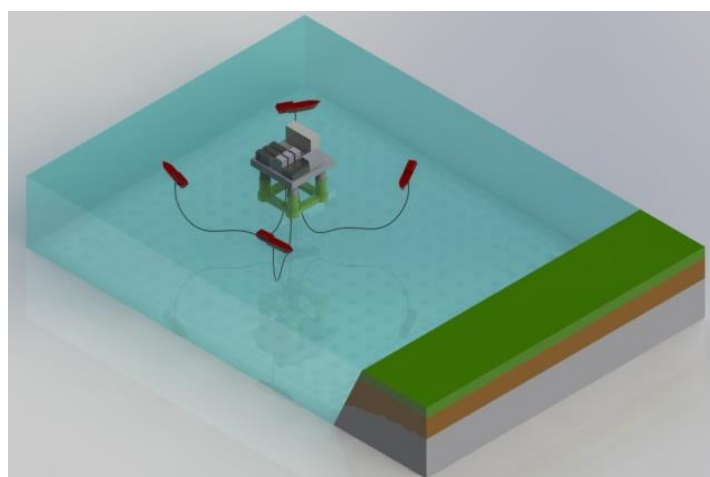
Figure 24 Power Hub Layout
Source: Elaborated by author based on DNV

One of the biggest challenges when optimizing power supply for offshore facilities, is to address large variations that electricity demands suffer over time. These variations cause equipment to run at very low loads for extended periods of time, reducing efficiency and increasing wear and equipment damage. In order to reduce these impacts, this study includes a timeline analysis, in which instead of optimizing for a single point, such as maximum load or maximum production, the algorithm optimizes sum of values overtime. A timeline analysis allows forecasting more precisely CO_2 emissions and fuel consumption

in part load periods. Additionally, it allows integrating fuel reduction, and a hypothetical electricity trade in the cost estimation.

First FPSOs in Brazilian Pre-salt started operations in recent years, therefore production values are based on forecasts and estimations. Oil production is the main driver for electricity demand. For this study, electricity demand for a generic Brazilian FPSO is based on Gallo et al (2017), in a 20 year period. The three FPSOs would have the same electricity demand characteristics, assuming that they would have similar well and exploitation block characteristics. The timeline considerations include an offset between commissioning and start of operation of each FPSO in two years. Table 5 shows a consolidated balance of the lifetime electric demand, considering the onsite cogeneration turbine for heat demand. Detailed analysis of heat demand is not part of the scope of this work.

Table 5 Electric Demand Integration

Year	Demand (MW) FPSO 1	Demand (MW) FPSO 2	Demand (MW) FPSO 3	Total Demand	Power Hub Demand
0	0			0	0
01	30	-	-	30	5
02	35	-	-	35	10
03	70	30	-	100	50
04	77	35	-	112	62
05	80	70	30	180	105
06	80	77	35	192	117
07	80	80	70	230	155
08	80	80	77	237	162
09	80	80	80	240	165
10	80	80	80	240	165
11	80	80	80	240	165
12	80	80	80	240	165
13	80	80	80	240	165
14	80	80	80	240	165
15	80	80	80	240	165
16	77	80	80	237	162
17	60	80	80	220	145
18	51	77	80	208	133
19	50	60	80	190	115
20	45	51	77	173	98
21	30	50	60	140	65
22	-	45	51	96	46
23	-	30	50	80	30
24	-	-	45	45	20
25	-	-	30	30	5

Source: Author based on Gallo et al (2017)
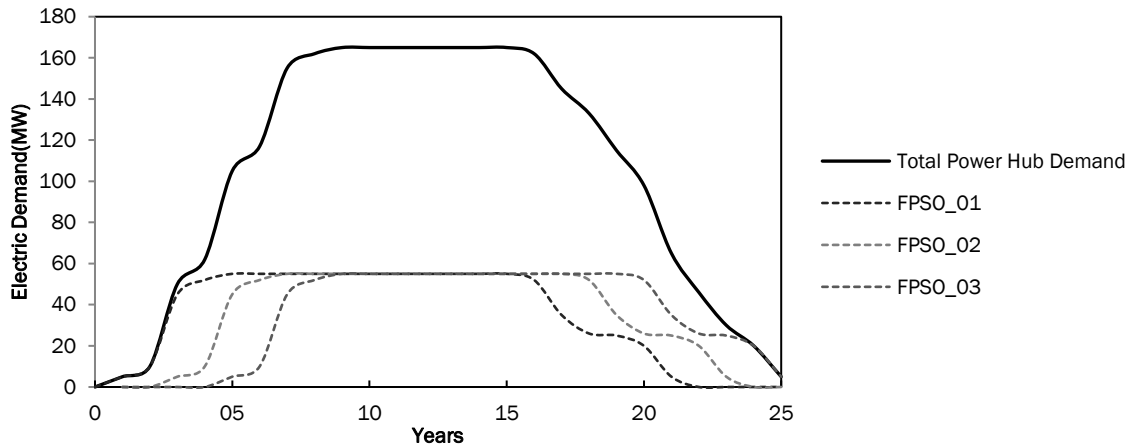
Figure 25 Power Hub/FPSO Electricity demand over time
Source: Author, based on Gallo et al (2017)

Figure 25 is a graphical representation of the aforementioned electric demand behavior over time. It is possible to observe three differentiated periods along the Power Hub lifetime. From years 0 to 7, there is a constant increase in electricity demand with visible variations on with the entrance of each FPSO in the grid. From years 8 to 16 there is a constant electricity demand. Even though real demand fluctuates even in a daily basis, it is assumed that this period will be characterized by an overall stable load. Finally, from years 17 to 25 there is a more continuous decrease in electricity demand, with no clear distinctions of the decommissioning points of each FPSO.

The electricity demand is one of the main frames to start the Power Hub design. The maximum load is one of the main design bounds. And after the design is completed the part-load conditions depends on the electricity needed, particularly in transition periods such as years 0 to 7 and 17 to 25. This section intended to establish the bases for the Power Hub design, which included main premises and considerations for rearranging FPSO power modules and concentrating them into a single Power Hub. The following sections, establish in-detail the design of the equipment contained in the Power Hub, through Thermodynamic, Economic and Dimensioning points of view, to finally address the optimization procedure.

5.2 Thermodynamic analysis

The thermodynamic properties of each point of the combined cycle are crucial data to determine design capacities and ratings for equipment. Those are obtained by applying

mass and energy balances and determining inputs and outputs characteristics in each component. The first principle of thermodynamics along with the respective ideal gas and heat transfer considerations are the main concepts to apply in this step. The thermodynamic balances of both Rankine and Brayton cycles, which compose the combined cycle, allows creating a calculation structure, utilized in the optimization processes. Each component is analyzed separately and all thermodynamic equations correspond to steady state conditions. The modeling process and considerations for each one of them is further explained in the following sections.

5.2.1 Gas Turbine

The gas turbine is the first equipment to be analyzed, since all downstream components design and performance will depend on the characteristics of its exhaust gases. In this study, gas turbine analysis has two different approaches. One of them corresponds to the single-objective optimization. In this case, a group of commercial gas turbines were selected to determine which one is best for a specific objective. The second approach is used in the multi-objective optimization and it is based on a hypothetic turbine modeled with corresponding governing equations.

Continuous Analysis – Gas turbine parameter design

In the multi objective optimization approach, the gas turbine parameters will be modeled from the governing thermodynamic equations. Gas turbine design and performance depends on the selected arrangement. As stated in Saravanamuttoo et al. (2009), twin spool gas turbines observe a reduction in operating mass flow when working at lower net power outputs, in contrast with single shaft gas turbines. This behavior can be seen in commercial gas turbines for combined cycles; therefore, the twin-spool gas turbine arrangement is used for this modeling case.

Four components constitute the gas turbine, compressor, combustor, compressor turbine and power turbine, as seen in Figure 26. The parameters defining the design of the gas turbine are, in this case, the pressure ratios, the turbine inlet temperature and compressor and turbine efficiencies. This allows the optimization search among continuous and smooth variables. Toffolo and Lazzaretto (2002) applied multi-objective optimization for a single-shaft gas turbine. For this study, a similar optimization structure is proposed, considering a double shaft gas turbine. For this arrangement, there must be compatibility between the work delivered by the compressor turbine and the compressor power requirements. Additionally, there must be flow compatibility all along the expansion processes. Thermodynamic considerations and main design equations are derived in Saravanamuttoo et al. (2009). Main equations follow after Figure 26.
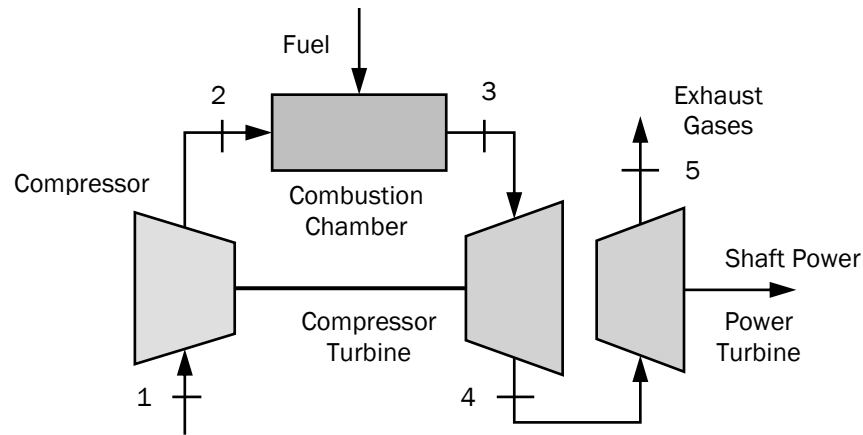
Figure 26 Two Shafts Gas Turbine Simplified Scheme
Source: Elaborated by author

Compatibility between compressor and compressor turbine:

$$\dot{W}_{ct} = \dot{W}_{co} \tag{1}$$

$$\eta_m c_{pg} \Delta T_{34} \dot{m}_{gas} = c_{pa} \Delta T_{12} \dot{m}_{air} \tag{2}$$

Mass balances for the air, fuel and gases flows:

$$\dot{m}_{gas} = \dot{m}_{air} + \dot{m}_{fuel} \tag{3}$$

$$\dot{m}_{air} h_2 + \eta_{cb} \dot{m}_{fuel} LHV = \dot{m}_{gas} h_3 \tag{4}$$

Pressure losses in the combustor:

$$p_3 = (1 - \Delta p_{cb})p_2 \tag{5}$$

Power turbine calculation:

$$\Delta T_{45} = \eta_{tp} T_4 \left[1 - \left(\frac{1}{p_4/p_a} \right)^{(\gamma-1)/\gamma} \right] \tag{6}$$

$$\dot{W}_{gt} = \dot{m}_{gas} c_p \Delta T_{45} \tag{7}$$

The considerations for the previous equations are based on the simplifications made by Saravanamuttoo et al (2009) in which is stated that for real gases in the average operation conditions in gas turbines, assuming a mean specific heat is usually sufficiently accurate. One of the reasons is that γ and c_p vary in opposed senses, and the differences are compensated in the product $c_p \Delta T$, especially when calculating the power output. Even though, temperature profiles would not be very accurate. However, for the objectives and scope of this thesis, these approximations are considered approximate enough. Additionally, real specific heat variations should be calculated through iterative processes that could hamper the optimization algorithm.

Discrete Analysis – Commercial gas turbines

For the single objective optimization, the gas turbine output properties are selected among a group of commercially available gas turbines. This approach is more practical when dealing with scenarios that are more realistic. It is common for offshore operators and companies to purchase gas turbine packages, which are specially designed or adapted to operate in maritime applications. This process is possible by linking the combined cycle model to Thermoflex®. This software possesses a broad library of gas turbines. This database allows obtaining commercial gas turbines characteristics and estimating their performance in different conditions.

Table 6 Main properties of selected gas turbines under ISO conditions

GT Model	PR	TET (K)	Air Flow (t/h)	Nominal Power (kWe)	LHV efficiency
GE LM2500+PV	21,5	773	299	30.340	39,9
GE LM6000 PA	29,5	751	439	41.020	39,1
Siemens SGT-700-33	18,7	811	330	32.215	36,9
Siemens SGT-800-50	21,1	826	474	50.504	38,3

Source: Thermoflex

To span a considerable range of possibilities, four gas turbines were selected. (i) GE LM2500 and (ii) SGT-700, both are commonly used gas turbines for offshore applications like FPSO vessels and Floating Liquified Natural Gas (FLNG). Particularly LM2500 has been widely studied and it is functioning in two of the operating offshore combined cycles. From a scale economy and efficiency point of view, larger turbines closer to what is actually used in on-shore applications are also considered: (iii) GE LM6000 among its applications of interests, it is used for larger scale combined cycles and for cruise and ship propulsion. (iv) SGT-800, which has the largest power rating among the studied turbines, is mostly used in simple/combined cycle and cogeneration applications. A summary of most important characteristics at ISO conditions is shown in Table 6.

It is important to note that gas turbine performance is deeply affected by environmental conditions. Power output reduces considerably with the increase of air inlet temperature. In this study, weather conditions correspond to averages obtained for Rio de Janeiro. It is expected that associated gases obtained from oil extraction operations would be used as fuel for the gas turbines. This associated gas is actually a mixture of several compounds.

The actual composition is unknown, however, there are several production scenarios covering a wide range of situations. The composition selected to carry out the simulations is detailed in Table 7. This information is obtained from one of the expected production scenarios. The fuel composition affects its heating value, which in turn has an important effect on power output.[1]

---

[1] Environmental considerations are also valid for the continuous variable approach of the gas turbine modeling

Table 7 Fuel gas composition

	Substance	Molar [%]
Methane	CH_4	75,6
Ethane	C_2H_6	10,9
Propane	C_3H_8	6,6
Carbon Dioxide	CO_2	2,9
n-Butane	C_4H_{10}, n	1,5
Isobutane	C_4H_{10}, iso	0,9
Nitrogen	N_2	0,5
n-Pentane	C_5H_{12}, n	0,3
Isopentane	C_5H_{12}, iso	0,2
Hexane	C_6+	0,1

Source: (GALLO et al., 2017)
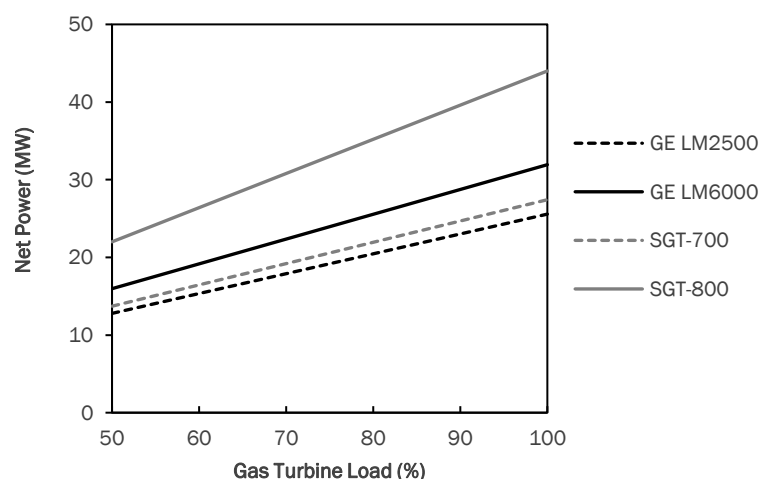
Figure 27 Power output chart at established conditions
Source: Author, based on Thermoflex

Outlining and applying the environmental and fuel factors makes possible to estimate the gas turbines performance and behavior in its actual location by using Thermoflex®. Most important variables to be extracted from gas turbine modeling are power output, fuel consumption, temperature of exhaust gases and CO_2 equivalent emissions. Another set of variables are constant and do not depend on environmental or off-design conditions. Instead they depend on the selection of the respective gas turbine model. Namely, purchasing costs and weight, which are further explained in the economic and dimensional modeling sections. Figure 27 and Figure 28 illustrate the gas turbines power output and efficiency performances at part-load conditions and under the specified weather and fuel conditions.
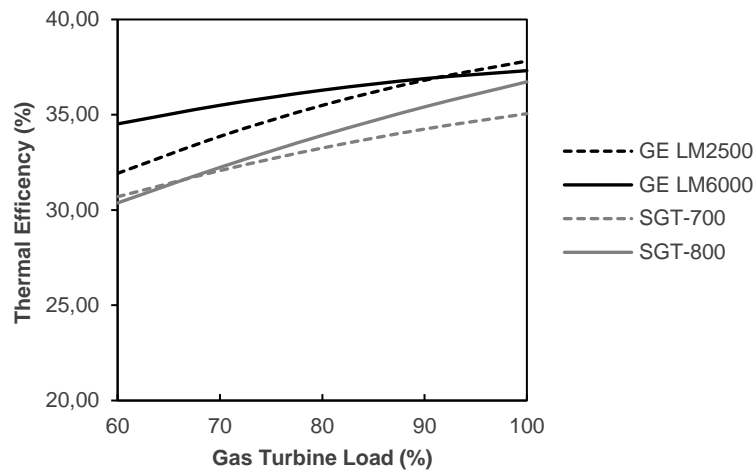
Figure 28 Efficiency output chart at established conditions
Source: Author, based on Thermoflex

5.2.2 Heat Recovery Steam Generator and Steam Cycle

A waste heat recovery unit (WHRU) is a critical part of the combined cycle. It is the main link between both cycles and its part load operation is closely related with the steam turbine off-design performance. Compact heat recovery units such as the Once-Through-Boiler (OTB) have been studied for off-shore oil platforms, (NGUYEN et al., 2014b; PIEROBON et al., 2013). Even though OTB have several important characteristics for off-shore design, such as faster response to varying operating conditions, and smaller footprints, (GULE, 2016), The concept of a power island allows integrating more efficient equipment, without a strict space limitation. Therefore, the WHRU configuration can be similar to an on-shore power plant. Heat Recovery Steam Generators (HRSGs) are widely used for on-land power plants and are generally considered more efficient for subcritical cycles, as the difference between water and gas heat transfer curves is reduced.

Considering the preceding statements two arrangements of Heat Recovery Steam Generators will be analyzed in this study: one pressure level and dual pressure HRSGs. Both HRSGs are horizontal drum type, without supplementary firing. In this case, the gas flows in a horizontal direction, while steam flows in an arrangement of vertical tubes. The main purpose of realizing a thermodynamic analysis to the HRSG, is to obtain a temperature profile, which will be useful when estimating dimensional and economical parameters. One pressure and double pressure arrangements will be analyzed for single and multi-objective

optimizations. Supplementary firing is not considered in this thesis, nevertheless it could be adapted in further studies.

Single Pressure Heat Recovery Steam Generator

HRSG for one pressure level is divided in three main sections: economizer, evaporator and super-heater, other additional parts such as re-heaters are not considered for the thermodynamic analysis. A preliminary temperature and energy balance of the HRSG is performed as in Ganapathy (2003), using the Pinch Point to carry out the mass flow calculations.

Figure 29 shows a simplified system layout, with main flows and components. Additionally, a typical one-pressure temperature profile is seen in Figure 30, including the respective temperature and flows nomenclature for this case. [2]
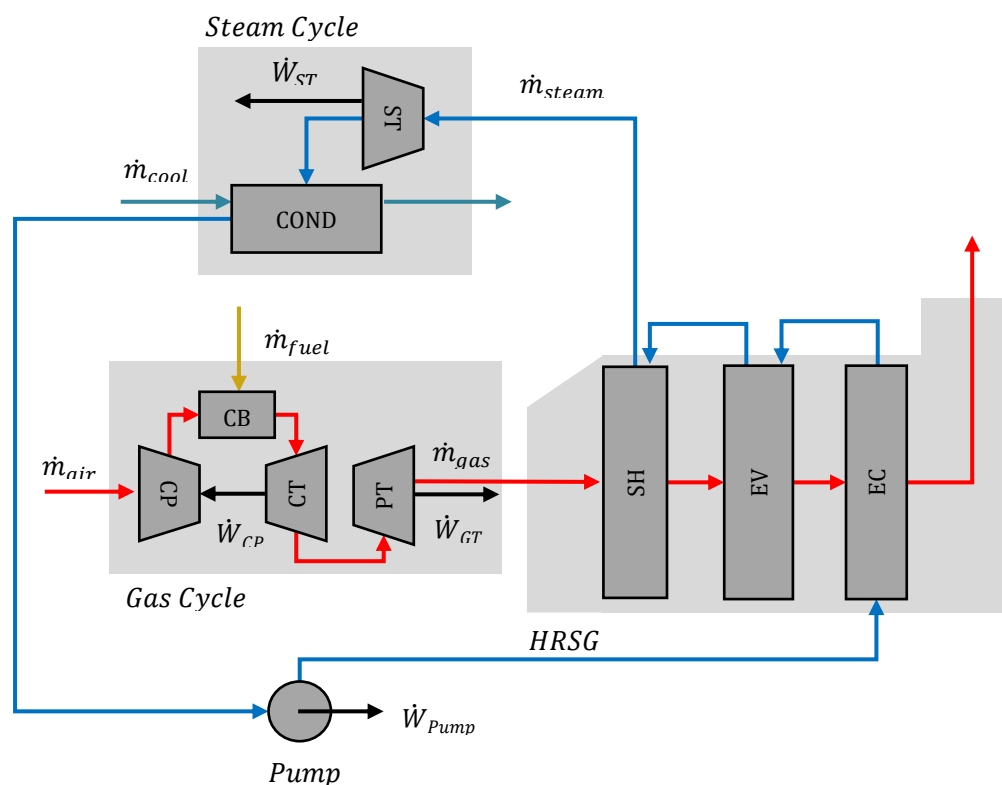
Figure 29 Simplified One Pressure Level Layout
Source: Elaborated by Author

---

[2] In Figure 29 the letter "T" represents temperatures for the gases, "t" the temperatures for the water/steam. Number "1" stands for inlet, and "2" for outlet. The subscripts: ec, ev, and sh, indicate economizer, evaporator, and super heater respectively.

$$PP = T2_{ev\_gas}\text{-}\ T_{sat} \rightarrow T2_{ev\_gas} = PP +\ T_{sat} \tag{8}$$

$$Q_{ev\_sh} = \dot{m}_g Cp_g\left(T_{exh\_GT}\text{-}\ T2_{ev\_gas}\right) = \dot{m}_w \Delta h \tag{9}$$
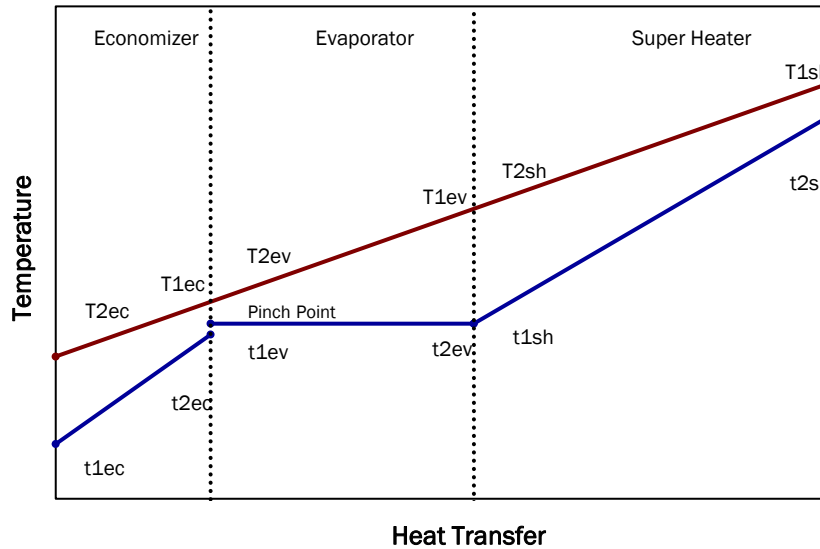
Figure 30 Temperature Profile
Source: Elaborated by Author

The steam cycle corresponding to one pressure level HRSG is determined by the HRSG outlet steam temperature or live steam temperature, and the outlet pressure. Ambient conditions also affect the steam cycle, as the condensation pressure is limited by the ambient temperature. The condenser is assumed to be of shell-tube type, in which the cooling fluid would be treated seawater, and the operational pressure would be set by the optimization iterations.

Dual Pressure Heat Recovery Steam Generator

The dual pressure arrangement is based on typical configurations as studied by Manassaldi et al. (2011). In this case there are two economizers, super-heaters and evaporators, thus doubling the quantity of sections of the previous arrangement, and therefore adding more complexity to the system. The order and disposition of these sections is as seen in Figure 31.

At the entrance, the low-pressure economizer handles one stream of water flow, which then divides at its outlet. One stream is sent to a pump to follow the high-pressure sequence to the evaporator and super-heater, the remaining mass flow is directed to the low-pressure sections. This system has a low-pressure pump, handling the complete stream of water flow, and a high-pressure pump which increases the pressure of the high-pressure water mass flow.

The calculations for estimating mass flows are similar to the single-pressure arrangement. This case considers two different streams, a low-pressure and a high-pressure stream, established by the pinch point methodology in their respective evaporators. These considerations, along with energy balances on each section, create an equation system which results in the temperature profile and HRSG main design parameters.
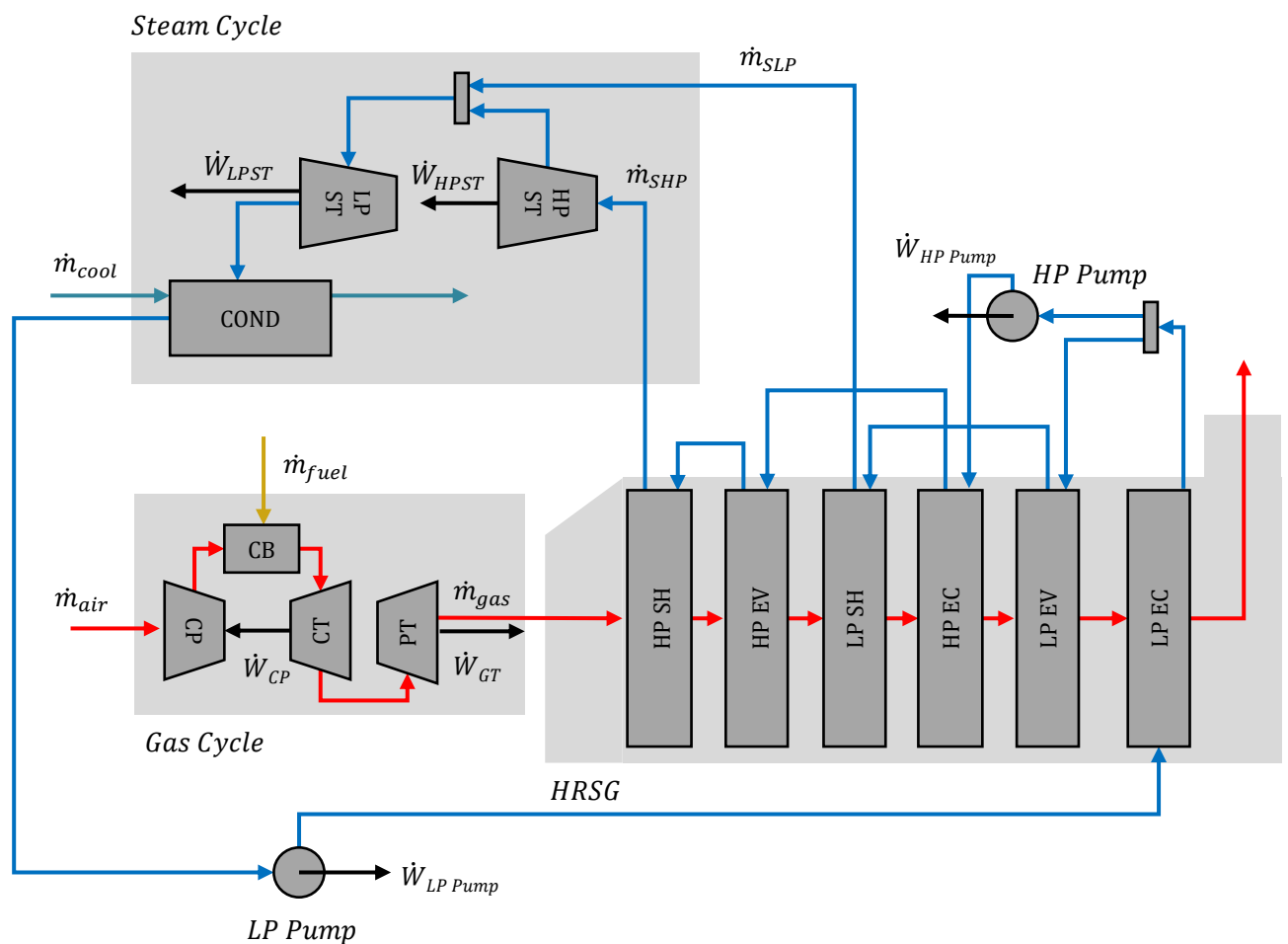
Figure 31 Two Pressure HRSG Simplified Layout
Source: Elaborated by Author

In this case, there is a steam turbine for each pressure level. The high-pressure steam turbine receives the live steam from the HRSG and expands down to the low-pressure level. At this point the high-pressure stream is mixed with the stream coming from the low-pressure super-heater, to enter the second turbine, and finally expanding to the condenser operational pressure

$$\left[\dot{Q}_{ec,ev,sh} = \dot{m}_{gas}C_p(T_{in} - T_{out}) = \dot{m}_{water/steam}(h_{out} - h_{in})\right]_{LP,HP} \tag{10}$$

$$\dot{W}_{LPST} = \dot{m}_{SHP}(h_{2shH} - h_{2shL}) \tag{11}$$

$$\dot{W}_{HPST} = (\dot{m}_{SHP} - \dot{m}_{SLP})(h_{2shL} - h_{cond}) \tag{12}$$

$$\dot{W}_{ST} = \dot{W}_{LPST} + \dot{W}_{HPST} \tag{13}$$
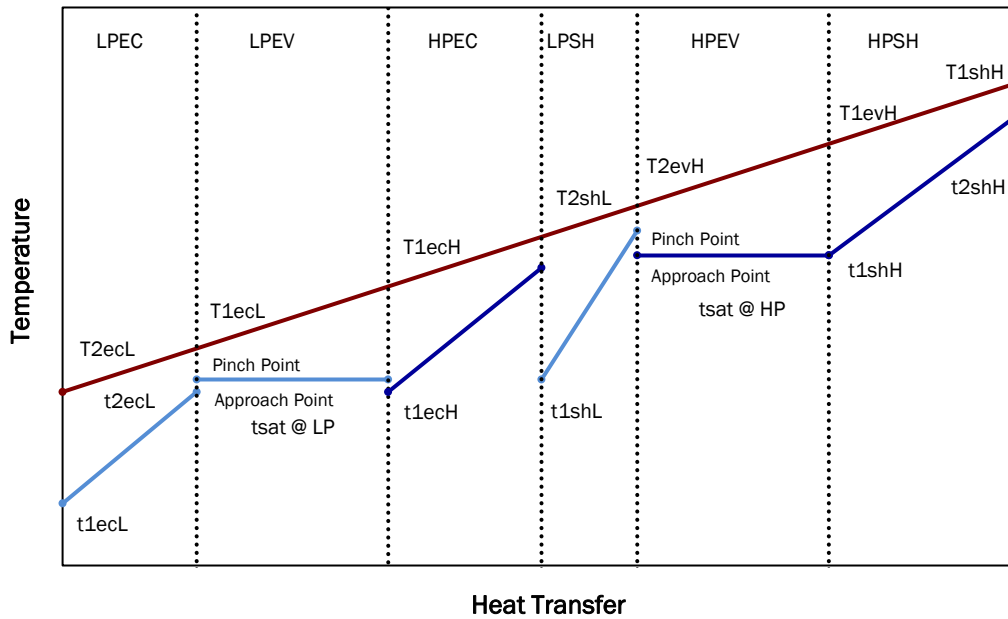
Figure 32 Temperature profile two pressure levels
Source: Elaborated by author

5.2.3 Exergy and Energy efficiencies

Reduced fuel consumption and carbon dioxide emissions are closely related to increased efficiency of the combined cycle. The introduction of a bottoming cycle may increase efficiency up to 53~54%, as it is commonly seen in onshore power plants. Efficiency for simple cycle gas turbines is around 34~37%, particularly in offshore

applications this efficiency is reduced due to constant off-design operation. Energy efficiency will be evaluated as follows:

$$\dot{W}_{CC} = \Sigma\dot{W}_{GT} + \Sigma\dot{W}_{ST} - \Sigma\dot{W}_{AUX} \tag{14}$$

$$\eta_{cc} = \frac{\dot{W}_{CC}}{(\Sigma\dot{m}_f)LHV_f} \tag{15}$$

From an exergetic point of view, the maximum available capacity for the bottoming cycle is given by the exergy of the exhaust gases, as seen in Gülen et al (2012). Exergy performance of the bottoming cycle can be analyzed through Eqs. 13 and 14.

$$W_{BT,max} = e_4 = c_p(T_4 - T_1) - T_1 c_p \ln\left(\frac{T_4}{T_1}\right) \tag{16}$$

$$\varepsilon_{BT} = \frac{W_{BT}}{W_{BT,max}} \tag{17}$$

Where, $w_{BT,max}$ is the maximum theoretical obtained work. The subscript BT refers to the Bottoming Cycle, all values on Eq. 8 are referred to thermodynamic states in the gas turbine. ε_{BT} is the exergetic efficiency, and w_{BT} is the actual delivered work.

5.3 Weight and Dimensions Analysis

The offshore power hub should be located in a floating facility. Excessive space and weight needs have an impact on overall investment costs, as hull construction expenses may arise, compromising the project cost-effectiveness. Even though power hub would be dedicated to allocate the power island, space should be optimized to reduce investments for floating square meter requirements. This situation generates a tradeoff among costs, weight and efficiency. In order to study this tradeoff, dimensional estimations were carried out, as specified in the following sections.

5.3.1 Gas Turbine and Generator

It is common for gas turbine producers to offer packaged products for specific applications. In offshore facilities gas turbines are delivered as closed compact modules for better installation and maintenance. Power generation modules are coupled with a generator depending on the specific requirements. When selecting from one of the pre-established gas turbines, their associated dimensions and weight are addressed by their own manufacturer. Approximate values are supplied in Table 8.

Gas turbine weight is a very uncertain factor, as it is related with several auxiliary systems that may be installed or not in the gas turbine module, such as control systems and electric generator, depending on its application. The same gas turbine model can have different weights if it is used as a mechanical drive or to generate electricity. A correlation was established to assess this value, when dealing with a continuous gas turbine design, instead of a pre-selected gas turbine. A set of commercial gas turbines and their weights were assessed and aspects such as compact design, power generation, marine applications, combined cycle applications were considered to create the chart seen in Figure 33.

Table 8 Dimensions and weights for selected GT models

GT Model	Weight (tons)	Dimensions (m)		
		Length	Width	Height
GE LM2500	90,00	13,94	2,64	3,98
GE LM6000	136,98	16,51	4,31	4,91
SGT-700	169,00	19,00	5,00	4,00
SGT-800	320,00	20,00	5,00	15,00

Source: Manufacturer data
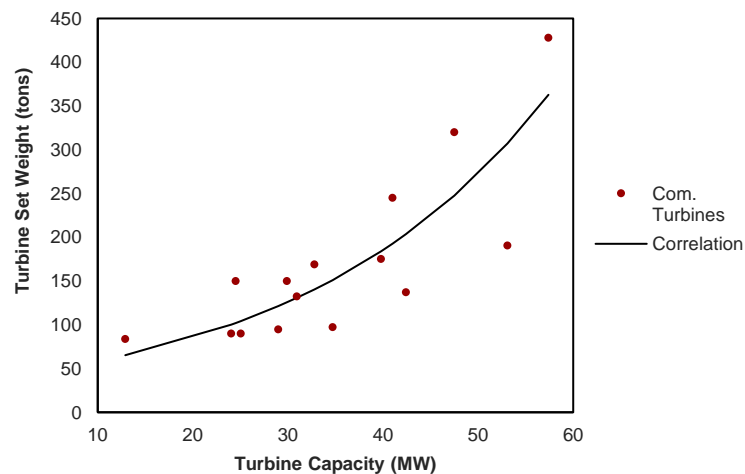
Figure 33 GT Weight correlation
Source: Manufacturer data and author

The turbines models selected to create the correlation (18) were carefully selected to maintain uniformity of design criteria, this correlation results in a R^2 value of 0,7755. Rivera-Alvarez et al (2015) generated a correlation using public data of a gas turbine group, however, the results are adequate for turbines below 25 MW and does not account for the electricity generator. For this work, all selected gas turbines are compact versions of their corresponding model and include their respective electricity generator. The correlation is based on the ISO condition net power of the gas turbine. Even though other variables such as mass flow or efficiency may affect gas turbine weight, a detailed analysis of the gas turbine weight is out of the scope of this thesis.

$$M_{GT} = 39660 \, e^{W_{GT}3,856 \times 10^{-5}} \tag{18}$$

5.3.2 Heat Transfer Equipment

Further heat transfer calculations need to be performed on the HRSG and condenser to evaluate their size and weight. Both equipment will be analyzed through the overall heat transfer coefficient. Once the HRSG dimensional structure is settled, that is, number of tubes, fins, height, width among other important magnitudes, an iterative procedure is realized, by calculating the pressure drops both in gas and steam sides and rejecting the solutions giving excessive pressure drop values.

Heat Recovery Steam Generators

Every section of the HRSGs will be evaluated under the same methodology. A bundle of finned tubes disposed vertically will conform each section. The air will flow horizontally through the tube bundle. All sections will be contained in an enclosure with continuous height and width. An example of the tube bundle with the most important dimensions is shown in Figure 34 and Figure 35. Dimension values cannot be assumed arbitrarily, as there is a strict trade-off among size, heat transfer and costs. Dimensions to

be evaluated are similar for each section of the HRSG. Subscripts mentioned previously distinguish among the dimensioning variables. Main dimensioning variables are stated in Table 9.

Table 9 HRSG variable sizing parameters

Symbol	Name
N_r	Number of tubes rows
N_t	Number of tubes per row
L_f	Length of finned tube
P_t	Transversal pitch
P_l	Longitudinal pitch
d_i	Internal tube diameter
d_o	External tube diameter
n_f	Fin spacing
l_f	Fin length
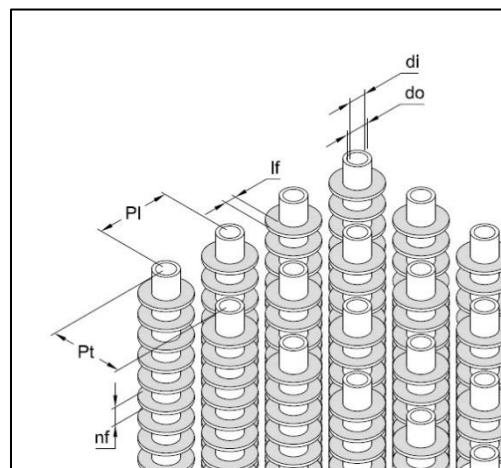
Figure 34 Detailed view and dimensions of tube bundle
Source: Elaborated by author

The overall heat transfer coefficient method is applied to determine heat transfer areas in each HRSG section, as seen in the following equations. An inline arrangement with plain fins is considered to calculate the heat transfer coefficient (HTC), adapting the methodology applied by Dumont and Heyen (2004), in which the HTC is a function of several parameters as seen in Eq. (20)

$$\frac{1}{U_o} = \frac{1}{h_o} + R_w + \left(\frac{1}{h_i} + R_{fi}\right)\left(\frac{A_o}{A}\right) \tag{19}$$

$$h_o = f(J, E, d_{f,o}, h_c) \tag{20}$$
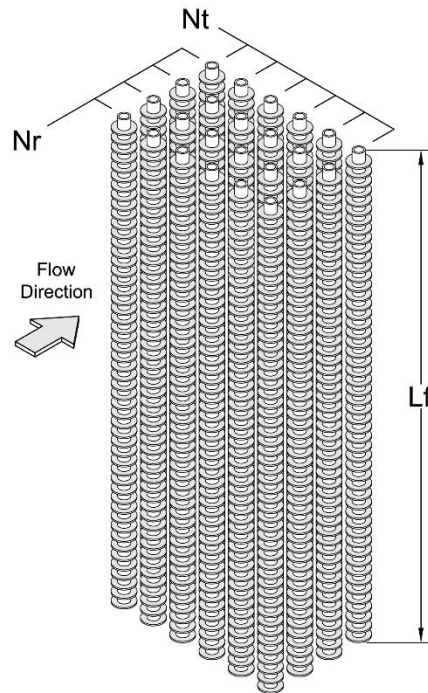
Figure 35 Tube bundle example
Source: Elaborated by author

This last method is based on the outside heat transfer area. The outside heat transfer coefficient is a function of the Colburn Factor, outer diameter and fin diameter, the gases properties and a term including the efficiency of heat transfer in fins. This methodology was developed specially for finned tubes in heat recovery steam generators by ESCOA (1979) and adapted by Dumont et al. (2004). A sequence of areas calculation must be carried out to determine the total available area through the finned tubes, as seen in Eqs. (21) to (25).

$$A_{po} = \pi d_o (1 - n_f t_f) \tag{21}$$

$$A_o = \pi d_o (1 - n_f t_f) + \pi n_f [2l_f(d_o + l_f) + t_f(d_o + 2l_f)] \tag{22}$$

$$A_{fo} = A_o - A_{po} \tag{23}$$

$$A_c = d_o - 2l_f t_f n_f \tag{24}$$

$$A_n = A_d - A_c L_f N_t \tag{25}$$

Once the cross-sectional area is determined, the calculation of the outside flow heat transfer coefficient can be performed. The mass velocity and the Reynolds number of the flue gases are determined in Eqs. (26) and (27). Afterwards, a series of non-dimensional factors must be calculated in order to determine the Colburn Factor in Eq. (31).

$$G_n = m_{gas}/A_n \tag{26}$$

$$Re = G_n d_o/\mu_b \tag{27}$$

$$C_1 = 0{,}25 Re^{-0{,}35} \tag{28}$$

$$C_3 = 0{,}20 + 0{,}65 e^{(-0{,}25 l_f/s_f)} \tag{29}$$

$$C_5 = 1{,}1 - [0{,}75 - 1{,}5 e^{(-0{,}70\,N_r)}]\left[e^{(-2{,}0 P_l/P_t)}\right] \tag{30}$$

$$J = C_1 C_3 C_5 (d_f/d_o)^{0{,}5}[(T_b + 460)/(T_s + 460)]^{0{,}25} \tag{31}$$

The Colburn factor allows calculating an initial heat transfer coefficient for the flue gases in Eqs. (32) and (33), it must be noted that the radiation contribution on the heat transfer coefficient calculation (h_r) is negligible. This initial value must be corrected through a fin effectiveness factor (E).

$$h_c = J G_n c_p (k_b/c_p \mu_b)^{0{,}67} \tag{32}$$

$$h_o = 1/[(1/(h_c + h_r)) + R_{fo}] \tag{33}$$

The initial methodology to calculate the fin effectiveness factor was based in graphic solutions. Values were obtained through joining lines in a nomograph. However, a numerical approximation of this method in Eqs. (34) to (37).

$$b = l_f + (t_f/2) \tag{34}$$

$$m = [h_o(t_f + w_s)/(6 k_f t_f w_s)]^{0{,}5} \tag{35}$$

$$X = (\tanh mb)/mb \tag{36}$$

$$E = X(0,9 + 0,1X) \tag{37}$$

After performing the aforementioned calculation, the thermal resistance of the fluid flowing outside the tubes can be defined in Eq.(39).Thermal resistance due to wall material is calculated in Eq.(40).

$$h_e = h_o(EA_{fo} + A_{po})/A_o \tag{38}$$

$$R_o = 1/h_e \tag{39}$$

$$R_{wo} = (t_w/k_w)(A_o/A_w) \tag{40}$$

Heat transfer coefficient for fully developed turbulent flows inside the tubes, that is water and steam, is determined according to the correlations proposed by Gnielinski (2013), displayed in Eq. (42).

$$f = 1/\sqrt{1.8 * \log(Re) - 1,5} \tag{41}$$

$$Nu = [(f/8) * (Re - 1000) * Pr] \tag{42}$$
$$/\left[1 + 12.7 * \sqrt{(f/8)} * (Pr^{2/3} - 1)\right]$$

$$h_i = Nu * k_i/d_i \tag{43}$$

$$R_{io} = ((1/h_i) + R_{fi}) * (A_o/A_i) \tag{44}$$

Finally, the overall heat transfer coefficient is calculated through the sum of the thermal resistances, Eq. (45) and (46). Using the temperature profile previously calculated with the application of the pinch point and the thermodynamic equilibrium in each section, it is possible to calculate the total heat transfer area for each HRSG section.

$$R_{to} = R_o + R_{wo} + R_{io} \tag{45}$$

$$U_o = 1/R_{to} \tag{46}$$

$$\left[U_o A_o = \frac{Q}{LMTD}\right]_{EC,EV,SH} \tag{47}$$

$$A_{HRSG} = \sum \frac{Q_{EC}}{U_{EC}LMTD_{EC}} + \sum \frac{Q_{EV}}{U_{EV}LMTD_{EV}} + \sum \frac{Q_{SH}}{U_{SH}LMTD_{SH}} \tag{48}$$

The geometry proposed according to the steps above is valid only if the pressure drops are between established limits. Excessive pressure drops for the flue gases affect gas turbine performance, diminishing its power output as a result of restrictions in the expansion process. In a similar way, excessive pressure losses on the steam side diminishes energy drop in the steam turbine expansion.

Pressure drop is calculated according to the same methodology derived by ESCOA (1979), detailed in Eqs. (49) to (56).

$$C_2 = 0,07 + 8,0Re^{-0,45} \tag{49}$$

$$C_4 = 0,11[0,05\,P_t/d_o]^{[-0,7(l_f/s_f)^{0,2}]} \tag{50}$$

$$C_6 = 1,1 + \left[1,8 - 2,1e^{(-0,15N_r{}^2)}\right]\left[e^{(-2,0P_l/P_t)}\right] - [0,7 \tag{51}$$
$$- 0,8e^{(-0,15N_r{}^2)}]\left[e^{(-0,6P_l/P_t)}\right]$$

$$\beta^2 = (A_n/A_d)^2 \tag{52}$$

$$a = [(1 + \beta^2)/4N_r]\rho_b[(1/\rho_2) - (1/\rho_1)] \tag{53}$$

$$f = C_2C_4C_6(d_f/d_o) \tag{54}$$

$$\Delta P_{gas} = (f + a)G_n{}^2N_r/\rho_b \tag{55}$$

$$\Delta P_{water/steam} = (f\rho u^2)\left(N_rL_f/2d_i\right) \tag{56}$$

Condenser

The condenser is assumed to be of shell-tube type, in which the cooling fluid would be treated seawater, and the operational pressure would be a decision variable set by the optimization procedure. For the condenser case it is estimated that the total weight would

be governed by the piping installed in it, by establishing a fixed overall heat transfer coefficient.

5.3.3 Steam Cycle Components

Dimensional properties of three main components of the steam cycle were analyzed: steam turbine, electric generator and condenser. Haug (2016) carried out a very complete study for several weight and volume estimating methods. Particularly, the steam turbine weight is estimated to be proportional to the steam mass flow passing through it. A specific weight estimation is project dependent and relies on the features of each model and manufacturer. Following empirical authors suggestions that 30% of the combined cycle power comes from steam generation, power generated by the steam turbine is expected to be between 7 MW and 30 MW (considering for example between 25 and 90 MW in GTs). For these cases, the electricity generator may be heavier than the steam turbine itself. By performing a study of the several proposed correlations, it is found that the best fit for the steam turbine-generator set is obtained through equations (57) by Rivera-Alvarez et al (2015) and (58) by Haug (2016). The constant k_{st} is estimated between 202 and 238 kg/(kg/s)$^{3/2}$ and $M_{ST,0}$ between 654 and 2641 kg.

$$M_{ST} = k_{st}(\dot{m}_w)^{3/2} + M_{ST,0} \tag{57}$$

$$M_{GEN} = 0{,}835(\dot{m}_w) + 12{,}034 \tag{58}$$

HRSG plays an important role when determining cycle dimensions such as size and weight. HRSG and the steam cycle in general are more likely to be tailored equipment, instead of packaged catalogue products. HRSG weight, size and efficiency has been subject of several studies trying to improve and optimize its performance.

$$M_{HRSG} = k_{HRSG}(A_{HRSG}) + M_{HRSG,0} \tag{59}$$

Rivera-Alvarez et al (2015) demonstrates that an important and predictable part of HRSGs weight consists in the share occupied by piping. By determining the quantity of tubes and fins composing each section, a rough weight estimation can be calculated. When comparing piping weight with equations provided by the previously mentioned author, it is possible to note that the correlation derives in higher weight values, accounting for additional factors, like casing and drums weight. Hence, the correlation in Eq. (59) used to estimate a more precise weight of the HRSG. Constant values are between 8,5-9,5 kg/m2 for k_HRSG and 520 and 4650 kg for M_(HRSG,0).

5.3.4 Volumetric considerations

An optimized arrangement for the power hub must also consider the space that it requires to operate in an offshore vessel. In this matter, the concept of footprint and volume need to be introduced in the optimization to obtain more compact solutions. However, both footprint and space are very project dependent values, and they are related to specific engineering design of each component. In this case, the volume required for the combined cycle is established by the largest components, namely the Heat Recovery Steam Generator and the gas turbines.
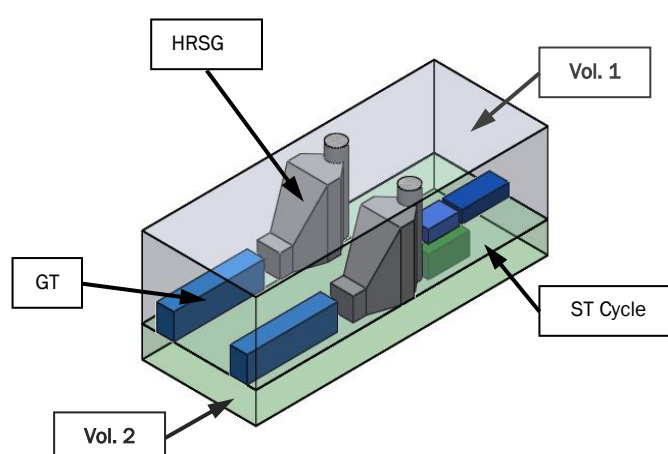
Figure 36 Combined Cycle Volumes
Source: Elaborated by author

An example of the required volume for a Combined Cycle block can be seen in Figure 36. In this example, the combined cycle is composed by two gas turbines coupled

to two HRSGs. The steam cycle is composed by one steam turbine and one condenser. Other equipment such as piping and bombs are not considered for the volumetric analysis due to the smaller space that they would require. To illustrate the block space demand, the combined cycle in Figure 36 is enclosed in two larger volumes, namely volume 1 and volume 2. Assuming that the gas turbines, steam generators and steam turbines would be on the deck enclosed by volume 1, and the condenser, pump and further equipment would be below the main deck, enclosed by volume 2.

$$L_{block} = L_{GT} + L_{HRSG} + (L_{ST} + L_{GEN}) + Clearances \qquad (60)$$

$$W_{block} = N * W_{HRSG} + Clearances \, / \, N * W_{GT} + Clearances \qquad (61)$$

$$H_{block} = H_{HRSG} + Clearances \qquad (62)$$

Preceding equations illustrate the approximate calculation of volume no.1 located on the upper deck. Width varies depending on the HRSG quantity. If just one HRSG is installed in the block, width is dependent on the gas turbine dimensions, Eqs. (60) to (62) considers both cases.

5.4   Off-design Analysis

The operation of gas turbines in offshore oil and gas industry is highly dependent on the properties of fluids being produced. Power generation is subject to sudden changes if unexpected pressure variations occur during the oil and gas extraction. Over time, power requirements also change, inducing large periods of operation. Thus, the off-design performance is a key aspect when considering alternatives to improve performance in offshore operations.

For the power island concept, larger scale concentrated power equipment response to power demand fluctuations would not be as harmful for off-design performance, as in smaller scale localized gas turbines. By gathering all power demands and supply through a concentrated power island, it is expected that combined cycle generation groups would not reach extremely low part-load operations.

5.4.1 Gas Turbine

Operating gas turbines at part-loads will affect efficiency and performance downstream of the combined cycle. This is due to changes in heat capacity of exhaust gases. As stated for the design process, main parameters to be observed during part load of gas turbines are: exhaust gases mass flow and temperature, net power output and fuel consumption. Each approach for Gas Turbine selection (continuous and discrete analyses) has its own part-load calculation procedure. For commercially available gas turbines modeled in The   ulations at different load co
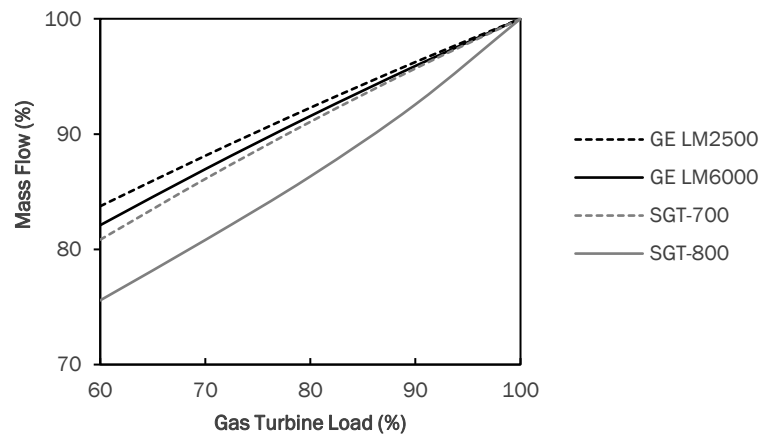
Figure 37 Mass flow part load performance
Source: Author based on Thermoflex data

Figure 37 to Figure 39 show how mass flow, fuel consumption and exhaust temperature perform over part load conditions. This information is introduced in the calculation as input for the part load performance of the heat recovery steam generator and steam cycle. The difference of single and double shaft gas turbines performances noticeable in the exhaust gases temperature. Unlike the other gas turbines, SGT-800 is a single shaft mode and it shows a negative curve slope for this parameter.
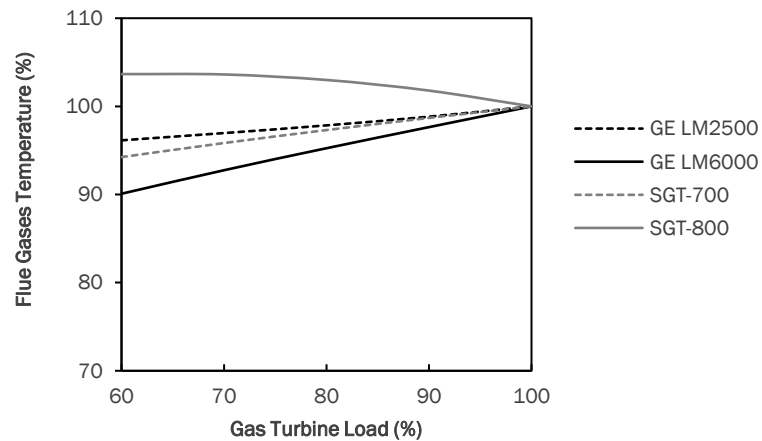
Figure 38 Flue gases temperature at part load
Source: Author based on Thermoflex data
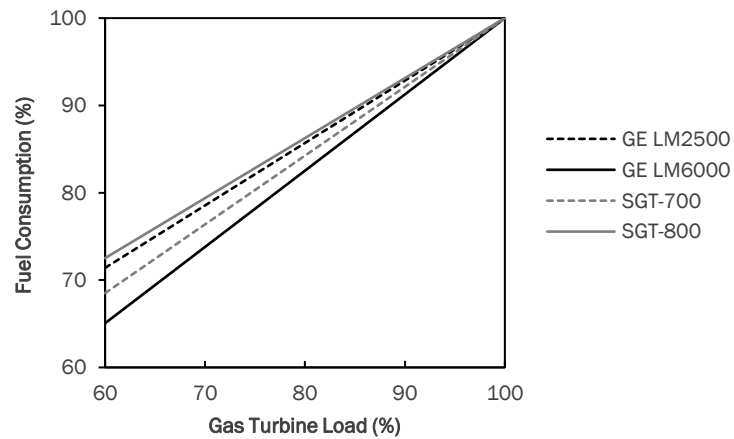
Figure 39 Fuel Consumption at part load
Source: Author based on Thermoflex data

In contrast with the previously described procedure, part-load calculation for the discrete analysis approach must start from the parameters obtained for the gas turbine design point. In this case, the gas turbine is not a commercial device, thus, manufacturer data is not available. The methodology outlined in this section is based on the simple model developed by Haglind and Elmegaard (2009). In order to calculate the part-load performance of a designed turbine, several considerations must be established.

- Gas cycle arrangement is based on the design criteria aforementioned; the gas turbine consist on a double shaft configuration, having a compressor, combustor, compressor turbine and power turbine.

- Flow control strategies such as variable inlet guide vanes for the compressor (VIGV) or variable area nozzles for the turbines (VAN) are not simulated. For calculation purposes, static geometry of both compressor and turbine is considered.

- Pressure losses along the mass flow path and mass flow bleeds will be considered as negligible. Combustion efficiency is established at $\eta_{CB} = 0,99$.

- Since the arrangement consist in two turbines in series, there must be flow and pressure compatibility between them. This poses an operational restriction on the pressure ratio of the compressor turbine. Particularly, in this restricted operational range, the variation of the isentropic turbine efficiency can often be assumed as constant. To maintain a suitable calculation procedure for this study, both compressor and turbine isentropic efficiencies will be assumed as constants. A deeper analysis of the turbine and compressor efficiencies is out of the scope of this study.

Charts and curves representing parameters of gas and compressors are often used to determine part load performances. In this case, the previously stated considerations will substitute the use of such method. However, as an example, curves are shown to represent the theoretical bases of the methodology applied in Figure 40. As the isentropic turbine efficiency is kept constant, the non-dimensional mass flow entering the power turbine $(m\sqrt{T_4}/p_4)$ becomes a function of the compressor turbine pressure ratio (p_3/p_4) and its non-dimensional mass flow $(m\sqrt{T_3}/p_3)$, according to the equations below.

$$\frac{m\sqrt{T_4}}{p_4} = \frac{m\sqrt{T_3}}{p_3}\frac{p_3}{p_4}\sqrt{\frac{T_4}{T_3}}$$

(63)

$$\frac{p_4}{p_a} = \frac{p_2}{p_1} \times \frac{p_3}{p_2} \times \frac{p_4}{p_3}$$

(64)

When the turbine swallowing capacity has reaches is limit, the curve slope tends to zero. This is an indication that the turbine has choked. Thus, an increase in pressure ratio will not produce any further significant increase on the non-dimensional mass flow. If the power turbine is choked, then the compressor turbine is constrained to operate at a fixed non-dimensional point, as seen in point (b) of the preceding figure, (SARAVANAMUTTOO et al., 2009)

Compressor Turbine   Power Turbine
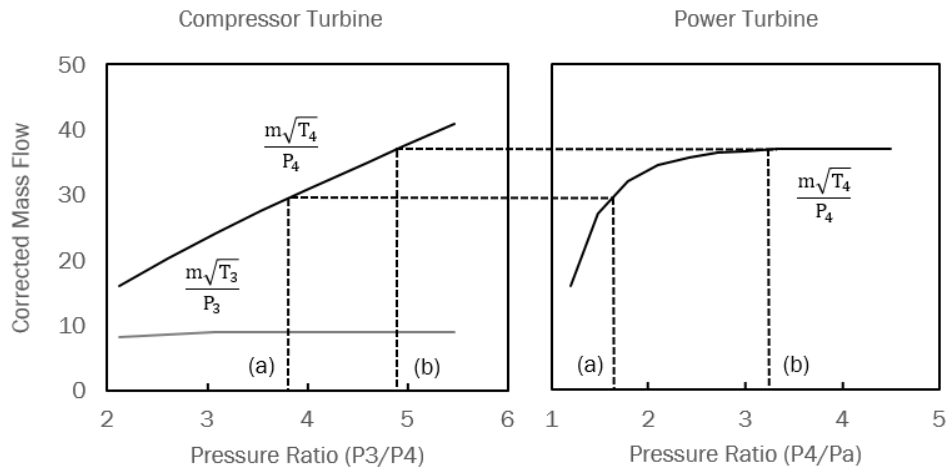
Figure 40 Compressor Turbine and Power Turbine Example Curves
Source: Author based on Saravanamuttoo (2009)
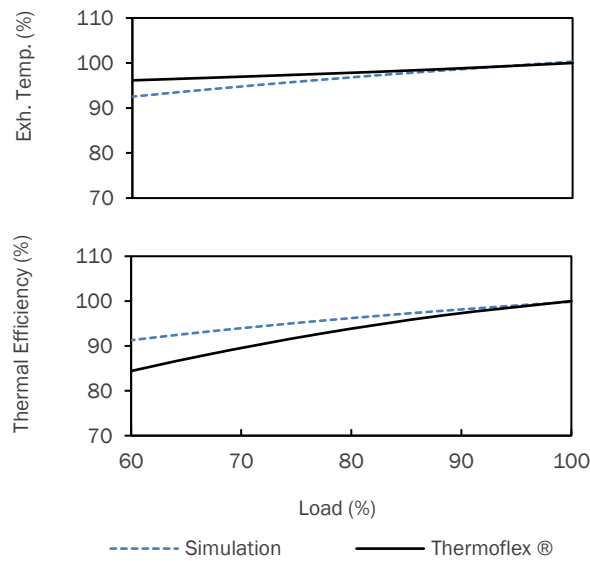
Figure 41 Simulation for LM2500
Source: Author and Thermoflex data

This method was structured to optimize the gas turbine design and off-design parameters. As a validation example, it was also applied to calculate the part load performance of three selected commercial gas turbines: LM2500, LM6000 and SGT-700, (Figure 41 to Figure 43) Turbine model SGT-800 part-load was not calculated because the formulated structure not compatible with single-shaft units
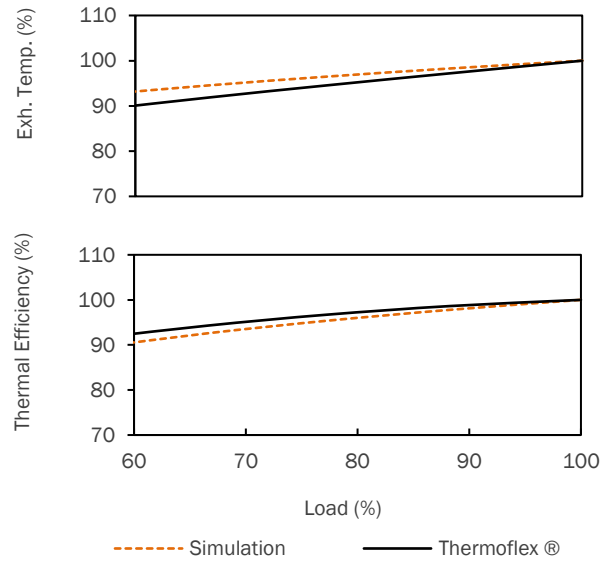
Figure 42 Simulation for LM6000
Source: Author and Thermoflex data
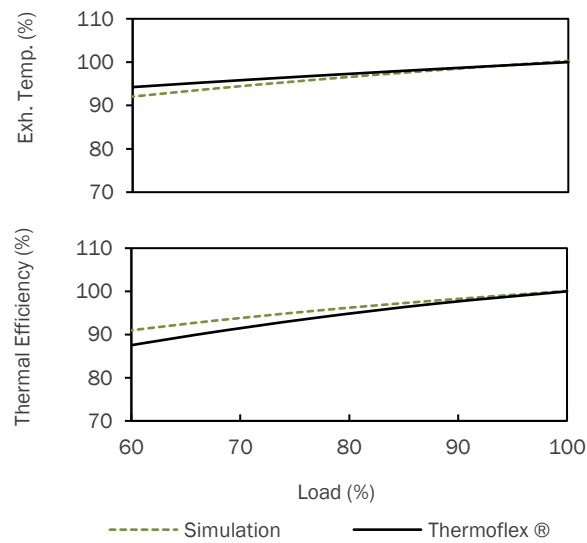
Figure 43 Simulation for SGT-700
Source: Author and Thermoflex data

5.4.2 Heat Recovery Steam Generator and Steam Cycle

The overall heat transfer coefficient approach is implemented to calculate the HRSG off-design performance, as denoted by and Ganapathy (2003) and Knopf (2012).

The HTC and heat transfer areas were calculated for the economizer, evaporator and super heater in the design point analysis. Those values are corrected applying a factor related to the variations of the gas turbine exhaust gases, as shown in Eq. (65).

$$\text{Correction Factor} = \frac{(m_{g\_des})^{0,6}}{(m_{g\_off})^{0,6}} \frac{\left(\dfrac{k^{0,7}C_P^{0,3}}{\mu^{0,3}}\right)_{des}}{\left(\dfrac{k^{0,7}C_P^{0,3}}{\mu^{0,3}}\right)_{off}} \tag{65}$$

Assuming a relatively small influence of the gas properties, the equation system can be simplified as seen in the Equations (66) to (70).

$$(UA)_{ec\_off} = (UA)_{ec} \frac{(m_g)^{0,6}}{(m_{g\_off})^{0,6}} \tag{66}$$

$$(UA)_{ev\_off} = (UA)_{ev} \frac{(m_g)^{0,6}}{(m_{g\_off})^{0,6}} \tag{67}$$

$$(UA)_{sh\_off} = (UA)_{sh} \frac{(m_g)^{0,6}}{(m_{g\_off})^{0,6}} \tag{68}$$

Off-design analysis of the steam turbine is carried out through the Stodola's Cone Law, (STODOLA, 1922). Correlating the off-design and design properties through a turbine constant, as seen in and Eq. (70).

$$\frac{\dot{m}_{w\_off}}{\dot{m}_w} = \frac{P}{P_{off}} \sqrt{\frac{T_{in\_off}}{T_{in}}} \tag{69}$$

$$CT = \dot{m}_w \frac{P}{\sqrt{T_{in}}} \tag{70}$$

Stodola's Law and Ganapathy's methodology for HRSG off-design create an equation system, which resolution is a set of variables that determine the combined cycle off-design behavior. Steam turbine performance is directly related to gas turbine load. Nevertheless, some operation artifices may vary the steam turbine behavior and avoid some undesirable operational situations. The model considers a sliding pressure

regulation, in which pressure, mass flow and power output decrease proportionally. Which means that a pressure regulating valve at the steam turbine entrance is not needed.

5.5   Model Validation

The calculation structure presented so far allows running a preliminary optimization in order to verify model consistencies and accuracy. A double pressure HRSG arrangement is optimized, taking the combined cycle thermal efficiency as a single minimizing objective. Thermoflex is employed to carry out the validation process against the model developed in this thesis. The combined cycle sections are configured in an analogous way, as seen in Figure 44. This software simulates the thermodynamic phenomena, according to the obtained parameters, such as Pinch Point and efficiencies defining the equipment. Additionally, it is possible to introduce the optimized dimensions for the HRSG, namely, the number of tubes, lengths, diameters, fin characteristics and so on. to further determine the impact of these physical properties in the model.
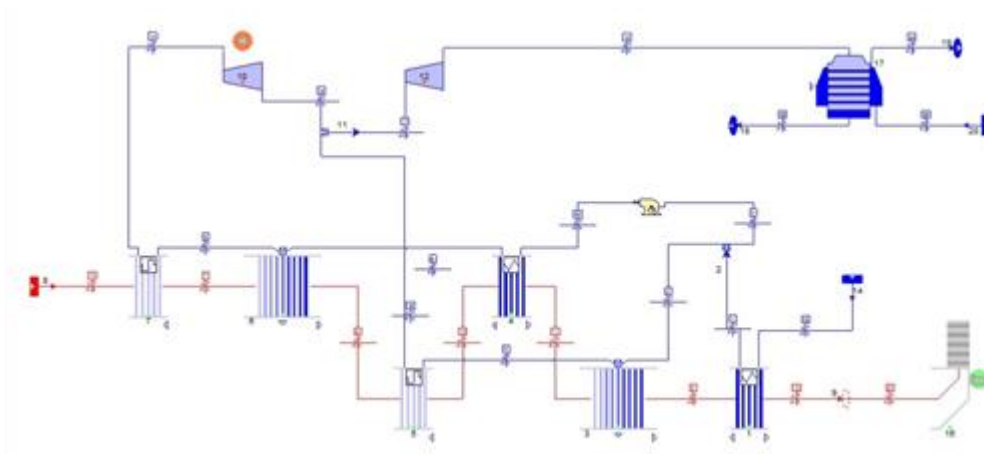
Figure 44 Thermoflex 2P Validation Model
Source: Author and Thermoflex data

A Steam Cycle assembly contains both Steam Turbine and HRSG sub-assemblies. Each input and output have a parameter node, which contains temperature, pressure, enthalpy and mass flow data. Table 10 shows important parameters for the design point, such as total power output, which is the sum of both high-pressure and low-pressure steam turbines results, yielding an error of 0,68%. Table 11 and Table 12 display a comparison between both the calculated model and Thermoflex temperature profiles, i.e. temperature

in each node, for the design condition. The temperature profile comparison yields very low error levels, ranging 0,66 and -0,58%.

Table 10 Main parameters comparison

Parameter	Model	Thermoflex
Steam Turbine Power Output (MW)	11,03	10,96
Mass Flow HP (kg/s)	8,25	8,52
Mass Flow LP (kg/s)	2,08	2,04
High Pressure (bar)	79,91	78,67
Low Pressure (bar)	10,60	9,91
Steam Turbine Inlet Temperature (K)	749,32	742,40

Source: Author and Thermoflex data

Table 11 Exhaust Gases Temperature Profile Validation (K)

HP	T1shH	T2shH	T1evH	T2evH	T1ecH	T2ecH
Calc. Model	793,3	731,5	731,5	578,2	575,7	519,5
Tflex	793,3	735,8	735,8	576,5	574,2	517,3
Error (%)	0,00	-0,58	-0,58	0,29	0,27	0,43
LP	T1shL	T2shL	T1evL	T2evL	T1ecL	T2ecL
Model	578,2	575,7	519,5	465,7	465,7	383,6
Tflex	576,5	574,2	517,3	463,4	463,4	383,9
Error (%)	0,29	0,27	0,43	0,49	0,49	-0,08

Source: Author and Thermoflex data

Table 12 Water/Steam Temperature Profile Validation (K)

HP	t2shH	t1shH	t2evH	t1evH	t2ecH	t1ecH
Calc.Model	749,3	568,1	568,1	568,1	558,1	445,6
Tflex	742,4	567,0	567,0	567,0	553,1	439,7
Error (%)	0,93	0,19	0,19	0,19	0,90	1,34
LP	t2shL	t1shL	t2evL	t1evL	t2ecL	t1ecL
Model	492,2	455,6	455,6	455,6	445,6	300,0
Tflex	489,2	452,6	452,6	452,6	437,7	300,0
Error (%)	0,62	0,66	0,66	0,66	1,80	0,00

Source: Author and Thermoflex data

In general, results obtained above are between acceptable values of error, indicating an appropriate accuracy for the model in design conditions. For the off-design validation, gas turbine temperature and mass flow inputs range between 70% to 100%. These inputs are modified from the exhaust gases stream inlet. The HRSG dimensional parameters are left constant. Figure 45 displays both model and validation curves, along with the correspondent error in each load operation. Even though error values increase at lower part-load operations, it is still acceptable for the current application. Highest error value is of 1,75% at 70% load. Both curves remain very close for almost all the analyzed load range.
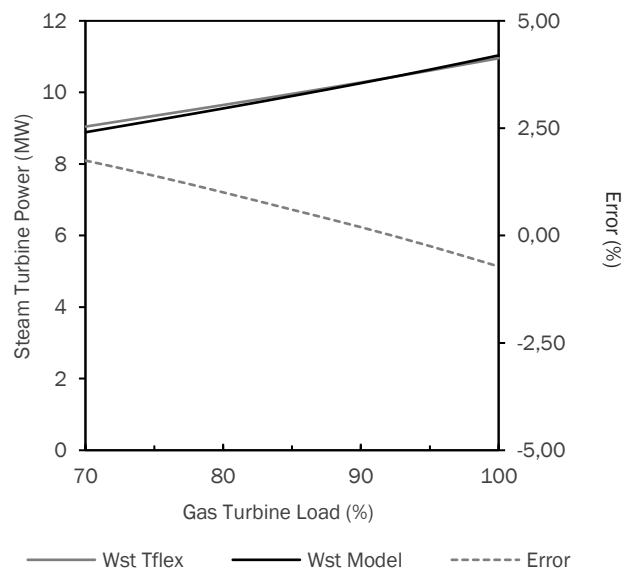
Figure 45 Steam Turbine Off-design validation
Source: Author and Thermoflex data

A comparison for the gas turbine model was performed in previous sections (see Figure 41 to Figure 43). It is necessary to note this comparison was based on three gas turbines available in Thermoflex libraries. Design parameters of efficiencies, pressure ratios and turbine inlet temperatures, needed to be estimated, which can cause deviation from the actual turbine performance. However, the overall results show acceptable error margins, especially for the range 70-100% load.

5.6   Economic Analysis

This section is devoted to estimate the economic performance of the power hub. Capital cost for the equipment purchase will be calculated, through correlations in which main inputs are thermodynamic or physical properties. More realistic forecasts can be observed when performing a VPN analysis. In this case, information respecting fuel consumption, fuel costs and fuel savings need to be included in the forecast. Power hub arrangements providing the highest values of VPN, are considered to be more cost-effective, and thus more likely to produce economical revenues and avoid economic losses.

5.6.1   Purchase Equipment Costs (PEC)

The first step to perform an economic forecast is estimating purchasing costs of equipment. For the single optimization approach, reference and updated costs of commercially available gas turbines are extracted from Thermoflex ®. These values were also verified through additional information research, such as manufacturers brochures and previous cost studies, as shown in Table 13.

Table 13 Gas Turbine Costs

Gas Turbine Model	Reference Cost (USD)	Updated Cost (USD)
GE LM 2500	14.807.310	15.547,680
GE LM 6000	19.248.110	20.210,510
SGT-700	14.028.630	14.730,060
SGT-800	17.248.400	18.110,820

Source: Thermoflex

On the other hand, cost estimation for sized equipment is performed by applying the correlations shown in equations (71) to (77). The correlation in (GAS TURBINE WORLD,

2016) provides an estimation for the gas turbine purchasing costs, according to the regular prices in the market.

$$C_{GT} = W_{GT}[(7.7 \times 10^3)\, W_{GT}^{-0.275}]$$ (71)

The following equations corresponds to the costs related to the steam turbine, HRSG, condenser, pumps, and generator, respectively. These correlations were formulated by Frangopoulos and updated by Carapellucci and Giordano (2013) and Roosen et al. (2003). All correlations result values in USD.

$$C_{ST} = 5075,5\, W_{ST}^{0,7}[1 + (0,05/1 - \eta_{ST})^3][1 + 5e^{(T_{ST\,in} - 866/10,42)}]$$ (72)

W_{ST}: Net Steam Turbine Power Output (kW), η_{ST}: Steam Turbine Isentropic efficiency, $T_{ST\,in}$: Live steam temperature (K).

$$C_{HRSG} = 5404,2\, \Sigma A + 17500,2\, \Sigma B$$ (73)
$$A = [0,097/(P/30) + 0,9][1 + e^{(Tstout - 830/500)}][1 + e^{(Tgout - 990/500)}(Q/\Delta TLM)^{0,8}]$$
$$B = [0,097/(P/30) + 0,9]m_{st} + 1948,4\, m_{gas}^{1,2}$$

P: Operating Pressure (MPa), $T_{ST\,out}$: Steam outlet temperature (K), $T_{G\,out}$: Gases outlet temperature (K). Q: Heat duty (kW). ΔTLM: Logarithmic Mean Temperature (K). m_{st}: Steam mass flow (kg/s). m_{gas}: Flue gases mass flow (kg/s).

$$C_{CD} = 248\, A_{CD} + 69\, m_{CW}$$ (74)

A_{CD}: Heat transfer area (m²), m_{CW}: cooling water mass flow (kg/s).

$$C_{PUMP} = 940 W_p^{0,71}[1 + (0,2/1 - \eta_P)]$$ (75)

W_p: Pump power input (kW), η_p: pump isentropic efficiency.

$$C_{GEN} = 4028,1 \; W_{ST}^{0,58} \tag{76}$$

W_{ST}: Steam Turbine Net Power Output (kW)

Purchase Equipment Costs (PEC) will be the sum of the resulting values of applying the aforementioned correlations. Each device cost is multiplied by the quantity established in the combined cycle block structure. For example, if the power hub is composed by two blocks of three gas turbines each and shared HRSG, the resulting breakdown will be 6 GT, 2 ST and 2 HRSGs. Gas turbine and Heat Recovery Unit quantities are determined by Mixed Integer Non-Linear Programming (MINLP). The block combined cycle structure and MINLP are resumed in Eq. (77). Indexes indicating quantities of equipment are similar as used in the total weight calculation.

$$C_{Total} = TQG \; (NTR \; C_{GT} + HXI \; C_{HRSG} + C_{ST}) \tag{77}$$

5.6.2 *Capital Costs*

Purchasing cost are the base indicator to carry out and economic analysis of a power plant, it is usually used to estimate further installation, engineering and commissioning costs. Bejan et al. (1995) present a methodology to estimate such costs by establishing ranges for diverse items in a cost breakdown. Table 14 was elaborated according to guidelines established by Bejan et al. (1995). However, these guidelines are generic, and some consideration must be made in order to relate these correlations to offshore equipment.

Total capital investment (TCI) is the sum of the fixed capital investment (FCI) and other outlays costs (OO). The most important share of the total capital investment is related to the Direct Costs (DC), which include the purchased-equipment costs, and the additional costs linked to installation and supplementary equipment. For a floating power hub, most equipment is installed in a module basis, instead of a single power plant block. Manufacturers build specific arrangements for compact gas and steam cycles, for use in offshore applications. Therefore, its installation and engineering costs may be reduced.

Additionally, other costs related to land use, construction and facilities are not considered, as the power plant would be installed directly in the hosting floating vessel.

Costs in piping are estimated as an average of the proposed range in Beján et al. (1995). This reference states that solid-fuel based power plants have less piping needs than liquid fuel based. However, it is expected that compact modules reduce the quantity of connections. Instrumentation, control and electrical equipment are also based on range averages, as advised in Beján et al. (1995), for this type of combined cycle.

For instrumentation and control, power plants costs range between 6% and 40% for a standard level of automation. An average of 23% of purchased equipment cost corresponds to medium-high automated power plants, which is the case of the current design, and the value to apply in the cost breakdown. A similar consideration applies to costs related to Electrical Equipment and Materials, in which average power plants range between 10% to 15%. An average value of 12.5% is considered for the current analysis, even though Beján et al. (1995) states that 11% is more frequent, it is possible that some additional electrical equipment may be included into the Combined Cycle to be more stable regarding tension and frequency.

Table **14** Approximate Cost Breakdown

Total Capital Investment	TCI
I. Fixed-capital investment	FCI
A. Direct costs	DC
1. Onsite Costs	ONSC
- Purchased-equipment cost	PEC (Calculated)
- Purchased-equipment installation	30% PEC
- Piping	25% PEC
- Instrumentation and controls	23% PEC
- Electrical equipment and materials	12.5% PEC
2. Offsite Costs	OFSC (N/A)
B. Indirect costs	IC
1. Engineering and supervision	6% DC
2. Construction costs including contractor's profit	10% DC
3. Contingencies	12% of B1 and B2
II. Other Outlays	OO
A. Startup costs	8.5% FCI
B. Working capital	10% TCI

Source: Author based on Beján cost structure

5.6.3 Offshore Costs

Hosting vessel

So far, cost have been calculated for combined cycle blocks. Even though this cost represents the largest share in overall Power Hub capital costs, there are further important considerations regarding maintenance, ancillary systems and staff facilities, to provide a more realistic cost estimation. All systems that compose the power hub must rely on a hosting vessel, which costs cannot be neglected. Weight and volume are crucial parameters to estimate the cost of a hosting vessel for the power hub. There are two different approaches for evaluating the ship structure and size, which will be the base for a cost estimation. A simple cost estimation is enough to fulfill the objectives of this study, as a deep analysis of the hosting vessel structure and cost is out of the scope.

Weight is a very important parameter to determine materials and dimensioning of the hosting vessel. However, there are many equipment with specific dimensions that must fit either in upside or downside main deck of the vessel, therefore a volumetric approach is more convenient to perform the hosting vessel cost estimation. The cost estimation methodology is based on Watson et al. (1998). Eq. (79) represents main design equation, and its details are presented below.

$$V_h = (V_r - V_u)/K_c \tag{78}$$

V_h: Hull Volume (m³). V_r: Total cargo capacity required (m³). V_u: Cargo capacity above the upper deck (m³). K_c: Ratio of cargo capacity below the upper deck, to the total moulded volume.

$$L = \left[\frac{V_h(L/B)^2(B/D)}{C_{bd}} \right]^{1/3} \tag{79}$$

L: Length (m), B: Breath (m), D: Depth (m). C_{bd}: Block coefficient at the moulded depth

The equation presented above determines the length according to some dimensional ratios, which are typical for each ship type, for this case, typical ratios (L/B) and (B/D) of oil tankers are selected, in accordance of Watson et al. (1998) guidelines. Section 2.3 addressed the calculation of the total volume of the ship below and above the deck, which depends on the combined cycle layout configuration. Besides of the combined cycle equipment, the upper deck section also contains two additional main spaces. A building to host the crew and staff working in the Power Hub and a space for an electricity transforming station. Gallo et al (2017) performed an energy analysis of a FPSO crew accommodation building, based on an approximate Brazilian FPSO layout design. Even though it is possible that the quantity of accommodation space required varies between an FPSO and the Power Hub, a good approximation is done by considering a similar volume of the FPSO accommodation building.

Regarding the space of the electricity transformation equipment, it varies depending on the type of transformation required in the offshore grid. If High Voltage Direct Current (HVDC) transformation is needed, there would be additional costs and volume required to perform such current transformation. The space occupied by a HVDC transformation station for offshore applications is estimated by ENTSO-E (2011). A 400 MW Voltage Source Converter (VSC) station, would measure 50 x 33.5 x 22 m and weight approximately 3300 t.

The total volume is then composed by the Combined Cycle equipment volume, the Accommodation Building volume and the Electricity Transformation Unit volume. By determining those magnitudes, it is possible to apply the ship design equation presented by Watson et al. (1998), in order to estimate ship dimensions. When ship dimensions are calculated, an approximate ship lightweight can be obtained, in the equation (80) according to Malla et al. (2014). Watson et al. (1998) presents a cost estimation through equation (81), which depends on the ship lightweight and steelwork. Reference prices are updated to 2017.

$$M_{ship} = C_b C_h LBD \tag{80}$$

$$C_{ship} = 1,69\, M_{ship}\left[-610,5\, Ln(M_{ship}) + 7850,5\right] \tag{81}$$

Grid Connections

This study proposes two grid connection scenarios for analysis. First scenario considers a closed grid composed solely by the Power Hub and FPSOs. Therefore, all electricity demand must be equal to the energy produced. In this case, connections between FPSOs and the Power Hub rely on submarine gas piping to transport produced gases to the combined cycle blocks in the power hub, and connection cables between the power hub and each FPSO for electricity supply. This configuration produces a small-scale electricity grid, where each FPSO is located approximately ten kilometers away from the Power Hub. A High Voltage Alternate Current (HVAC) configuration is convenient for grids with relatively small distances. However, in a closed grid, there would still be idle capacity at some point of the oil production life time.

A second scenario addresses this aspect, by including a long-range connection to the mainland through an High Voltage Direct Current transmission line (HVDC). Submarine HVDC cables would run an approximate 300 km distance to mainland. Power demand on the FPSOs remains the same. However, electricity production in the Power Hub would be more constant, as an important surplus could be sent to the main grid onshore. This could improve both economic and thermodynamic performance. Nevertheless, the inclusion of a HVDC transmission line and AC/DC transformers increases the capital costs. References of cost estimation for submersible cables and AC/DC converter station are found in ENTSO-E (2011), as presented in Table 15.
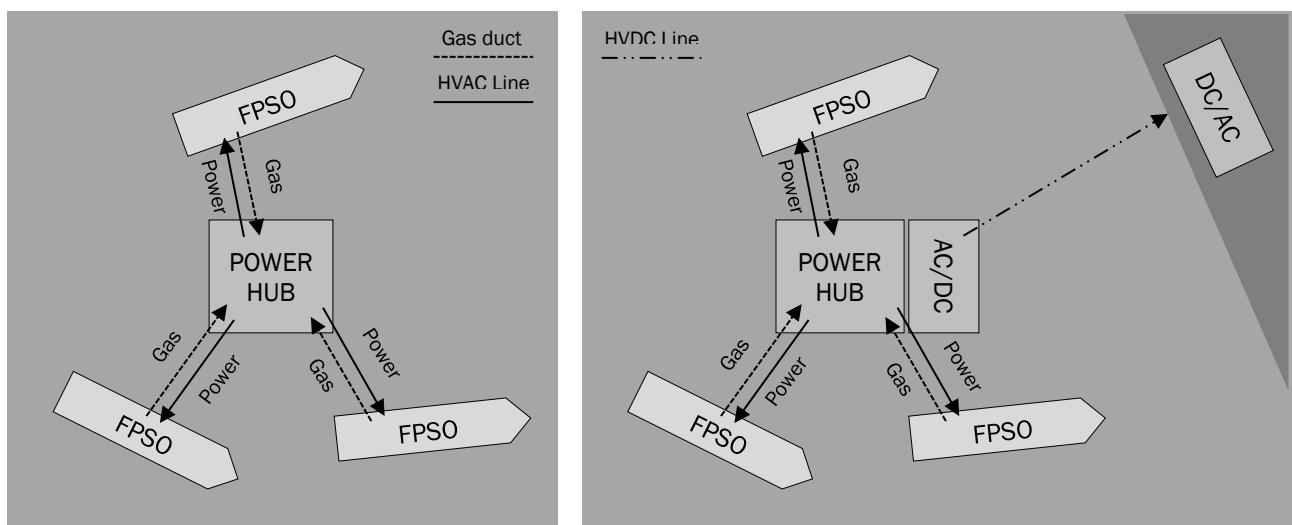
Figure 46 Grid Configurations - Isolated (left) - Onshore link (right)
Source: Elaborated by author

Table 15 Grid Connection Estimated Costs

Item	Closed Grid	Onshore Connection
Submarine Ducts	~2200 USD/m, ~35 km	
Submarine HVAC cables	~834 USD/m, ~35 km	
Submarine HVDC cables	N/A	~470 USD/m, ~300 km
AC/DC Transforming Station	N/A	~ 88 MM USD

Source: ENTSO-E (2011)

5.6.4 Reference scenario

One of the main drivers of exploring the concept of a floating power hub is to reduce fuel consumption. In this case fuel is considered to have no cost since it comes directly from the production well, and even in some specific production periods it could be reinjected. Nevertheless, using less fuel would be profitable to export the surplus production to more valuable uses, through submarine piping or Liquefied Natural Gas Carriers. Profits of installing such type of projects would rely on the opportunity cost of the associated gas, or electricity exports depending on the connection case. In order to calculate this quantity, it is necessary to compare a reference scenario against power-hub impacts in a year-to-year basis.

The reference scenario is a business-as-usual case in which the power generation remains isolated in each FPSO. Fuel consumption and CO_2 emissions (without considering flare and fugitive emissions) are divided in two main sources, turbo generators which are part of the power supply module, and turbo compressors which energize the CO_2 compression train. CO_2 emissions related to power supply either mechanical drive or electricity, are directly related to fuel consumption, so it is feasible to assume that a reduction of fuel consumption derives in a proportional CO_2 emission decrease.

Figure 47 depicts both CO_2 emissions and fuel consumption variations over time. Since CO_2 emissions considered in this analysis are produced by gas turbine combustion, they are proportional to fuel consumption. Then, the distinction between values in the figure is established through different axes. In the case of Turbo-Generators, emissions and consumption characteristics have a close relation with the Electric Demand curve, shown in the first part of this chapter. Turbo-Compressors demand is more related to production characteristics and associated gas composition. The present study considers

three FPSOs connected to the Power Hub, with a gap of two years in each start of operations, therefore, as performed in the electricity demand, total consumption/emissions is extended over a time frame of 25 years. Operational costs saving, related to diminishing fuel consumption, is given by Eq. (82), in which, for a specific year of the timeline, saved gas is equal to the reference scenario consumption, minus the consumption considering the installation of the Power Hub.
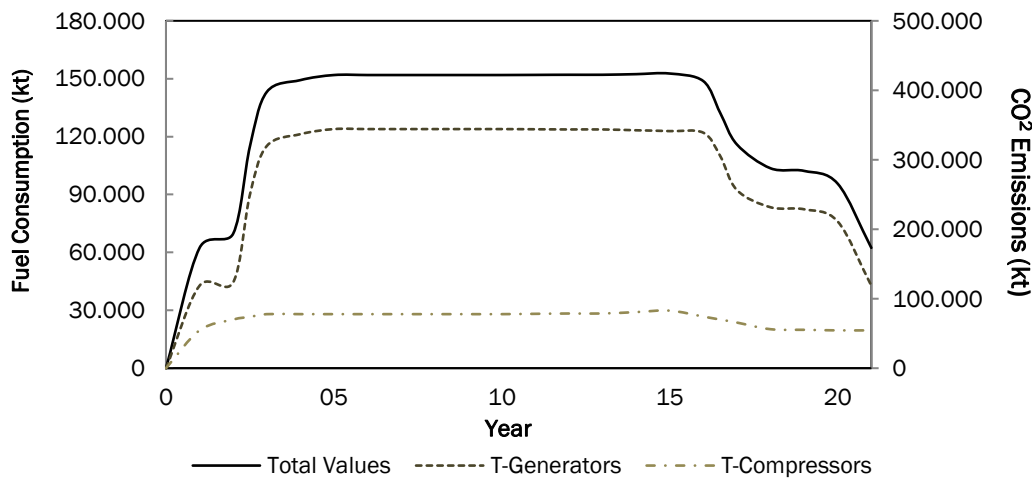
Figure 47 Reference scenario consumption/emissions over time
Source: Elaborated by author

$$C_{fuel} = C_{opp} \times \left[\left(\dot{m}_{f,TC} + \dot{m}_{f,TG} \right) - \dot{m}_{f,PH} \right] \qquad (82)$$

The previous equation applies also for CO_2 emissions, as stated before. In a scenario of electricity trade with the onshore system, emissions and fuel consumption would not be less than in the isolated grid case. Environmental benefits of this case come from reducing other fossil fuel generation on-shore and applying the gas-to-wire concept.

5.6.5 *Net present Value*

Previous sections explained both the Capital Costs and main Benefits related to installing a Floating Power Hub; in this section those parameters are integrated into an economic analysis. The indicator for signaling economic performance of each result in the present work is the Net Present Value (NPV). This method allows evaluating the project

economic performance along its lifetime, which is important when assessing the different fuel reductions of each year, depending on the oil and gas production and electricity demand.

The timeframe is divided in 25 years, each of them has single production characteristics which derive in diverse fuel consumption behavior. Operation and Maintenance costs are divided in fixed and variable. Variable cost is mostly related to material and fuel consumption. For this study, it is convenient to separate variable cost from O&M total costs, since the fuel consumption is addressed in a different manner, as explained in the previous item.

Therefore, considered O&M cost are composed by payroll of crew and staff in the power plant, and expenses of consumable supplies and equipment. Susskind et al. (1970) exposed a detailed cost structure, specifying staff and material cost according to average fossil-fueled power plants. According to this reference, estimated payroll expenses in an average power plant is 1,510 USD/MWh, updated to 2017 prices. In a similar manner, estimated cost of consumable supplies and equipment is 0,347 USD/MWh

$$PV = \frac{C_t}{(1 + i)^t} \tag{83}$$

$$NPV = -TI + \sum_{t=1}^{n} \frac{C_{fuel}}{(1 + i)^t} - \sum_{t=1}^{n} \frac{MWh \times C_{O\&M}}{(1 + i)^t} + \left[\sum_{t=1}^{n} \frac{C_{E.Sold}}{(1 + i)^t} \right] \tag{84}$$

5.7 Optimization

An optimization procedure localizes minimum or maximum points along a selected objective function. In some cases, it is possible to derivate the objective function in order to obtain maximum and minimum points. Nevertheless, in non-smooth problems, such as the one presented in this work, it is more adequate to perform optimization through derivative-free methods. Genetic algorithm (GA) optimization were selected because their versatility and capacity to deal with non-smooth objective functions.

Genetic algorithms are inspired in natural selection phenomena. When a GA starts, it establishes a random initial population of solutions, in which a variable vector represents

each solution. The quantity of members in an initial population depends on the problem nature and structure. GA evaluates the objective function in each solution to create an expectation or fitness factor, which categorizes the solution group in less or more optimal. Solutions with best expectations conform the elite group, which will produce new solutions group acting as 'parents' of this new population. Vectors representing each solution mutate in order to produce a new population, that is, a string of variables from one solution can be mixed with other one to produce a new member.

Given the previously explained nature of GA, it is necessary to define some important parameters which delimitate the quantity and quality of solutions provided. The population range determines the quantity of members that form the first random population set. The maximum number of generations limits the quantity of new members being created until finding an optimum solution. Maximum stall generations value stops the algorithm when a there is a clear fault in convergence. This is particularly critical for thermodynamic calculation, as the result must be voided if mass, pressure and temperature restrictions are not between reasonable values.

One of the reasons of selecting GA to perform the calculation is their ability to deal with non-linearities, in a reasonable amount of computing time. This model has several bounded integer variables that define quantities and layouts for the power hub. Those variables add complexity to the model, as it must select among a non-smooth combination of values. A series of combined cycle blocks compose the floating power hub. A combined cycle block can have diverse arrangements, one to four gas turbines can be combined with a single steam turbine. In the same way, one waste heat recovery unit can be shared by two or four gas turbines, in order to reduce space and weight requirements.

The overall calculation integrates several thermodynamic, sizing and economic methods, all equipment follows the same reasoning: first determine thermodynamic parameters, followed by a dimensional analysis and finishing with cost estimations. This framework is integrated in the optimization procedure. A fitness function and a constraint vector compose the GA calculation, which runs in MATLAB software (2018). A standard GA runs all optimization cases, optimization parameters are set as follows: crossover fraction 0.8, migration fraction 0.2, population size 200 and 4800 generations. The single objective algorithm converges in approximately 4800 – 5000 seconds and the double objective in about 80000 seconds, running in a 3.40 GHz Intel Core i7-3770 CPU. Areas and pressure calculations take longer, due to the large iteration processes to avoid unacceptable pressure levels.
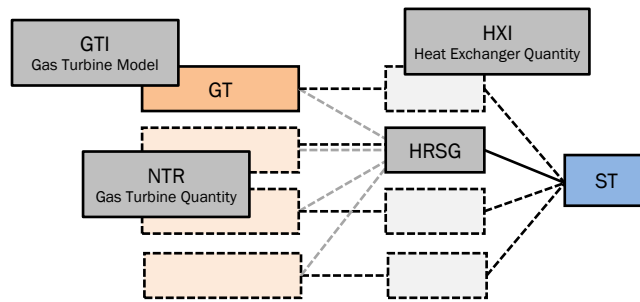
Figure 48 Combined Cycle Layout
Source: Elaborated by author

Integer and binary variables represent the size (GTI) and quantity (NTR) of gas turbines, and whether if each is coupled to a HRSG or one HRSG is shared by the GT group (HXI), as displayed in Figure 48. The introduction of such variables to the model makes it necessary to establish a Mixed Integer Non-Linear Programming (MINLP), in order to select among these discrete values.
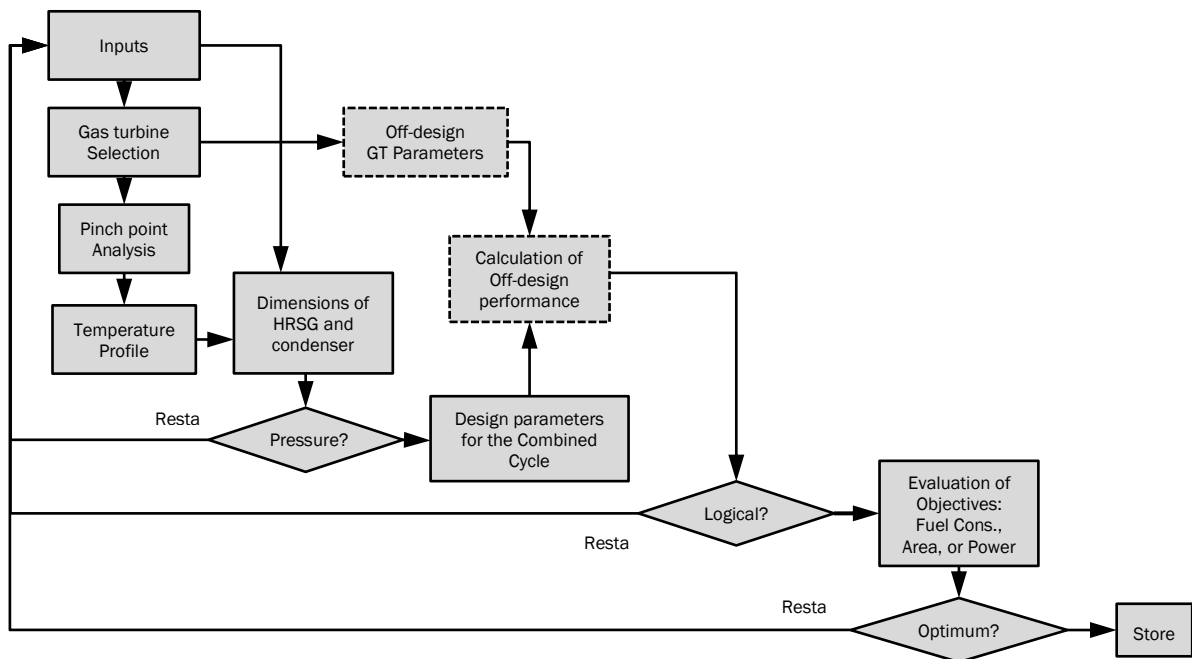
Figure 49 Simplified Algorithm Logic
Source: Elaborated by author

The structure of how the GA discards and accepts results can be seen in Figure 49. The model starts establishing design parameters for the gas turbine, which derive in a specific set of characteristics of the exhaust gases. Such characteristics are used to apply a Pinch Analysis, in order to determine heats and duties in each section of the heat

recovery steam generator. When the mass flows and enthalpies are determined, the steam turbine and condenser thermodynamic parameters are calculated. In this stage, the thermodynamic equilibrium in each component is verified, to avoid temperature crosses and fluid phase inconsistencies.

Solutions not meeting thermodynamic equilibrium in all nodes are discarded. If the candidate solution is consistent, then the physical properties of the components can be evaluated. The specific design for the HRSG is carried out and pressure drops are determined.

If total pressure drops on the gas side exceed 0.1 bar the solution is also discarded. Physical properties such as weight and size are also calculated for the gas turbine and condenser. The calculated transfer areas, duties, thermodynamic and physical properties are main inputs for the cost estimation of the combined cycle equipment. Solutions are evaluated in an iterative process until reach a minimum or maximum value.

The model construction has been composed by several scenarios and design options, regarding equipment selection and connections. This model structure aims to estimate the optimum power hub configuration. Because of the large number of variables and design options, the model is divided in two stages, in order to construct and organize results. In the following sections a broader vision of the model is presented along with the expected results of each stage.

Table 16 summarizes all variables involved in the calculation, with their respective analysis scenario and Table 17 shows the selected bounds for the GA model, the bound values are based on similar studies such as Manassaldi et al. (2011) and Pierobon et al. (2013). The overall calculation scheme can be seen in the Figure 52 at the end of this chapter.

5.7.1 HRSG and GT approach

The first stage of the power hub analysis consists in comparing two optimization approaches, single-objective and multi-objective optimization. This is an early stage of the analysis, in which only the design parameters are optimized. As explained in previous sections, single and multi-objective optimizations have differences regarding gas turbine selection. The single objective optimization considers a discrete analysis in which

commercial turbines are selected. The multi-objective optimization considers the tailored design of the gas turbine through its governing equations. Besides of the gas turbine, the HRSG presents two design options single pressure and double pressure arrangements. Both single and multi-objective optimization include the HRSG selection. The distinction between HRSGs allows understanding the tradeoff between weight and efficiency.

In this stage, space and weight may influence in the overall capital costs. Furthermore, as the main objective of a floating power hub is to improve efficiency in FPSOs energy supply and thus, reduce CO_2 emissions, the design procedure becomes a tradeoff among costs, weight and efficiency at design point.

$$f_1(X) = [PEC] \tag{85}$$

$$f_2(X) = [M_{cc}] \tag{86}$$

$$f_3(X) = [\eta_{cc}] \tag{87}$$
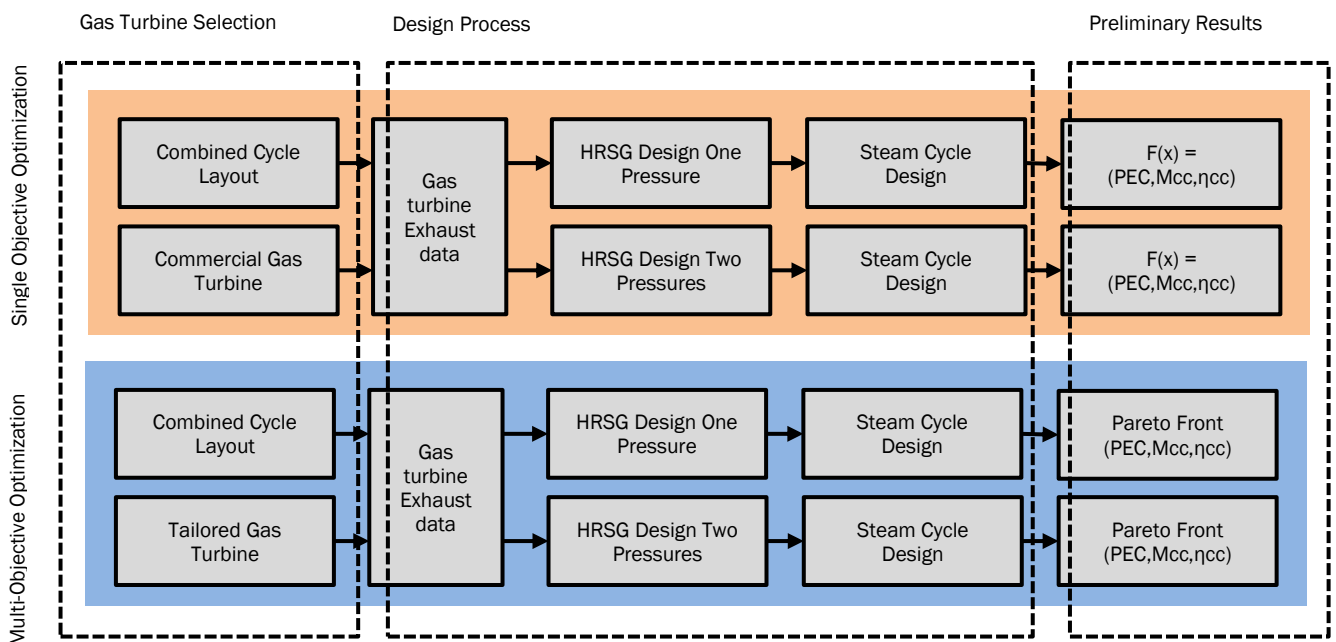
Figure 50 First stage of Power Hub Analysis
Source: Elaborated by author

The three objectives are assessed separately (single objective optimization) and as a vectorized three-dimensional objective for a trade-off analysis (multi objective optimization), figure 50 illustrates this case calculation scenarios. As seen in Eq. (85) to (87), a function containing thermodynamic, dimensional and economic modeling for the

combined cycle is applied to evaluate the established objectives. The vector X represents the decision variables, each input of this vector corresponds to design parameters of each component in consideration.

To assess such tradeoff three objectives are established: 1) Minimizing costs, which will be evaluated as the total purchasing equipment costs for the power plant: the sum of the individual costs of gas turbines, steam turbines, HRSGs, pumps and condensers. 2) Minimizing the total weight, resulting from the sum of the individual weights of the power plant aforementioned equipment. 3) Maximizing thermal efficiency, having as consequence reduction of fuel consumption and CO2 emissions.

5.7.2 Connection Scenarios

This stage evaluates only multi-objective optimization, with double pressure HRSGs and tailored gas turbines. A more detailed rationale of this selection is presented in the results section. The second stage includes the off-design calculation for the combined cycle. This is essential to understand how the proposed power plant performs along the production life time. Objectives are summarized in Eq. (86). One of the objectives of this work is to propose systems that operate more efficiently at different loads over time. Therefore, optimized values must reflect that variability. To address this aspect, one of the objectives is the average efficiency along the life time period. Thermal efficiency is closely related to fuel consumption. A higher average efficiency means less fuel consumption at the end of the evaluation period, and by consequence, less CO_2 emissions. The first stage includes an economic approach based on the capital costs; in this stage a more detailed economic analysis is performed. The off-design analysis and parameter evaluation overtime allows including all the net present value components, which depend on the yearly fuel saved costs and consumption. The net present value is hence selected as an objective to be maximized.

$$f(X) = [NPV, WTP, \bar{\eta}_{cc}] \tag{88}$$

Previous studies address the sizing minimization through weight-to-power ratio, as it is an important parameter for evaluating power plants offshore. This parameter allows comparing the present result with other systems. It also represents an indicator of the

combined cycle compactness, which is an important driver for selecting offshore systems. Even though, in this study, the volume and space are used to estimate the hosting ship costs, it is expected that in more complex design the weight and other several sizing parameters are considered. Figure 51 shows the possible scenarios for this optimization case.
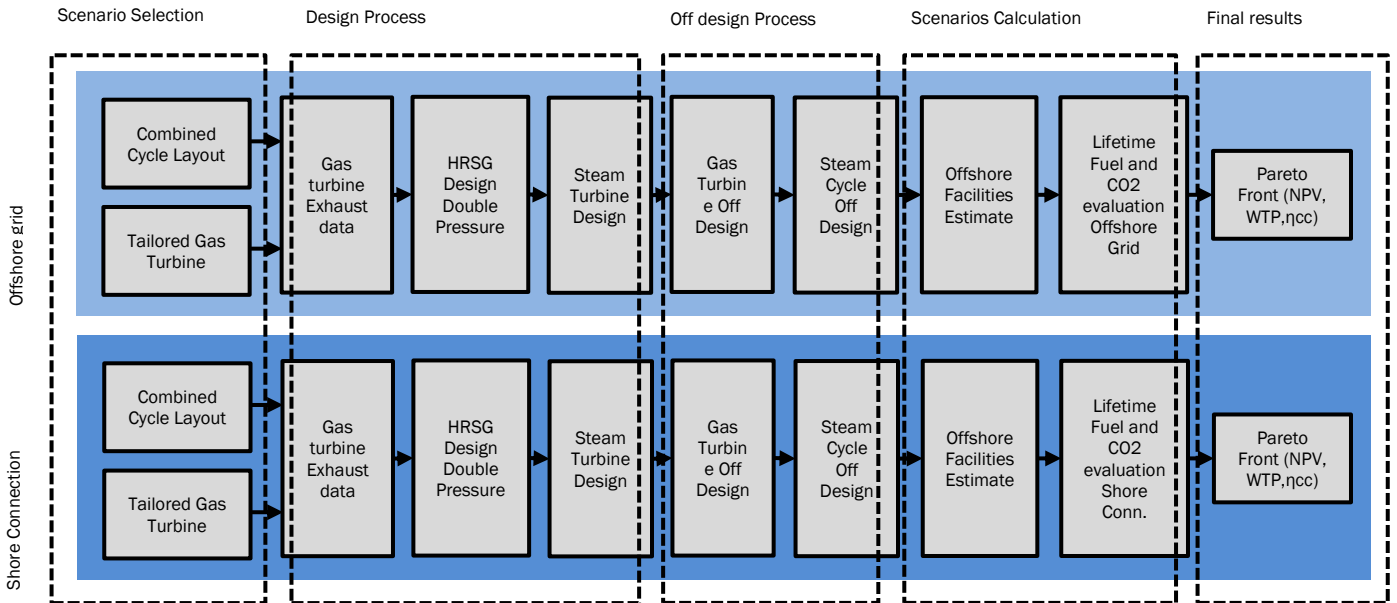
Figure 51 Second stage of Power Hub Analysis
Source: Elaborated by author

Table 16 Overall Variable Balance

Equipment	Case	Decision	Dependent	Fixed	Results
A. Gas Turbine	A.1 Commercial GT	NTR, GTI	$m_{air}, m_{fuel}, T_{exh} = T_{1sh}$	T_{amb}, x_{fuel}	PEC, M_{cc}, η_{cc} NPV, WTP, $\bar{\eta}_{cc}$ $W_{cc}, M_{CO2}, M_{fuel}$
	A.2 Tailored GT	NTR, r, η_{co}, T_3, η_t, W_{gt}			
B. HRSG	B.1 Single Pressure	$P, P_l, P_t, (d_o, N_r, N_t, n_f, l_f)_{ec,ev,sh}$ PP, W, L, HXI	$(d_i, U_o, HTA, LMTD, N_r)_{ec,ev,sh}$ $T_{exh} = T_{1sh}, \Delta P_{(w,gas)}$	t_f	
	B.2 Double Pressure	$\left[P, PP, (d_o, N_r, N_t, n_f, l_f)_{ec,ev,sh}\right]_{H,L}$ P_l, P_t, W, L, HXI	$\left[(d_i, U_o, HTA, LMTD, N_r)_{ec,ev,sh}\right]_{H,L}$ $T_{exh} = T_{1sh}, \Delta P_{(w,gas)}$		
C. Steam Turbine	C.1 Single Pressure	$t_{2sh}, P_{out} = P_{cond}$	m_w, W_{st}	η_{st}	
	C.2 Double Pressure		$[m_w, W_{st}]_{H,L}$		
D. Condenser	-	$P_{out} = P_{cond}$	m_{cool}, HTA	U_{cond}	
E. Offshore	E1. Offshore Grid	W_{ref}	$TB, TIC, L, B, D, Z_{ship}$	$[L, Z]_{cables,piping}$	
	E2. Onshore Connection		$TB, TIC, L, B, D, Z_{ship}, E_{sold}$	$[M, Z]_{AC/DC}$ $[L, Z]_{cables,piping}$	

Source: Author

Pre-processing

MATLAB

Post-processing

Thermoflex
(Four
comercial GTs)

Microsoft Excel

Integer variable (GT Selection)

Integer variables
Number of HRSG
Number of GTs

Microsoft Excel

Final Results

1 — Define GT Temperature and mass flow

Gas Turbine Design

4 — Determine Block Layout

10 — Raw variable and parameter vector results

2 — HRSG Temperature Profile

Steam turbine inlet temperature and pressure

5 — Determine component and ship cost and weight

9 — Calculate Consumption and efficiency

3 — Pressure losses

HRSG Dimensions

6 — Off-Design for GTs

8 — Calculate dispatch over time

Consistent?
Yes – Continue
No – Restart loop

7 — Off-Design for CC

Consistent?
Yes – Continue
No – Restart loop

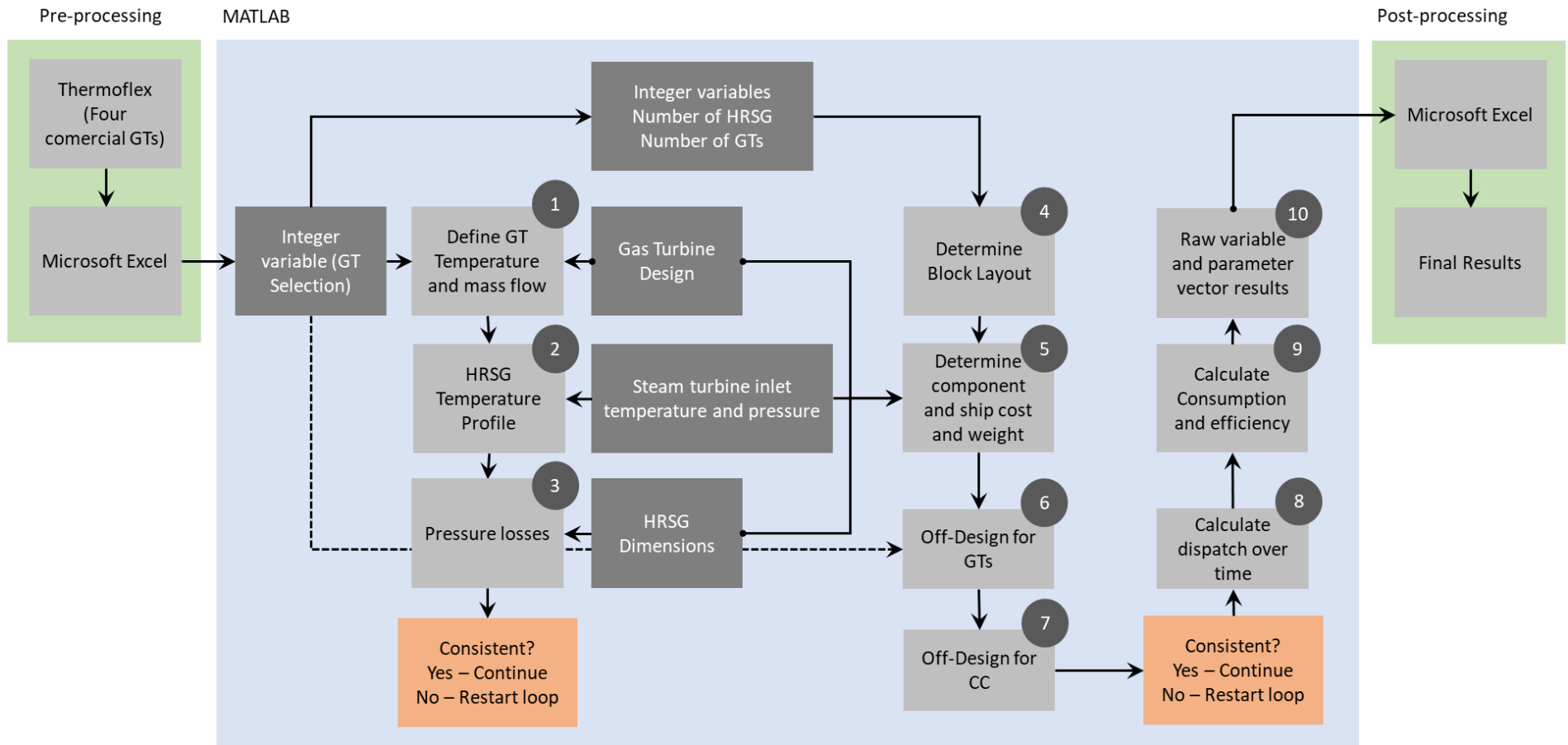**Figure 52** Algorithm stages and platforms
Source: Elaborated by author

Table 17 Variable Bounds

Variable	Lower Bound	Upper Bound
Integers		
NTR (adim)	1	4
HXI (adim)	0	1
Gas Turbine		
r (-)	19	28
η_{pt} (%)	0.7	0.9
TIT_{GT} (K)	1300	1600
η_{co} (%)	0.7	0.9
WTD (MW)	20	45
HRSG		
L_f (m)	7	18
W_t (m)	4	7
PP (K)	10	30
P (bar)	20	80
P_H (bar)	50	80
P_L (bar)	10	40
TIT_{ST} (K)	600	750
HRSG Sections		
d_o (m)	0.04	0.09
N_r (-)	1	20
N_t (-)	20	100
P_l (m)	0.05	0.1
P_t (m)	0.07	0.2
n_f (1/m)	100	200
l_f (m)	0.005	0.02
Condenser		
P_{cond} (bar)	0.5	10

Source: Author

6   RESULTS

This chapter is dedicated to represent the set of obtained results. It is divided according to the given solution approaches. Besides the first single-objective optimization, both approaches result in Pareto fronts, and are divided into a number of clusters. Cluster solutions are points with similar characteristics. The first gas turbine and HRSG approach is discussed from a focus of a design point. The second approach broadens the design vision to the off-design parameters and gives a lifespan insight of the overall Power Hub performance.

For the following results, the nomenclature used for representing the layout of the combined cycle blocks is simplified as follows: the number of gas turbines, followed by the number of heat recovery steam generators, and finally the number of steam turbines: GT(HRSG)xST. Therefore, a 2(1)x1 block configuration, has two gas turbines with a shared HRSG and one steam turbine.

6.1   Gas Turbine and HRSG Approach

Results in this case are divided in Single-objective and Multi-objective optimization subdivisions, the single-pressure and double-pressure HRSGs are also evaluated. In this case, the results from the different optimization methodologies are compared as follows.

6.1.1 Single-objective Optimization

This optimization procedure allows analyzing extreme points of the variable solution set. Table 18 and Table 19 highlight the most important parameters of the single-objective optimization procedure. There are similarities of the obtained arrangements for both pressure levels. The number of gas turbines and blocks are similar in both cases. Results in one objective

optimization tend to reduce blocks in 1(1)x1 arrangements. This allows improving the heat exchange by increasing the heat transfer area in HRSGs delivering steam for a single steam turbine, however, such layout results in a considerable increase in weight.

Optimized dual-pressure arrangements result in more compact combined cycles and smaller HRSGs when compared with single-pressure configurations. These results are mainly because achieving maximum efficiencies requires greater heat transfer areas when dealing with one pressure configurations. Likewise, weight minimization is obtained to the detriment of the heat transfer area. The results provide a less efficient system for the dual-pressure configuration, including one shared HRSG, and having the same model and quantity of gas turbines as the single-pressure case with three separated HRSGs.

Table 18 Single-objective single pressure optimization results

Optimization case	Efficiency (η_{cc})	Costs (PEC)	Weight(M)
Decision Variables Overview			
P (bar)	28.47	27.89	70.77
PP (K)	10.16	30.00	29.96
T_{LST}(K)	730	724	679
$P_{ex,ST}$ (bar)	0.05	0.93	0.05
L_f (m)	16.18	12.58	7.00
X_t (m)	5.36	5.06	5.10
Combined Cycle Design			
GT Model	LM6000 PA	SGT-800-50	LM2500+PV
CC Layout	1(1)x1	1(1)x1	3(3)x1
Groups	4	3	2
HTA (m^2)	43182	19340	9145
W_{ST} (MW)	13.60	11.67	28.09
WTP (kg/MW)	12,943	9,922	4,998
Objective Values			
η_{CC} (%)	**53.28**	46.22	51.80
PEC (MMUSD)	122.02	**80.67**	130.00
M_{total} (ton)	2588	1895	**1262**
Fuel Consumption/CO_2 Emission Reductions			
BAU (%)[3]	23,4%	22,5%	20,1%

Minimizing equipment costs results in the lowest performance levels. Besides the lowest heat transfer areas for the whole system, minimizing costs also follows the lowest operating

---

[3] Fuel consumption and CO_2 emission reductions are considered proportional, this value corresponds to the reductions compared to the base scenario (BAU) at maximum demand. Lifespan values and reductions are presented in the Off-grid/Land-cx approach.

pressures in both the single and dual-pressure configurations. Reduced areas and low pressures decrease size of equipment, reducing its efficiency but not necessarily diminishing total weight; the main reason being the selection of gas turbine SGT-800 which holds the lowest cost per MW and the largest weight

In all cases, there are important reductions in fuel consumption due to the application of combined cycles. Diminishing fuel consumption is directly related to reducing CO2 emissions. Considering a business-as-usual scenario, in which the three FPSOs remain separated, estimated CO2 emissions are approximately 455.686 ton/year at full load. The results obtained in this work suggest that it would be possible to reduce those emissions in a range between 18.7 % and 27.2 % at peak demand for the dual-pressure steam cycle configuration by applying the weight minimization and efficiency maximization optimizations, respectively.

**Table 19** Single-objective double pressure optimization results

Objective	Efficiency (η_{cc})	Costs (PEC)	Weight(M)
Combined Cycle Design			
P_H (bar)	79.91	64.93	69.40
P_L (bar)	10.60	18.50	29.13
PP_H (K)	10.10	29.81	27.90
PP_L (K)	10.10	27.37	29.90
T_{LST}(K)	749	685	661
$P_{exh,st}$ (bar)	0.52	5.29	4.67
L_f (m)	11.03	10.54	8.54
X_t (m)	6.64	5.48	5.35
Combined Cycle Design			
GT Model	LM2500+PV	SGT-800-50	LM2500+PV
CC Layout	1(1)x1	1(1)x1	3(1)x1
Groups	5	3	2
HTA (m^2)	26297	18488	19306
W_{ST} (MW)	11.28	14.62	22.90
WTP (kg/MW)	8,341	8,761	4,307
Objective Values			
η_{CC} (%)	**54.64**	48.67	49.23
PEC (MMUSD)	123.00	**90.70**	133.00
M_{total} (ton)	1536	1540	**858**
Fuel Consumption/CO$_2$ Emission Reductions			
BAU (%)	27,2%	24,1%	18,7%
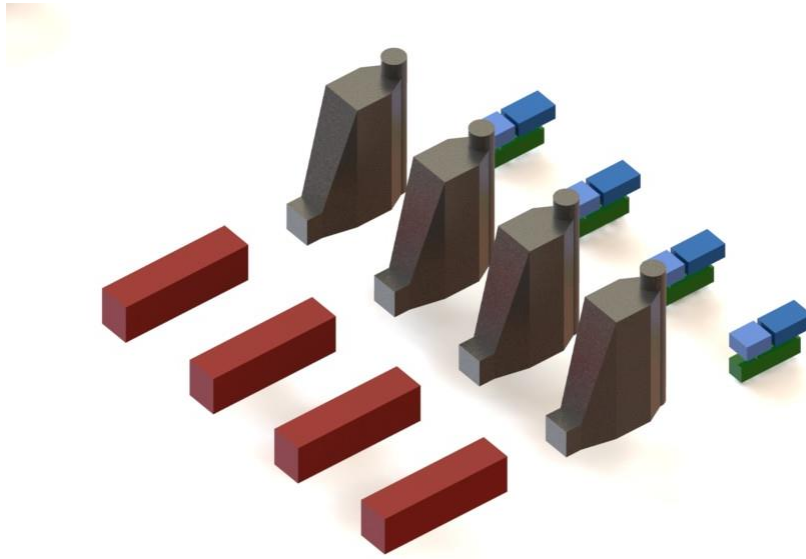
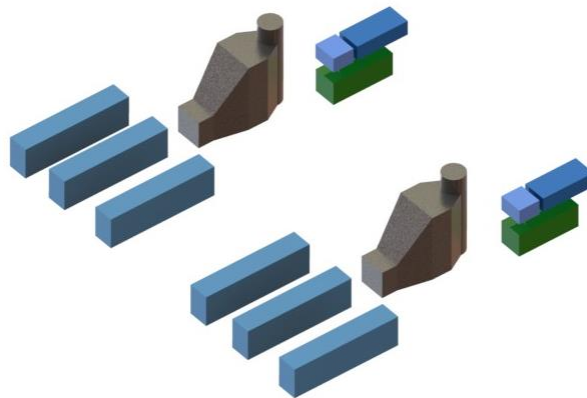**Figure 53** Efficiency Optimization, Single Pressure
4x GELM6000 1(1)x1 Source: Elaborated by author
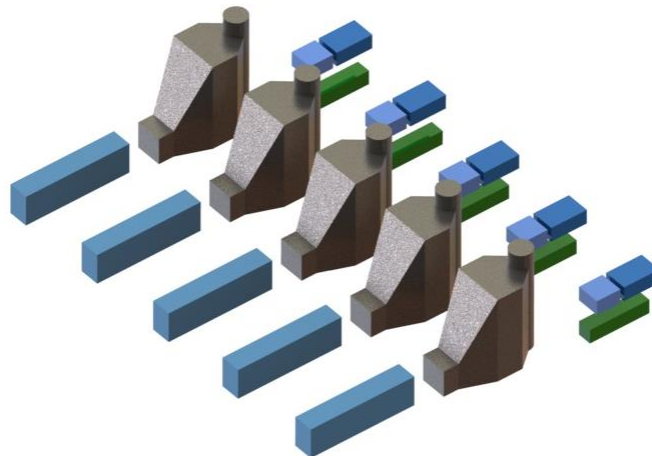
Figure 54 Efficiency Optimization, Double Pressure
5 x GELM2500 1(1)x1 Source: Elaborated by author
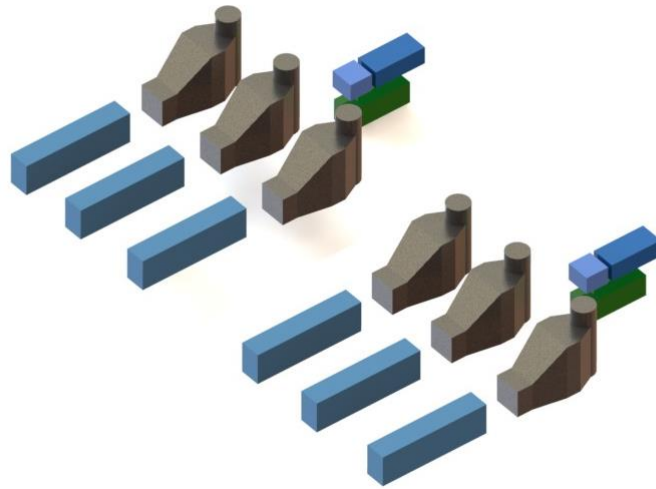
Figure 55 Weight Optimization, Single Pressure
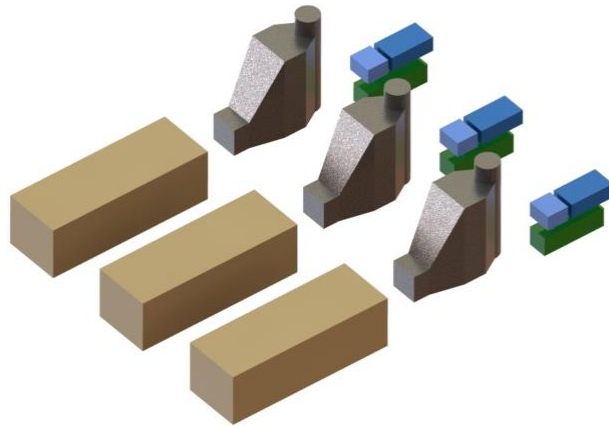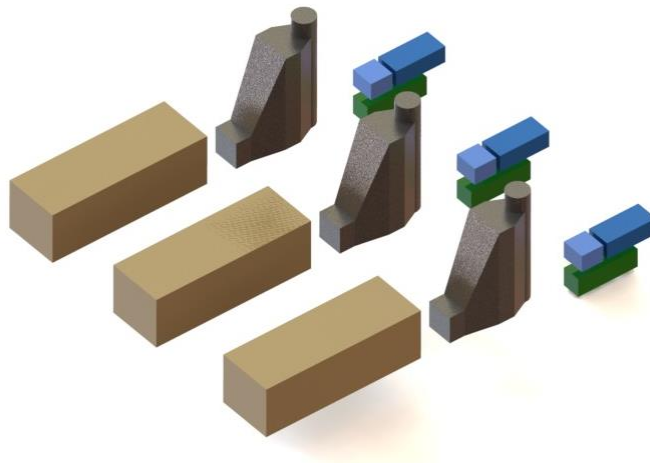2 x LM2500 3(3)x1 Source: Elaborated by author

Figure 56 Weight Optimization, Double Pressure
2 x LM2500 3(1)x1 Source: Elaborated by author

Figure 57 Equipment Cost Optimization, Single Pressure
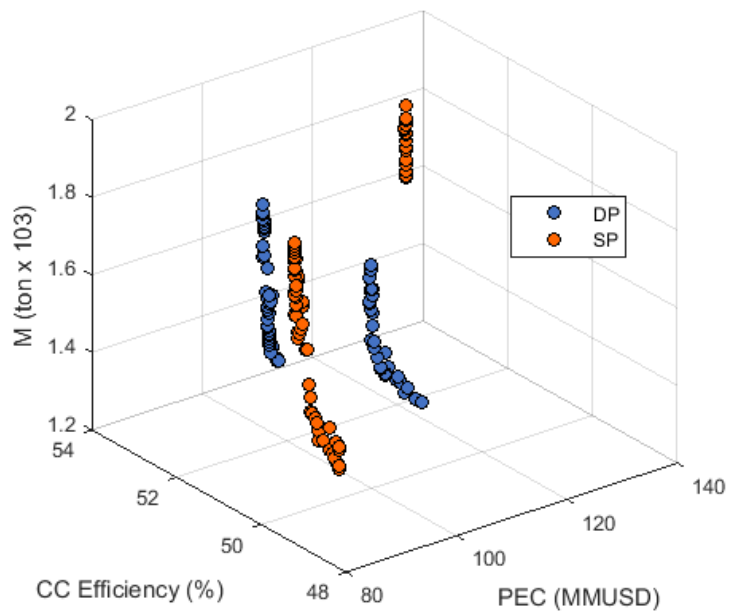3 x SGT800 1(1)x1 Source: Elaborated by author

Figure 58 Equipment Cost Optimization – Double Pressure
3 x SGT800 1(1)x1 Source: Elaborated by author

By using the obtained dimensions, it was possible to recreate the Combined Cycle components through CAD models in scale of each result. The CAD models allows comparing dimensions and volumetric aspects, in a more graphic manner. The result of this modeling can be seen from Figure 53 to Figure 58. All the Figures are in the same scale, so it is possible to compare sizes among them. It is possible to observe that the Layout is the main driver into determining the space required, the Steam Turbine itself represent a relatively small volume when compared to the remaining components

6.1.2 Multi-objective optimization

The results of the multi-objective optimization consist of a three-axis Pareto front, in which each axis represents one of the established objectives. In order to simplify the result visualization, three graphs are created. In each graph two objectives are analyzed, for both single-pressure and double-pressure arrangements. Each point of the Pareto front represents a feasible solution of the presented calculation. Thus, it also represents a set of variables and a specific arrangement for the combined cycle. As some variables are integer by nature, the Pareto front of both arrangements presents clusters of results with similar characteristics, clusters are not determined by clusterizing algorithms, as they are easily determined by layout characteristics. CO_2 and fuel consumption reductions, for both single and double-pressure optimization cases, are expected to be between the extreme points of the single-objective optimization values presented previously.

The single-pressure optimization results in three differentiated solution clusters. This distinction is most appreciable for the equipment costs objective. Higher, medium and lower cost clusters are visible in Figure 59 to Figure 62. The clusters are characterized by the total quantity of gas turbines in the whole power plant, being 6, 5 and 4, respectively for each cluster

Figure 59 3D Pareto Front Double/Single Pressure
Source: Elaborated by author
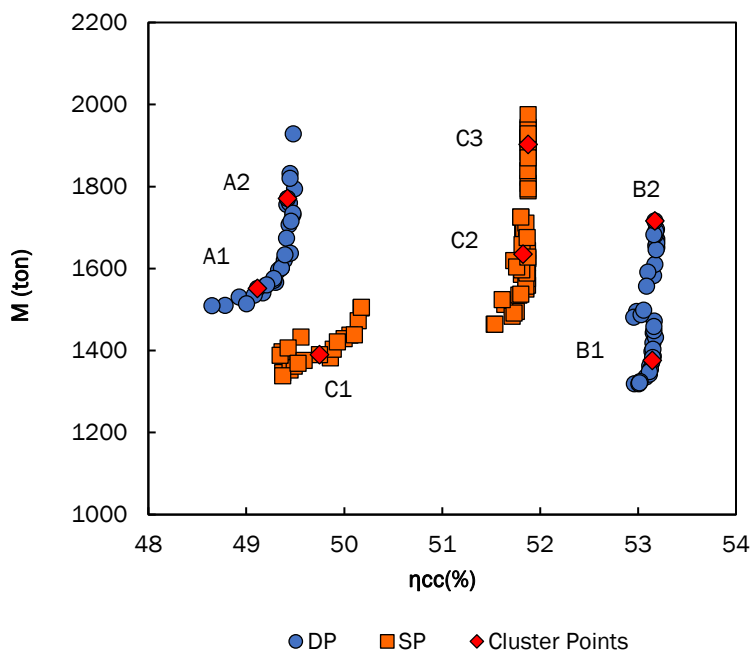
Figure 60 Pareto Front – Efficiency vs. Weight
Source: Elaborated by author
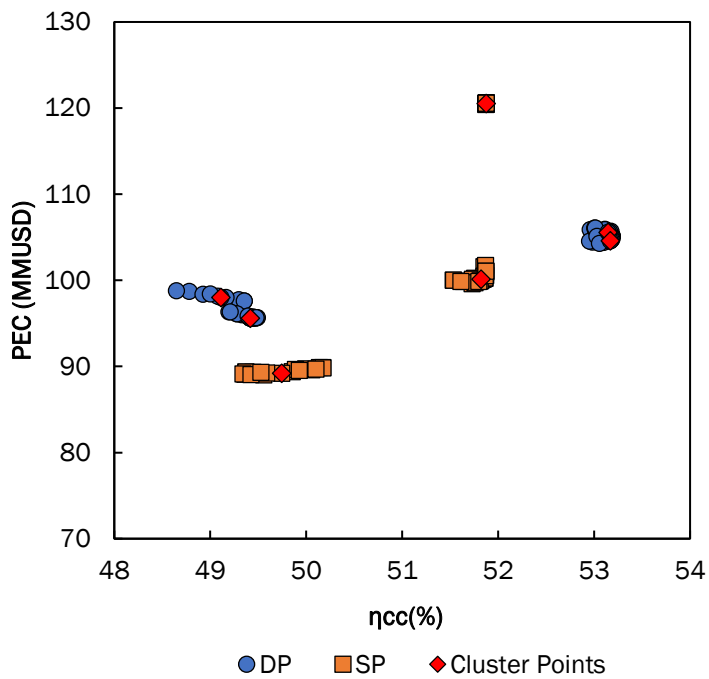
Figure 61 Pareto Front – Efficiency vs. Equipment Cost
Source: Elaborated by author

Figure 62 Pareto Front – Weight vs. Equipment Cost
Source: Elaborated by author

As an overall trend, gas turbine efficiency increases, reducing the exhaust gas temperature. This characteristic produces a rise in heat transfer area, in order to obtain high overall combined cycle thermal efficiencies. This reflects in an increase of HRSGs size and cost along with downstream components. The gas turbine inlet temperature is in average 1506 K for all single pressure results. The three objecti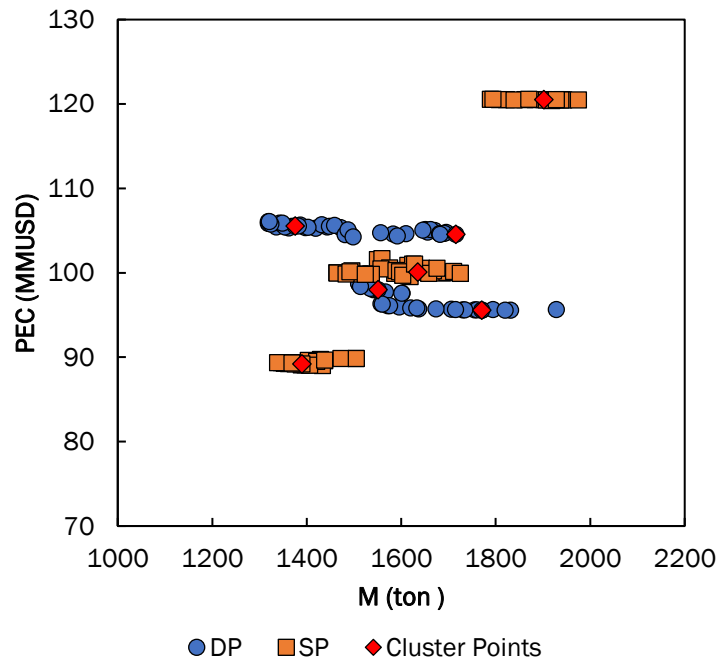ves show an overall positive correlation when considering all results, meaning that weight, cost and efficiency increase all together and vice versa. However, this trend is not visible among each cluster values, especially weight objective tends to be more disperse and less correlated with the other objectives. An overview of each cluster details is shown below.

Low cost solutions, seen in Figure 60 as a cluster around 90 MMUSD, are characterized by gas turbines with higher ratings and lower isentropic efficiencies; η_{pt} = 87.1-87.3% and η_{co} = 88.5-89.6%. The power plant would be composed by four 35.52 MW gas turbines, in combined cycle blocks of 1(1)x1 or 2(2)x1. For this cluster, the influence of pinch point and isotropic efficiencies on the overall thermal efficiency are more noticeable, as they have larger variation spans when compared with medium and higher costs clusters. The combination of low pinch points, varying 5 K along the cluster, and high isentropic efficiencies results in overall higher thermal efficiencies.

The results indicate that the medium cost level power plants have five blocks, with gas turbine ratings ranging 32.29 to 32.92 MW in 1(1)x1 CC layouts. In addition to having an influence on the block arrangement, the power plant costs are influenced by small changes on the gas turbine rating. Larger ratings produce higher costs, and vice versa. The influence of the pinch point is similar as the one explained for the previous cluster with a narrower variation span (2 K). The isentropic efficiencies in the gas turbines present limited variations, thus having limited effects on the performances.

Finally, the results indicate that the three-block arrangements have the highest costs. In this cluster, combined cycle blocks are arranged in two gas turbines of 32.35 MW, i.e. 2(2)x1. Design parameters are more constant and their variation span is negligible, and thus their influence in result does not present a specific trend. Specifically, pinch point value averages 20 K, and isentropic efficiencies in the gas turbine are at the upper bound, $\eta_{pt} = \eta_{co}$= 90%. The relation between gas turbine rating and overall costs is similar as described for the medium cost cluster.

The Pareto front for dual-pressure arrangement presents two main result clusters, namely, power plants featuring four and six gas turbines. Four gas turbine arrangements appear in a cluster surrounding efficiencies around 49% in Figure 60. Six turbine arrangements are the cluster with average efficiency of 53% in the same figure. In this case, the cluster results are highly differentiated, due to the large gap between average gas turbine ratings between the two clusters, being 34.26 MW and 25.05 MW, respectively. The gas turbine inlet temperature also presents an approximate gap of 100 K between the clusters. Another differentiation feature is the presence of combined cycle blocks with a shared HRSG among the gas turbines, instead of a separate HRSG for each gas turbine. High HP pinch points and low LP pinch points are related to better thermal efficiencies in both clusters. Clusters details are presented as follows.

The first cluster of lower efficiencies is formed by two configurations containing four gas turbines, two CC blocks 2(2)x1 or one block 4(4)x1. In this cluster, objectives and variable trends are more correlated. As compressor isentropic efficiency decreases, so does the thermal efficiency and overall weight. On the contrary, it produces an increase in overall costs. An increase in steam cycle high pressure results in a weight reduction and in cost increase. Optimal gas turbine inlet temperature is about 1452 K with very small variation span. The results suggest that the cost increases when splitting four gas turbines into two blocks, due to the introduction of additional steam cycle components. This block distribution also affects the thermal efficiency, as in one CC block there are four HRSG, meaning a larger heat transfer area, thus increasing the thermal efficiency compared with the two-block arrangement. Even though block distribution is discrete, cost and thermal efficiency variations are smooth among the results and they also depend on gas turbine properties.

The second cluster is characterized by power plants having six gas turbines in two blocks of three gas turbines each. The cluster is divided into power plants having two types of blocks, 3(3)x1 or 3(1)x1. This cluster presents the highest thermal efficiencies of all multi-objective optimized results, ranging from 53.0 % to 53.2 %. The main difference between both clusters is the shared HRSG. This characteristic, along with fact that some design values are close to their bounds, make the relation among variables more disperse. Isentropic efficiencies in the gas turbine are in average $\eta_{pt} = \eta_{co} = 89\%$. The gas turbine inlet temperature varies between 1525 and 1537 K. As the isentropic efficiencies remain constant, small changes in the LP pinch point (varying from 16.8 to 17.6 K) affect the overall thermal efficiency (52.9% to 53.2%). The HP pinch

point remains almost constant around 26.8 K for all solutions. As detailed for the previous cluster, also in this case, the cost is influenced by the block layout and gas turbine properties.

**Table 20** Single/Double Pressure Cluster Results

Case	PEC (MMUSD)	WEIGHT (ton)	EFF (%)	Blocks	GTs per Block	GT Rating (MW)	HRSG per Block	ST Rating (MW)	Total Capacity (MW)
DP (A1)	98,00	1.551	49,11	2	2	34,32	2	19,45	176,18
DP (A2)	95,61	1.770	49,42	1	4	34,20	4	38,95	292,60
DP (B1)	105,56	1.376	53,15	2	3	25,06	1	17,78	168,17
DP (B2)	104,58	1.716	53,17	2	3	24,98	3	17,72	203,04
SP (C1)	89,21	1.390	49,75	2	2	35,53	2	17,02	176,16
SP (C2)	100,11	1.635	51,82	5	1	32,34	1	6,45	168,14
SP (C3)	120,53	1.902	51,88	3	2	32,36	2	13,00	220,17

## 6.2 Offshore Grid and Onshore Connection Approach

The Genetic Algorithm provides six Pareto fronts for the three objectives: Mean Efficiency, Weight-To-Power Ratio and Net Present Value. The Pareto fronts show the differences between both cases, isolated grid and on-land connection, and the tradeoff among the objectives, as seen in Figure 63 to Figure 66. Each point on the Pareto front represents an optimized solution containing 42 variables. As discussed in previous sections, these variables represent the physical and thermodynamic design of the Power Hub. As overall results, combined cycles for offshore grid are more restricted in weight and efficiency due to their operation conditions. On the other hand, an onshore connection provides a significant improvement in economic performance and a broader range of results for weight and efficiency. Points in Pareto Fronts form clusters of results with similar characteristic, average values are shown in Table 21. In below sections, a detailed analysis of both cases.
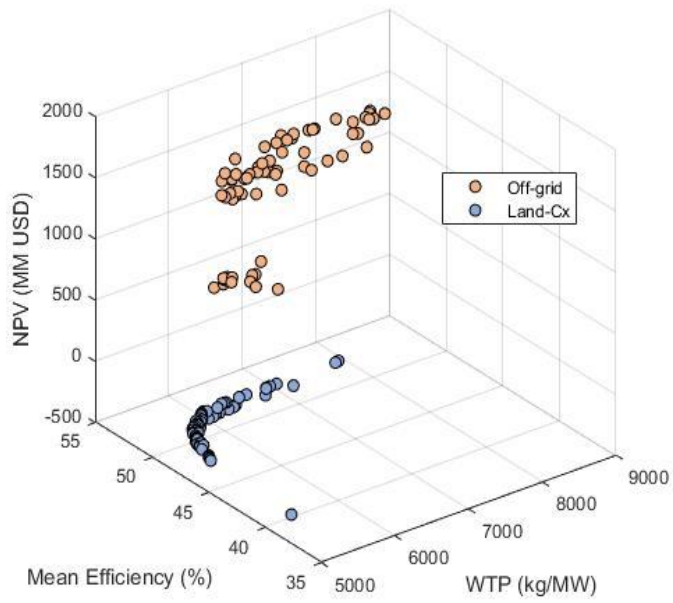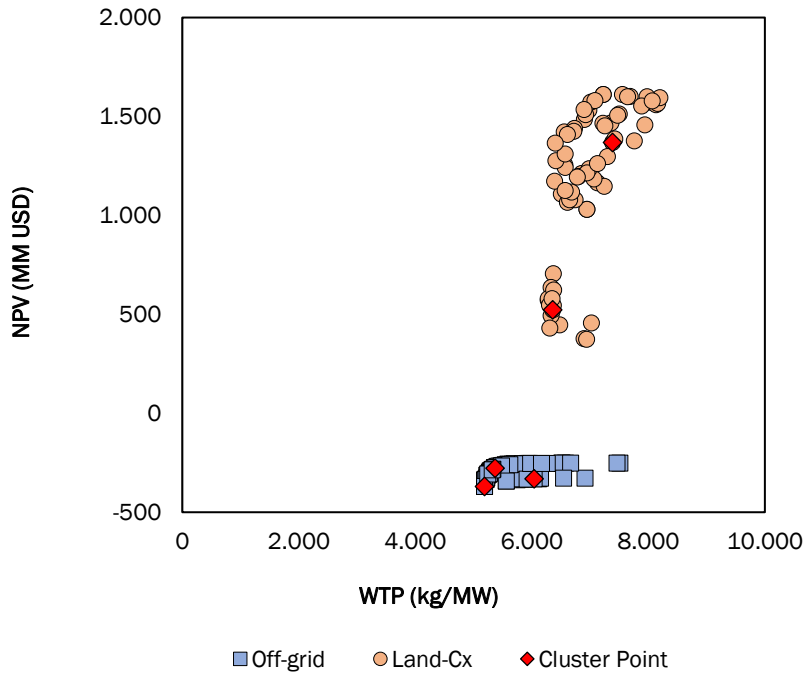
Figure 63 3D Pareto Front Off-grid/Land-cx
Source: Elaborated by author
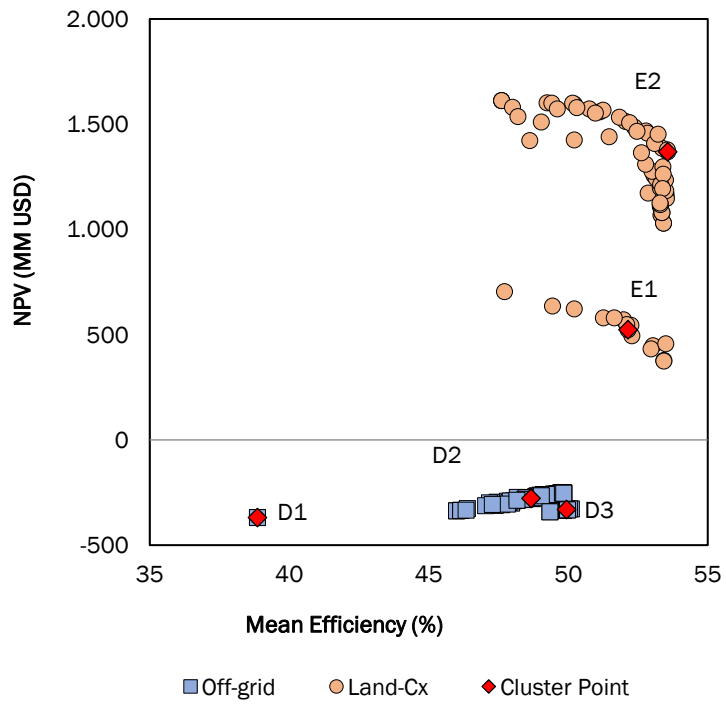
Figure 64 Pareto Front – Efficiency vs. Net Present Value
Source: Elaborated by author
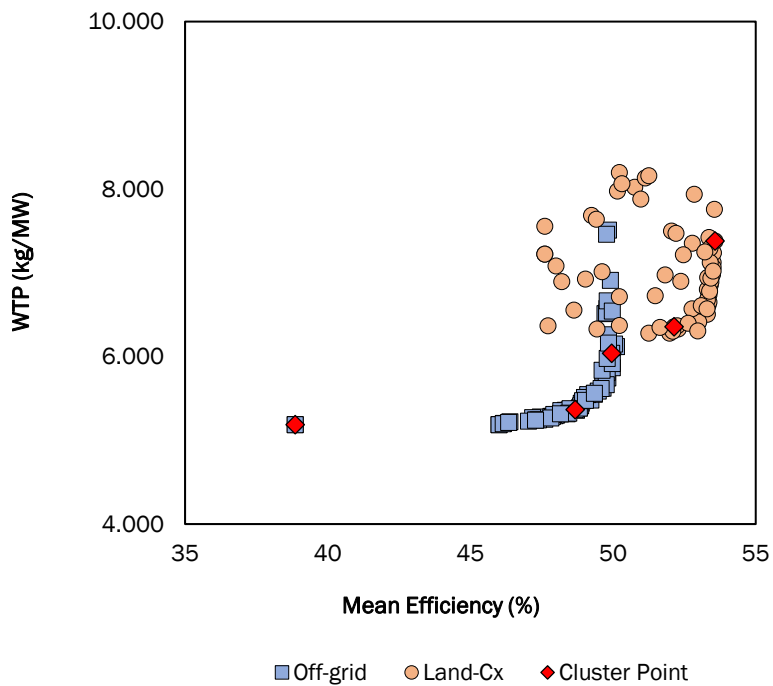
Figure 65 Pareto Front – Efficiency vs. Weight-to-Power
Source: Elaborated by author

Figure 66 Pareto Front – Weight-To-Power vs Net Present Value
Source: Elaborated by author

Table 21 Land Connection/Offshore Grid Cluster Results

Case	WTP (kg/MW)	EFF (%)	NPV (MMUSD)	Blocks	GTs per Block	GT Rating (MW)	HRSG per Block	ST Rating (MW)	Total Capacity (MW)
Off- grid (D1)	5.187	38,86	-369	4	1	31,94	1	15,89	191,32
Off- grid (D2)	5.365	48,67	-277	5	1	29.29	1	9,21	193,51
Off- grid (D3)	6.037	49,94	-330	6	1	28.17	1	7,97	216,86
Land-cx (E1)	6.357	52,14	524	2	3	32.95	3	26,68	251,07
Land-cx (E2)	7.381	53,57	1.369	2	4	34.26	4	35,10	344,28

6.2.1   Offshore grid

For an isolated offshore grid, optimized objectives result in some steady trends. In general, higher average efficiencies are related to lower GT capacities and thus, to ST capacities. When comparing between the clusters, higher efficiencies are related to better economic performance, but this is not a trend when comparing the diverse solutions within the clusters. Higher average efficiencies are related to higher WTP ratios. This relation is asymptotic and at some point, increase in WTP result in a marginal increase of efficiency. A similar trend is observed in WTP vs NPV, with higher WTP ratios having better economic performances. Reductions in fuel consumption and consequently CO_2 emissions range from 13.14% and 23.44% with respect of a Business-As-Usual Scenario. The economic results indicate that the off-grid case is not cost-effective, indicating that the advantages obtained by a reduction in gas consumption would not be enough to implement an isolated grid. Further mechanisms, a carbon trading scheme could improve NPV results. In this sense, prices above 92 USD/ton would be necessary to make this layout cost-effective. This cost is relatively high, as some other projects could sell carbon certificates at considerably lower prices. Offshore grid results are divided in three clusters, where the main difference is the GTs capacity. NPV values decrease with the increase of total installed capacity. The clusters are detailed as follows.

- Cluster D1 has the minimum values of WTP of all results, presenting the most compact layouts for the power hub. However, this minimization has marginal benefits, since slightly higher values present better economic and thermodynamic performances. It also presents

the lowest values of NPV, with four combined cycle groups and average 31.9 MW of GT capacity. Economic performance is heavily penalized due to the low thermal efficiency.

- Cluster D2 presents the best NPV results for the off-grid scenario. Even the most optimistic values are not economically feasible. This cluster has five combined cycle groups and 29.2 MW GT average capacity. The economic performance result is a balance of reducing the combined cycle blocks to reduce capital costs, while maintaining a reasonable efficiency to observe gains of reducing fuel consumption.

- Cluster D3 has the highest values of efficiency, penalizing WTP ratio and NPV, mostly because of increasing the number of groups of combined cycles. In this case the efficiency gains are marginal when assessing the economic penalties; there are high investments to obtain slight gains in efficiency. Best obtained efficiency is 50,1% (-328 MMUSD) against 49,8% (-252 MMUSD) in the second cluster.

For comparison purposes the WTP ratio was also calculated for the steam cycle only (Steam turbine, generator, HRSG and condenser), resulting in a range from 27 to 51 kg/kW an average value of 41 kg/kW. An optimized value of 34 kg/kW was obtained for the Norweigian case in Nord et al. (2014). The difference relies on the condenser cooling water temperature, which is considerably higher for the Brazilian case.

6.2.2 Land connection

This case presents a configuration of offshore grid connected to land through an HVDC line. This implies several considerations. As the scope of this case is to increase economic performance by selling surplus energy to the main grid, fuel consumption and emissions increase with respect of a Business-As-Usual scenario, in approximately 26% to 98%, depending on the Pareto front point. Benefits do not come from fuel savings but from electricity exchange with the main grid. Brazilian grid is based on a Hydrothermal generation, with complex price settings, an average price of 100 USD per MWh was considered for this case. Overall results show better economic performance when compared with the offshore grid case. Efficiencies achieve higher values because of normalizing the energy supply by exporting surplus energy to land, average efficiencies in this case range from 48% to 53%. WTP ratios in this scenario result in dispersed

values, not showing trends correlating either to efficiency or NPV. In this case NPV increases with Total Installed Capacity, dividing the results in two clusters, explained below.

- Cluster E1 layouts are composed by two blocks of three gas turbines and one steam turbine. NPV values range 374 and 705 MMUSD. Efficiencies for this cluster span a similar range as in the previous cluster, 48 to 53%. Installed capacity averages 251 MW compared to 345 MW of the first cluster. This configuration results in lower values of WTP ratio and more compact layouts.

- Cluster E2 results in layouts composed by two blocks of four gas turbines and one steam turbine, with separate HRSGs. This cluster presents the highest NPV of all results 1030 to 1612 MMUSD, because of the large installed capacity, 308 to 374 MW, and consequently, larger surplus energy to supply to the main onshore grid. The large size of the equipment causes an increase of required space and WTP, which is also the highest among obtained results, reaching 8 tons/MW. The increased capital costs are compensated with the benefits from electricity exchange.

6.2.3 Lifespan Comparison

One of the main drivers to perform off-design calculations is to understand how part-load operation could affect efficiency for the entire Power Hub lifetime. As the load is relatively constant in layouts considering a land connection, the Lifespan analysis becomes more interesting for the isolated grid results. Figure 67 show the efficiency of the optimized combined cycle layouts. There is a wide spread among results, D3 has the highest efficiency performance and D1 the lowest, all efficiency curves have a similar behavior over changing loads. However, average efficiency does not necessarily follow the same reasoning.

This is because not all combined cycles are operative at the same time, and at some points of the lifetime gas turbines operate in open cycle. Figure 68 to Figure 72 show the dispatch over the power hub lifetime, and it is possible to detail that 1x1 are prioritized in off-grid in order to avoid gas turbines operating in open cycles. Whilst, layout results in Land-cx resemble to conventional land combined cycles, with several gas turbines operating at full load along with the steam cycle (3x1 and 4x1). The fuel consumption in all cases increases to achieve a steady value,

according to the respective energy demand forecast. It increases with visible steps when commissioning each FPSO, until year 9, when it is steadier and start decreasing at year 16 until ending the lifetime in year 25. For the land-cx scenarios steps are clearer, because they only depend on the commissioning of the co-generation cycle in each FPSO to supply heat demand.
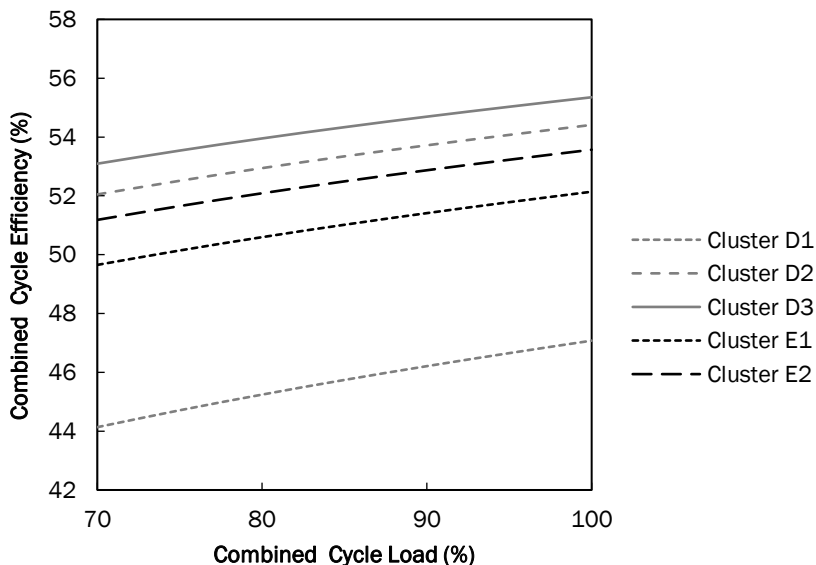
Figure 67 Combined Cycle Part Load Performance
Source: Elaborated by author
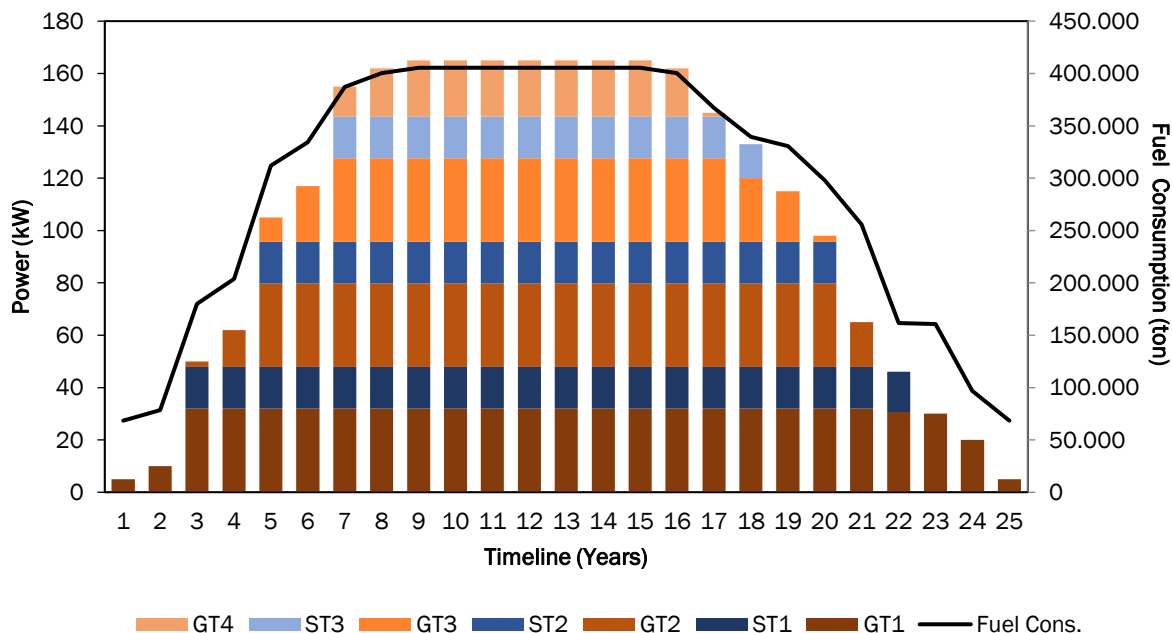
Figure 68 Lifespan performance Cluster D1
Source: Elaborated by author
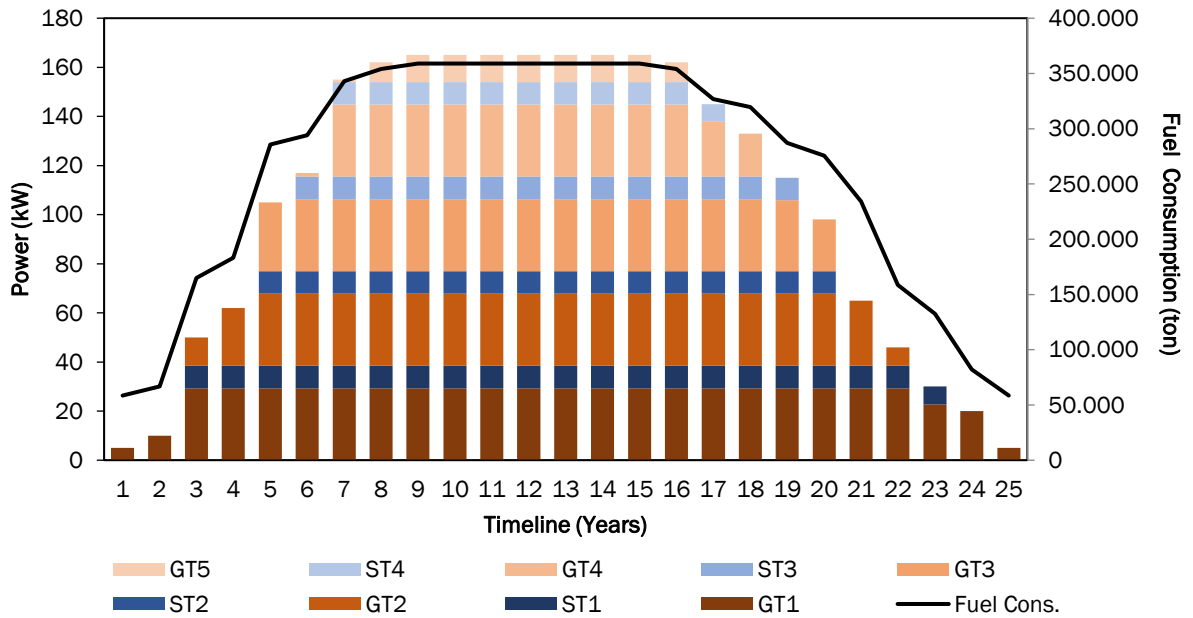
Figure 69 Lifespan performance Cluster D2
Source: Elaborated by author
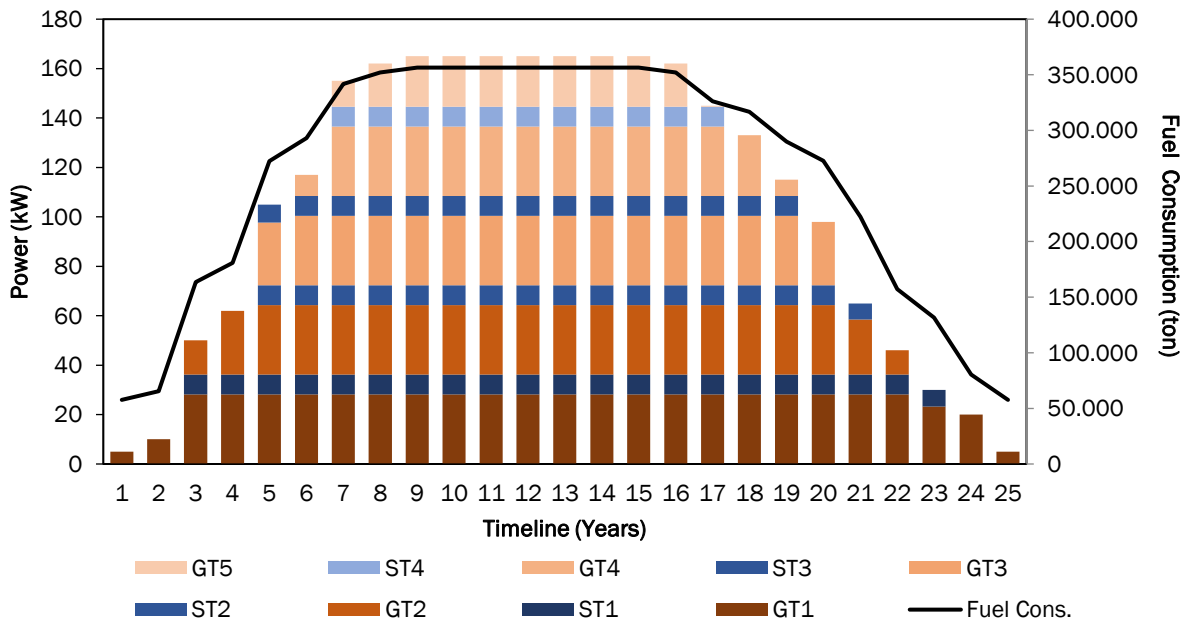
Figure 70 Lifespan performance Cluster D3
Source: Elaborated by author
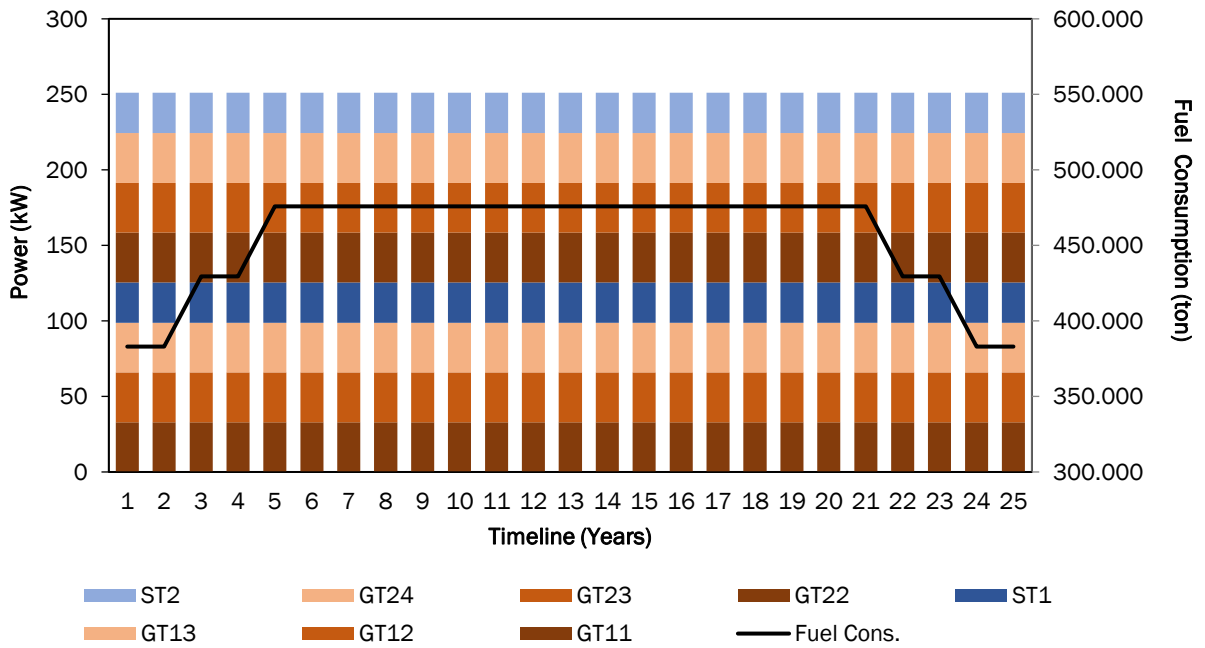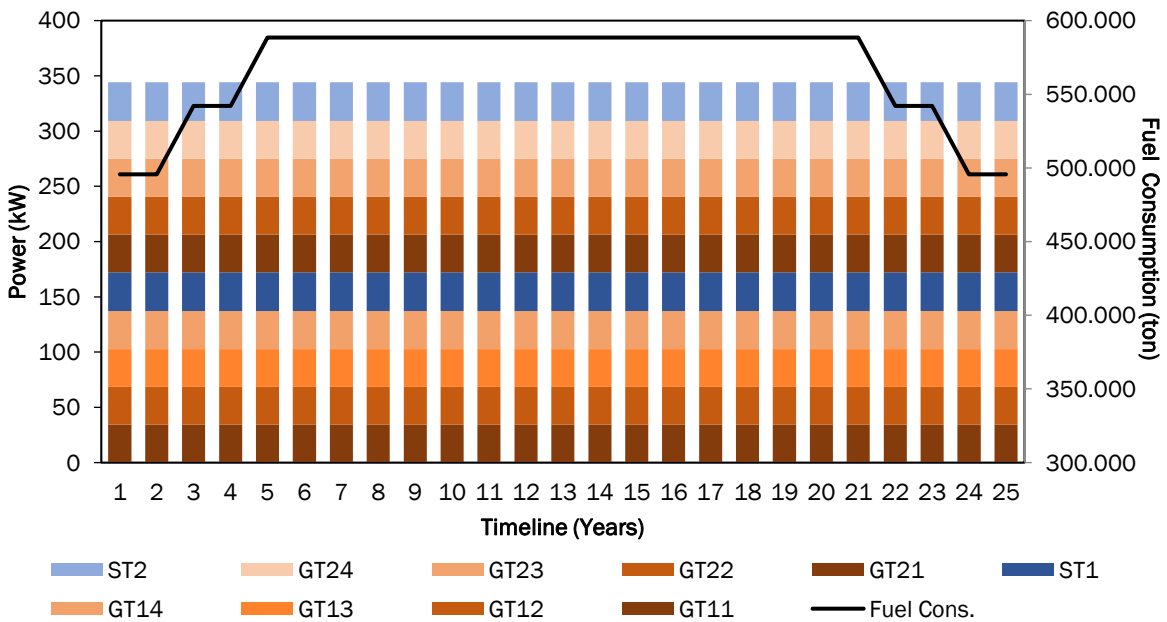
Figure 71 Lifespan performance Cluster E1
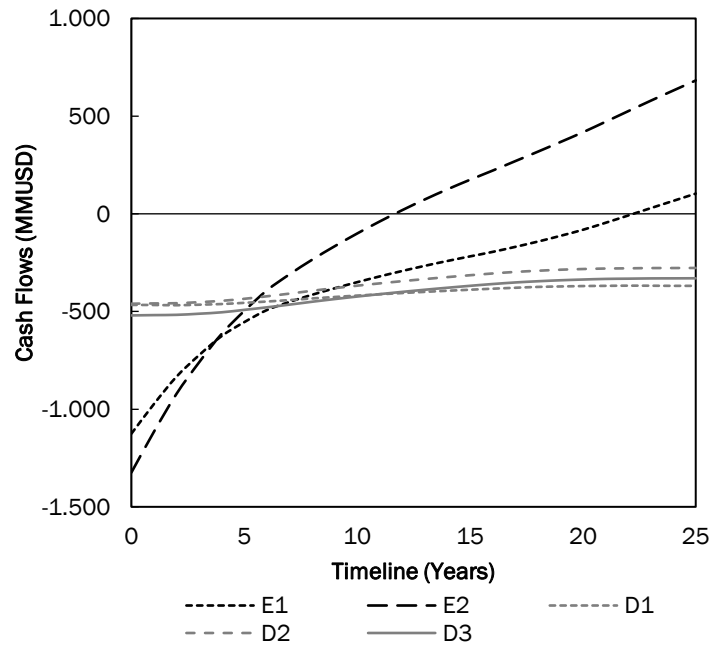Source: Elaborated by author

Figure 72 Lifespan performance Cluster E2
Source: Elaborated by author

In contrast with the efficiency curves shown earlier, layouts D2 (5 CC blocks, 38,5 MW each) and D3 (6 CC blocks, 36 MW each), even having different nominal efficiencies, result in a very similar consumption curve, as seen in Figure 73. Energy generated by the gas turbines is also similar, 18.160 GWh and 18.688 GWh respectively, this is because the 6th block in D3 remains without operation. Installing blocks of lower capacities are a way to smooth part load operation. However, this is may be penalized by weight and dimensional restrictions. More operational blocks may be obtained by soften the heat exchanger size bounds to be smaller.
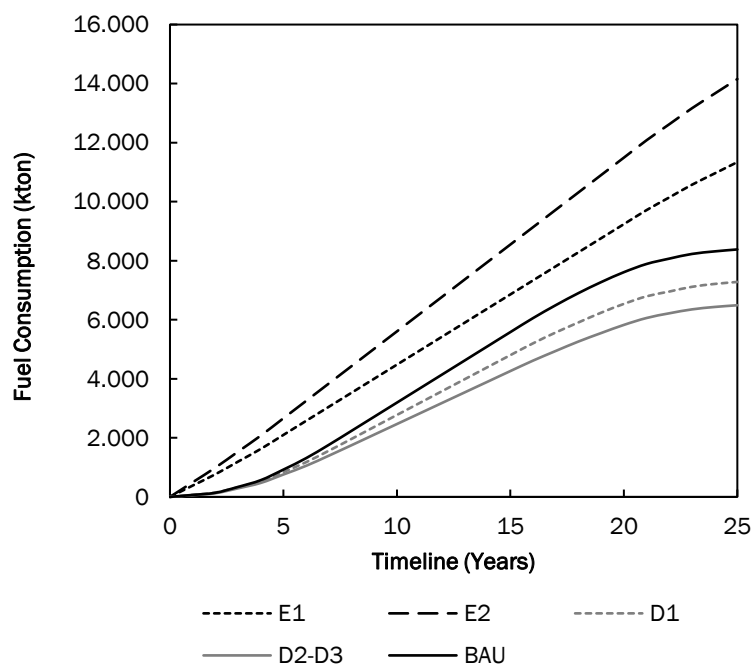
Figure 73 Accumulated Fuel Consumption
Source: Elaborated by author

Capital cost is another important aspect that limits block segregation. More blocks introduce higher cost and weight in equipment. This tradeoff is clearly visible in Figure 74 and Figure 75. Low investments in D2 mixed with acceptable efficiency performance makes it the best performant among Off-grid clusters. Regarding land connection scenarios, assuming that all surplus energy is sold, makes them more profitable and in theory, layouts are limited by the bounds of quantity of turbines and maximum installed capacity. However, in practice, this is strictly limited to Brazilian interconnected system operation, which prioritizes hydro sources, because of their lower costs.

Figure 74 Cash flows for all scenarios
Source: Elaborated by author
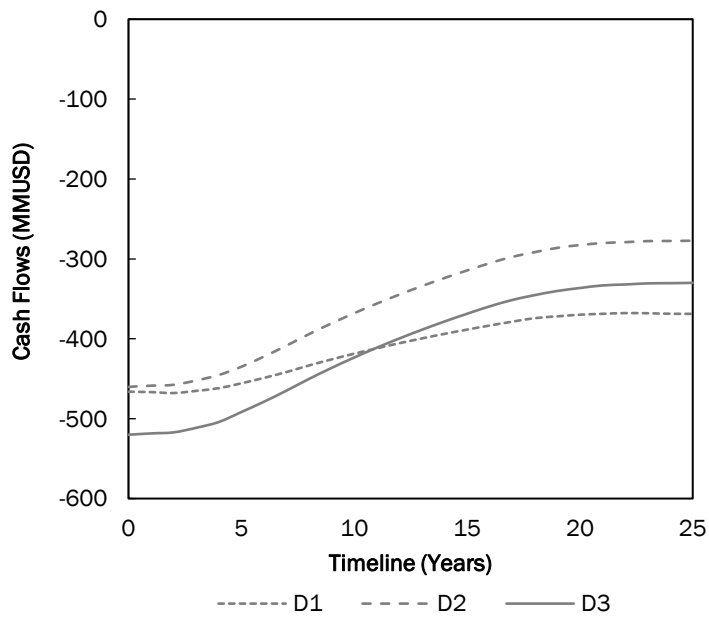
Figure 75 Cash flows for off-grid scenarios
Source: Elaborated by author

Capital costs consist, roughly, in equipment, engineering and infrastructure costs. Usually, land-based power plants do not consider costs related to size and weight of the system. Weight

and space constraints are quantified through an approximate ship cost, as seen in Table 22. In this case the ship hosting the floating power plant would be considerably smaller than a regular FPSO, as it would not carry crude oil. Results show that ship cost increases with the power plant size, however, they represent a relatively small share of the total capital costs, an average of 3,65% in off-grid layouts and 2,14% in land-connected layouts. Equipment costs increase more rapidly with the increase in total capacity, when compared to ship costs, as seen in Figure 76. This leads to understanding that ship costs become more critical when designing more compact solutions for offshore power hubs such as the off-grid layout. When there are further incomes, such as selling energy to land, ship cost becomes less representative.

Table 22 Ship design and cost per cluster

Cluster	L (m)	B (m)	D(m)	Mship (ton)	Cship (MMUSD)
D1	133	27	14	3.824	16.055.548
D2	136	27	14	4.101	16.903.679
D3	141	28	15	4.586	18.340.807
E1	164	33	17	7175,08	25.162.683
E2	173	35	18	8450,98	28.116.641
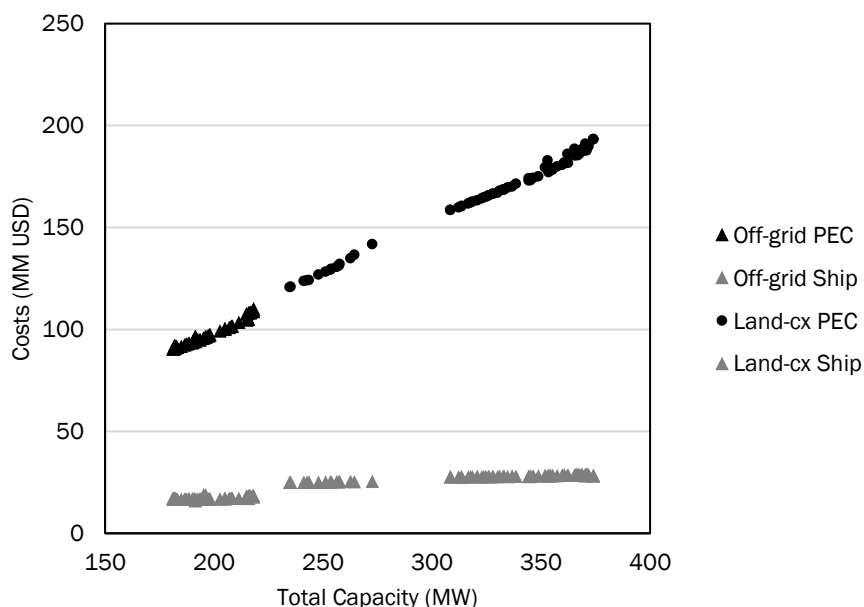
Figure 76 PEC cost and Ship cost depending on capacity
Source: Elaborated by author

Throughout this thesis, objectives have been related to diminish fuel consumption and increase efficiency. This is because the main objective of reducing CO_2 emissions, in this case, is

directly related to those two aspects. As the scope is to analyze and tackle power generation related emissions, a reduction in fuel consumption would be directly proportional to a reduction in CO_2 emissions. In that sense, trends of Figure 73 are equivalent for CO_2 emissions, and the analysis of the clusters remains the same. Table 23 shows both results in terms of absolute values, and reduced emissions. Considering reduced emissions as business as usual scenario emissions less the emissions of the new proposed layouts. Comparing to BAU scenarios all off-grid layouts reduce considerably CO_2 emissions. The analysis of the land connection layout emissions must consider that this would be a power plant connected to the main grid, and thus, the extra emissions would not necessarily mean an increase in emissions for the whole system. This is because the power hub would substitute another conventional fuel-based power plant onshore.

Table 23 Lifespan reduced Fuel Consumption and Emissions per Cluster

Cluster	Total Fuel (kton)	Total Emissions (kton)	Reduced Emissions (kton)	Compared to BAU
D1	7.281	19.733	2.984	13,14
D2	6.492	17.593	5.123	22,55
D3	6.429	17.422	5.295	23,31
E1	11.339	30.730	-8.013	-35,27
E2	14.156	38.362	-15.645	-68,87

6.2.4 Gas Turbine Designs Comparison

Next two sections present a more detailed analysis of the gas turbine design. Figure 77 shows dimensionless efficiency curves of the Gas Turbine designs. Results reinforce some aspects discussed before. D3 layout has the best performant gas turbine (its performance curves are displaced to the right when compared to the other gas turbines). It operates a higher range of part load at thermal efficiencies above 40%. In this layout, gas turbines part-load along all power hub lifetime is, in average, 88% the highest obtained value for all off-grid layouts.

This layout's high efficiency performance does not account for a better economic performance, since it needs higher investments. D2 layout has a similar fuel reduction, and its gas turbine efficiency curve is almost all below 40%. The slope in both D2 and D3 is similar, and

maintain reasonable performances along al load changes. In contrast D1 performance reduces quickly with load changes and its almost all below 30% thermal efficiency. Lower efficiency gas turbines allow for a higher share of energy generated by the steam turbine. However, it is penalized by operating at lower loads, in average 84%.
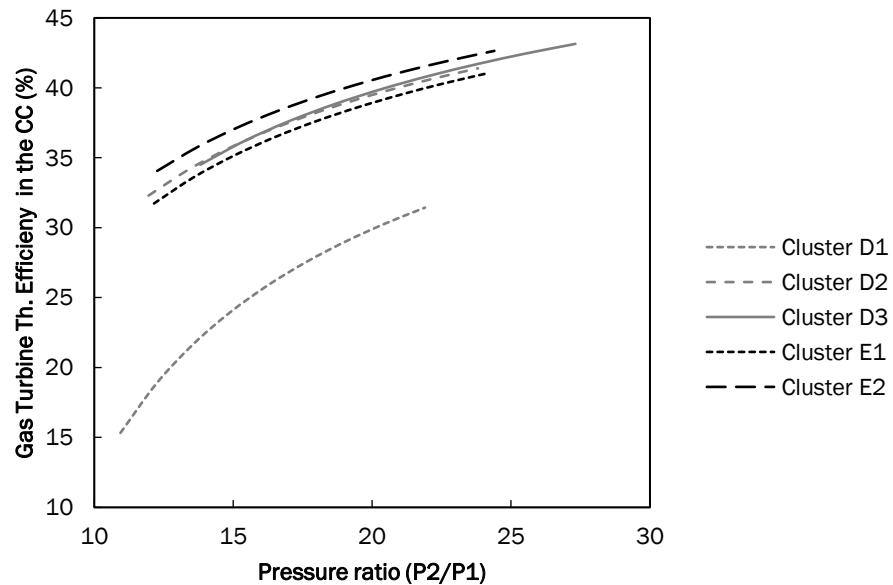
Figure 77 Off-design efficiency for GTs in Land-cx and Off-grid
Source: Elaborated by author
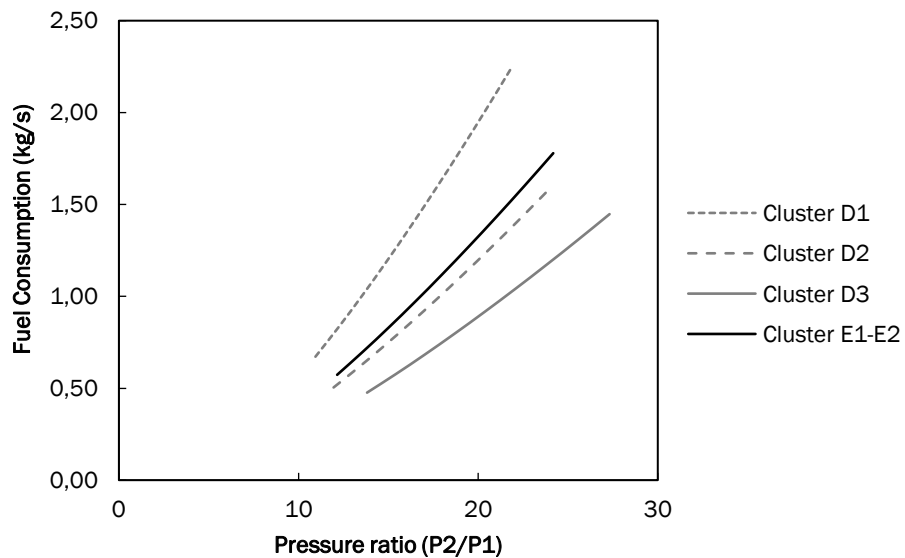
Figure 78 Off-design fuel consumption for GTs in Land-cx and Off-grid
Source: Elaborated by author
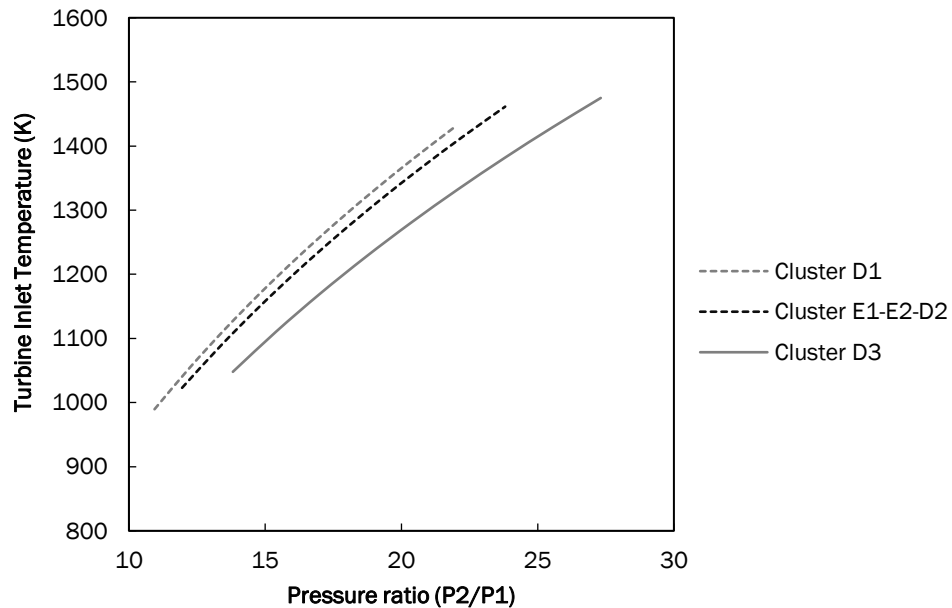
Figure 79 Gas Turbine Inlet Temperature for GTs in Land-cx/Off-grid
Source: Elaborated by author

For the fuel consumption seen in Figure 77 and the gas turbine inlet temperature in Figure 78, the turbine characteristics follow the same reasoning; D3, the most efficient layout, presents a gas turbine with curves that prioritize performance at part-load. For example, at 78% load D2 turbine has 39,8% thermodynamic efficiency and TIT of 1366K, whilst D3 has 41,7% thermodynamic efficiency and TIT of 1382K. Even not outperforming D1 gas turbine, D2 is also characterized by a low fuel consumption and a high TIT when compared with other obtained gas turbines. For comparison purposes Table 24 gathers gas turbines main design parameters for all calculated clusters. High installed capacity is prioritized in the case of land connection as it is assumed that all surplus energy would be sold to land. Higher mass flows correspond to less performant turbines. This table summarize some discussed results by showing the design point of the obtained turbines.

Table 24 Gas turbine Characteristics per Cluster

Cluster	m (kg/s)	W (MW)	P12	T05 (K)	T03 (K)	mfuel (kg/s)	etaThr (%)
A1	116,35	34,33	22,26	742	1450	1,98	38,35
A2	114,01	34,20	22,17	745	1453	1,97	38,55
B1	64,98	25,06	24,69	763	1536	1,29	43,06
B2	64,66	24,98	24,72	763	1537	1,29	43,08
C1	104,19	35,53	24,99	765	1506	1,96	40,14
C2	88,24	32,34	25,58	742	1506	1,66	43,20
C3	88,09	32,36	25,53	743	1507	1,66	43,20
D1	152,01	31,94	21,91	738	1428	2,25	31,44
D2	87,98	29,29	23,81	736	1461	1,57	41,40
D3	82,87	28,17	27,32	718	1475	1,45	43,14
E1	100,19	32,95	24,18	738	1469	1,78	41,06
E2	97,18	34,26	24,40	737	1480	1,78	42,64

Off-grid	Land-cx

6.2.5 Selection of Gas Turbine for offshore systems

Integrating the gas turbine into the optimization algorithm provided several design options, in terms its main design parameters, namely, TIT, pressure ratio, and isentropic efficiencies, seen in Figure 80, Figure 81 and Figure 82 respectively. Each point in the figures represents a gas turbine design for the respective conditions and cases, it is possible to observe some trends for each connection case. Trends for the off-grid scenario can be diffuse but follow some regular patterns; higher pressure ratios are more common in gas turbines with smaller capacity. TIT and isentropic efficiency trends also follow a negative correlation. For the off-grid scenario, trends show that more performant GTs are prioritized at lower power capacities. This distribution allows balancing the three objectives, specially WTP ratio which is not commonly optimized in land combined cycles; less performant GTs produce less efficient but lighter steam cycles. For the Land-cx scenario GT parameters do not follow consistent trends. Results are scattered for efficiencies and TIT, whereas for the pressure ratio remain almost constant, see Figure 83 to Figure 85.

Figure 80 Gas Turbine Inlet Temperature for GTs in Off-grid
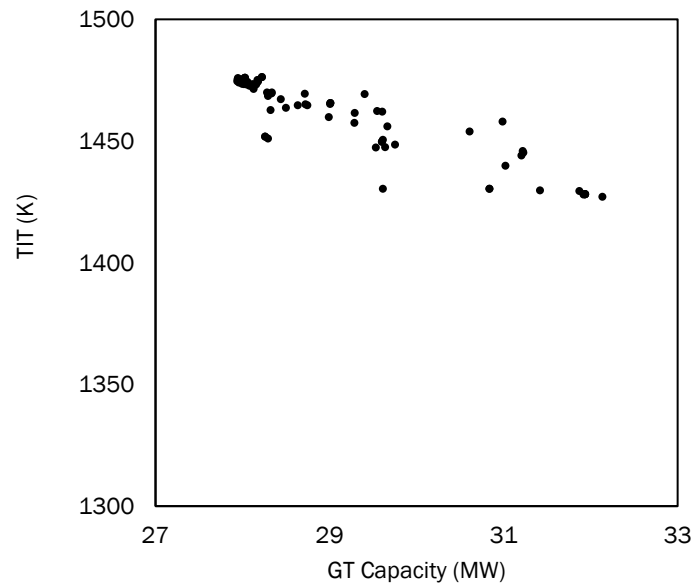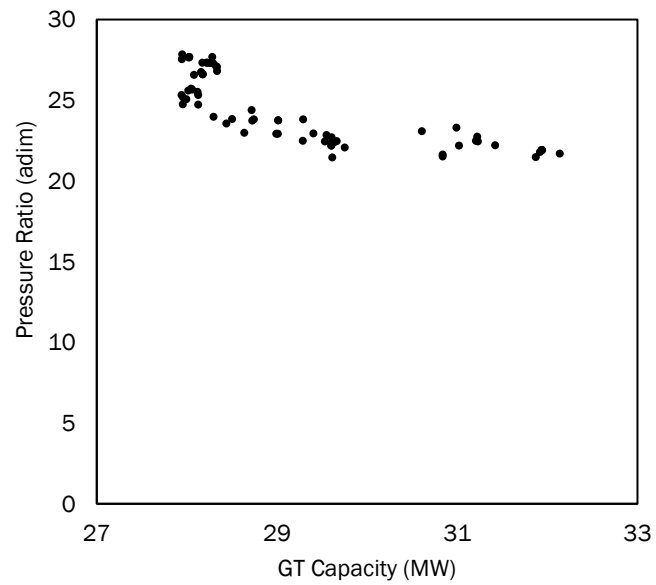Source: Elaborated by author

Figure 81 Pressure ratios for GTs in Off-grid
Source: Elaborated by author
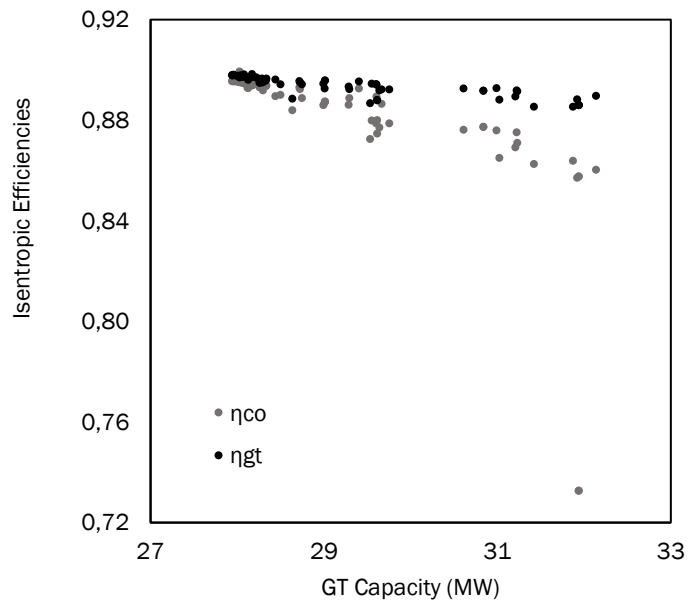
Figure 82 Gas Turbine and Compressor Efficiencies in Off-grid
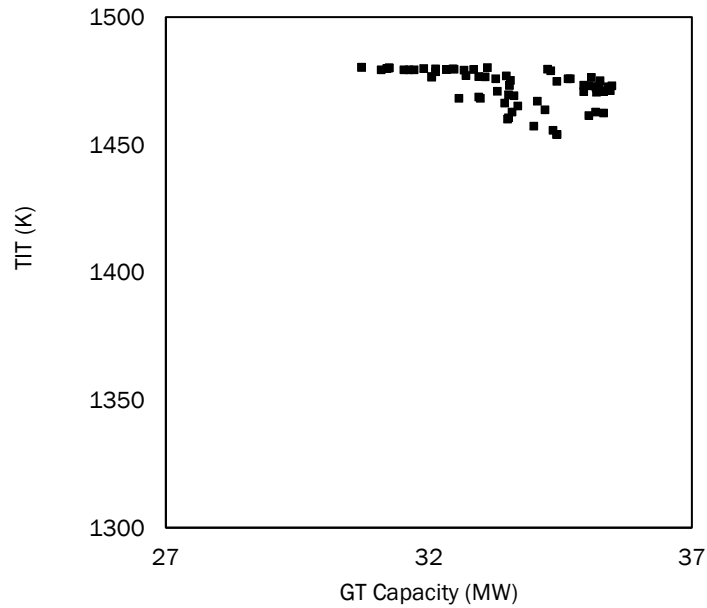Source: Elaborated by author

Figure 83 Gas Turbine Inlet Temperature for GTs in Land-cx
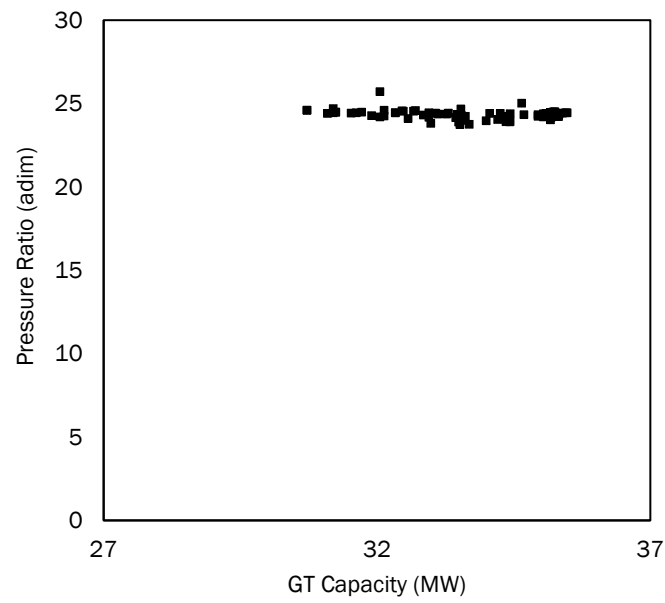Source: Elaborated by author

Figure 84 Pressure ratios for GTs in Land-cx
Source: Elaborated by author
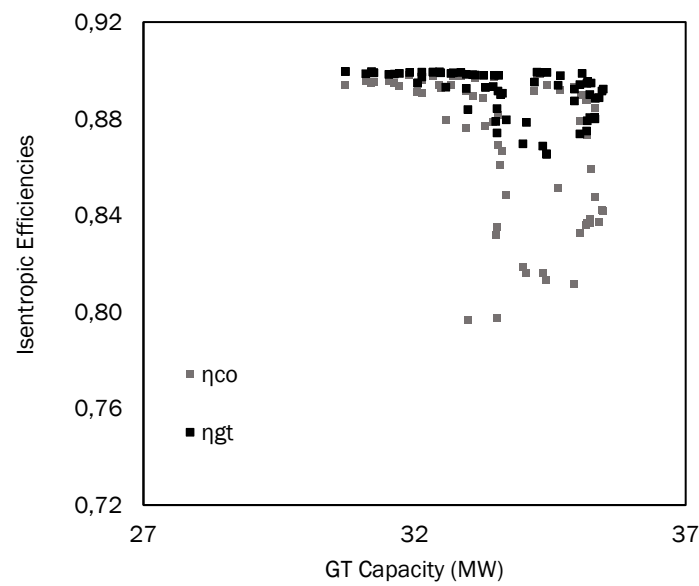
Figure 85 Gas Turbine and Compressor Efficiencies in Land-cx
Source: Elaborated by author

This analysis allowed understanding how the selection of gas turbines for offshore systems would affect the objectives (average efficiency, NPV and WTP), especially when considering load changes. For the off-grid scenario all objectives reduce their value when increasing the GT capacity. The average efficiency is higher because smaller capacities of GTs allow more blocks to operate at full load when changing electricity demands. For the Land-cx scenario, NPV and WTP decrease when decreasing GT capacity, whereas efficiency follows an erratic pattern.

The different trends in both scenarios can be related to the formation of combined cycle blocks. In an off-grid case, blocks are more compact to cope with the changing loads, increasing GT capacity would reduce the number of blocks needed (reduction of WTP ratio), however it would undermine the power hub efficiency. On the other hand, for the land-cx scenario blocks are more robust and composed by several gas turbines, increasing their size would directly increase benefits from electricity exchange, and as the block number is maintained, the WTP ratio would be increased.

7   CONCLUSIONS

Conclusions are divided in two sections. The first set of conclusions wraps-up the results of tradeoff between a customized and commercial gas turbine, along with the advantages and disadvantages of single pressure versus double pressure HRSG layouts. The second section presents the conclusions of the Land Connection and Offshore grid layouts, final remarks and recommendations for following studies.

7.1   Conclusion of preliminary results

Offshore oil platforms have very different needs when dealing with electricity and heat demand. Some previous research has pointed the applicability of installing a Power Hub with commercial Combined Cycles concentrating all electricity demand for various offshore platforms. This study presents a methodology for calculating a tailored and optimal Combined Cycle Power Plant for this type of offshore applications. Calculation was performed through the integration of modeling tools and methodologies, using Mixed Integer Non-Linear programming for discrete variables. Optimization approaches were separated in single-objective and multi-objective. Similarly, single and double-pressure HRSGs were considered. The proposed model allowed establishing optimum points through a wide range of alternatives, including the design and quantity of gas turbines.

Tradeoff among weight, costs and efficiency was assessed for both optimization approaches. Single-objective optimization allowed obtaining extreme points among the solution range. For this approach, there are not clear benefits of choosing single-pressure HRSGs. In order to obtain maximum thermal efficiency levels, heat transfer areas must increase when compared to double-pressure arrangements, resulting in high costs and weight. The effects of introducing commercial gas turbines is clear; highest efficiency rates were obtained with high efficiency turbines LM2500, whilst lower costs correspond with turbines having lower cost-to-power ratio, SGT-800-50.

For multi-objective approach, introducing the gas turbine specific design into the modeling provided more detailed results. Reducing compressor and turbine efficiency have deep negative impact in overall efficiency, but allows weight and cost to stabilize, as the overall size of the steam cycle is also reduced. Results show, that in order to maintain the required installed capacity, gas turbine ratings increase to compensate the reduction in efficiency. Gas turbines ratings span approximately 25MW to 35MW, with corresponding theoretical compressor efficiencies from 90% to 83%.

As a general remark for both single and multi-objective approaches, penalty in cost and weight objectives occurs due to the introduction of heavier components in downstream equipment, such as the steam turbine and condenser. In single-objective optimization this is noticeable because of the quantity of blocks, which is reflected in an increased number of steam cycle components. On the other hand, for multi-objective optimization there is an additional impact of the gas turbine and compressor efficiency. Weight and costs tend to be more related, they are both strongly dependent on the heat transfer area, particularly for the single pressure arrangements. Nevertheless, costs are additionally affected by the quantity of gas turbines, HRSGs and combined cycle blocks.

Intermediate results in the Pareto Front of double-pressure arrangements could introduce an interesting option for the Power Hub. Particularly arrangements having 3(1)x1, due to the reduction on weight and costs maintaining a reasonable thermal efficiency of around 53.15%. Any of the solutions presented results in an important CO2 emissions and fuel consumption reduction. Even though nowadays CO2 is not penalized by carbon taxes in Brazil, introducing a concentrated power hub may diminish carbon dioxide emissions approximately in 18.7% to 27.2% from original FPSO design. Further agreements or Carbon Market cooperation may produce an economic impact together with fuel savings and better allocation of such resources.

7.2 Conclusions of offshore Grid and Onshore Connection Approach

Three objectives were analyzed through a multi-objective optimization and mixed integer non-linear programming, Weight-To-Power ratio, Net Present Value and Mean Efficiency. Combined cycle design and off-design included main components, Gas Turbines, Steam Turbines,

HRSGs and condensers. Two approaches were established, an isolated Offshore grid and an onshore connection through HVDC lines. In order to establish such scenarios, it was necessary to make considerations about energy pricing and supply particular of the Brazilian market.

The methodology and considerations derived in results showing that an offshore power hub could be a promising way to reduce fuel consumption and CO_2 emissions. CO_2 total lifetime emissions could reduce from 13,4% and 23,4% when compared to the current scenario. Current Brazilian regulations do not consider carbon taxes, which undermines the economic performance of an offshore isolated grid. A carbon credit trading scheme, with prices above 92 USD/ton could make this type of offshore grid more viable. It is possible, but unlikely that carbon credits at high prices would be attractive to a slow carbon trading market. However, in a close future more strict compromises regarding emissions, could improve this scenario. On the other hand, a second scenario considering an onshore connection results in better economic results, with additional revenues from energy exchange to the main onshore grid. Surplus energy from the power hub would be sold at 100 USD/MWh. Electricity energy prices in Brazil are very volatile as they depend on the rain seasons. A break-even price from 47 to 123 USD/MWh depending on the quantity of gas turbines per combined cycle block. Brazilian regulations prioritize hydro sources for electricity supply, which could be a barrier for selling energy to the main grid. A pricing analysis is out of the scope of this study.

This work presented a distinct approach of combined cycle design for offshore power systems, by integrating most important combined cycle components to propose an optimized tailored arrangement for a new system instead of a previously installed one. It additionally included a layout design to optimize space and weight which had a clear impact of NPV results. Further studies may focus on the electrical equipment and electrical stability of the offshore grid as a part of the viability of offshore power hubs

References

AHMADI, P.; DINCER, I.; ROSEN, M. A. Thermodynamic modeling and multi-objective evolutionary-based optimization of a new multigeneration energy system. **Energy Conversion and Management**, v. 76, p. 282–300, 2013.

BARRERA, J. E.; BAZZO, E.; KAMI, E. Exergy analysis and energy improvement of a Brazilian floating oil platform using Organic Rankine Cycles. **Energy**, v. 88, p. 67–79, 2015.

BEJAN, A.; TSATSARONIS, G.; MORAN, M. **Thermal Design and Optimization**. Hoboken: John Wiley & Sons, 1995.

CAN GULEN, S.; JOSEPH, J. Combined Cycle Off-Design Performance Estimation: A Second-Law Perspective. **Journal of Engineering for Gas Turbines and Power**, v. 134, n. 1, p. 11801, 2012.

CARAPELLUCCI, R.; GIORDANO, L. A comparison between exergetic and economic criteria for optimizing the heat recovery steam generators of gas-steam power plants. **Energy**, v. 58, p. 458–472, 2013.

CARRANZA SÁNCHEZ, Y. A.; DE OLIVEIRA, S. Exergy analysis of offshore primary petroleum processing plant with CO2 capture. **Energy**, v. 88, p. 46–56, 2015.

CASAROSA, C.; DONATINI, F.; FRANCO, A. Thermoeconomic optimization of heat recovery steam generators operating parameters for combined plants. v. 29, p. 389–414, 2004.

DE OLIVEIRA, S.; VAN HOMBEECK, M. Exergy analysis of petroleum separation processes

in offshore platforms. **Energy Conversion and Management**, v. 38, n. 15–17, p. 1577–1584, 1997.

DRANKA, G. G.; FERREIRA, P. Planning for a renewable future in the Brazilian power system. **Energy**, v. 164, 2018.

DUMONT, M.-N.; HEYEN, G. Mathematical modelling and design of an advanced once-through heat recovery steam generator. **Computers & Chemical Engineering**, v. 28, n. 5, p. 651–660, 2004.

ENTSO-E. **Offshore Transmission TechnologyWntsoe**. Brussels: [s.n.]. Disponível em: <www.entsce.eu>.

EPE. **Plano Decenal de Expansão de Energia 2027**. Disponível em: <http://epe.gov.br/pt/publicacoes-dados-abertos/publicacoes/plano-decenal-de-expansao-de-energia-2027>.

ESCOA. **Fin Tube Technology**. 1. ed. Oklahoma: [s.n.].

FØLGESVOLD, E. R. **Combined heat and power plant on offshore oil and gas installations**. [s.l.] NTNU, 2015.

*GALLO, W. L. R. et al. Exergy analysis of the compression systems and its prime movers for a FPSO unit. **Journal of Natural Gas Science and Engineering**, v. 44, p. 287–298, 2017.*
GANAPATHY, V. **Industrial Boilers and Heat Recovery Steam Generators**. New York -

Basel: Marcel Dekker, Inc., 2003.

GAS TURBINE WORLD. **Performance Specs**Fairfield, CT. USAPequot Publishing Inc., , 2016.

GE. **Where only the most powerful and efficient survive**. Disponível em: <https://www.ge.com/power/about/insights/articles/2016/04/gas-turbine-boot-camp>. Acesso em: 2 dez. 2018.

GNIELINSKI, V. On heat transfer in tubes. **International Journal of Heat and Mass Transfer**, v. 63, p. 134–140, 2013.

GODOY, E.; BENZ, S. J.; SCENNA, N. J. A strategy for the economic optimization of combined cycle gas turbine power plants by taking advantage of useful thermodynamic relationships. **Applied Thermal Engineering**, v. 31, n. 5, p. 852–871, 2011.

GODOY, E.; BENZ, S. J.; SCENNA, N. J. Optimal economic strategy for the multiperiod design and long-term operation of natural gas combined cycle power plants. **ATE**, v. 51, n. 1–2, p. 218–230, 2013.

GODOY, E.; SCENNA, N. J.; BENZ, S. J. Families of optimal thermodynamic solutions for combined cycle gas turbine (CCGT) power plants. **Applied Thermal Engineering**, v. 30, n. 6–7, p. 569–576, 2010.

GORENSTEIN, J.; HAKVOORT, R. A. A review of the North Seas offshore grid modeling :

Current and future research. **Renewable and Sustainable Energy Reviews**, v. 60, p. 129–143, 2016.

GUARINELO, F. **Análise termodinâmica de ciclo combinado operando fora das condições de projeto**. [s.l.] UNICAMP, 2012.

GULE, M. **Dynamic process simulation of heat recovery steam generator designed for offshore oil and gas installations**. [s.l.] Norwegian University of Science and Technology, 2016.

HAGLIND, F.; ELMEGAARD, B. Methodologies for predicting the part-load performance of aero-derivative gas turbines. **Energy**, v. 34, n. 10, p. 1484–1492, 2009.

HAUG, K. C. **Weight Estimation of Steam Cycle for CO2 Capture System on Offshore Oil and Gas Installation**. [s.l.] NTNU, 2016.

HETLAND, J. et al. Integrating a full carbon capture scheme onto a 450 MWe NGCC electric power generation hub for offshore operations: Presenting the Sevan GTW concept. **Applied Energy**, v. 86, n. 11, p. 2298–2307, 2009.

IEA. **Oil Market Report**. Disponível em: <https://www.iea.org/oilmarketreport/omrpublic/>. Acesso em: 1 dez. 2018.

INTERNATIONAL ENERGY AGENCY. **Tracking Clean Energy Progress 2017**. [s.l: s.n.].

JAY, S. A.; TOONEN, H. M. Ocean & Coastal Management The power of the offshore (super-) grid in advancing marine regionalization. **Ocean and Coastal Management**, v. 117, p. 32–42, 2015.

KAVIRI, A. G.; JAAFAR, M. N. M.; LAZIM, T. M. Modeling and multi-objective exergy based optimization of a combined cycle power plant using a genetic algorithm. **Energy Conversion and Management**, v. 58, p. 94–103, 2012.

KEHLHOFER, R. et al. **Combined-Cycle Gas & Steam Turbine Power Plants**. 3d. ed. Tulsa, Oklahoma: PennWell Corporation, 2009.

KNOPF, F. C. **Modeling , Analysis and Optimization of Process and Energy Systems**. New Jersey: Wiley, 2012.

KORPÅS, M. et al. A case-study on offshore wind power supply to oil and gas rigs. **Energy Procedia**, v. 24, n. 1876, p. 18–26, 2012.

KURZKE, J. How to get map component map for aircraft gas turbine performance calculations. **ASME**, 1996.

MALLA, U.; KARRI, K. **Approach for Effective Design and Cost Estimation of New build / Conversion FPSO**. Society of Naval Architects And Marine Engineerings Convention. **Anais**...2014

MANASSALDI, J. I. et al. A discrete and continuous mathematical model for the optimal

synthesis and design of dual pressure heat recovery steam generators coupled to two steam turbines. **Energy**, v. 103, p. 807–823, 2016.

MANASSALDI, J. I.; MUSSATI, S. F.; SCENNA, N. J. Optimal synthesis and design of Heat Recovery Steam Generation (HRSG) via mathematical programming. **Energy**, v. 36, n. 1, p. 475–485, 2011.

MARVIK, J. I.; ØYSLEBØ, E. V.; KORPÅS, M. Electrification of offshore petroleum installations with offshore wind integration. **Renewable Energy**, v. 50, p. 558–564, 2013.

MEHRGOO, M.; AMIDPOUR, M. Constructal design and optimization of a dual pressure heat recovery steam generator. **Energy**, v. 124, p. 87–99, 2017.

NGUYEN, T.-V. et al. On the definition of exergy efficiencies for petroleum systems: Application to offshore oil and gas processing. **Energy**, v. 73, p. 264–281, 2014a.

NGUYEN, T.-V. et al. Oil and gas platforms with steam bottoming cycles: System integration and thermoenvironomic evaluation. **Applied Energy**, v. 131, p. 222–237, 2014b.

NGUYEN, T. VAN et al. Exergetic assessment of energy systems on North Sea oil and gas platforms. **Energy**, v. 62, p. 23–36, 2013.

NORD, L. O.; BOLLAND, O. Design and off-design simulations of combined cycles for offshore oil and gas installations. **Applied Thermal Engineering**, v. 54, n. 1, p. 85–91, 2013.

NORD, L. O.; MARTELLI, E.; BOLLAND, O. Weight and power optimization of steam

bottoming cycle for offshore oil and gas installations. **Energy**, v. 76, p. 891–898, 2014.

OPEC. **World Oil Outlook 2040**. Vienna: [s.n.].

ORLANDINI, V. et al. Dynamic performance of a novel offshore power system integrated with a wind farm. **Energy**, v. 109, p. 236–247, 2016.

ORTIZ, H. Y. **Análise exergética de um sistema de injeção de CO2 para uma plataforma FPSO e sua integração com ciclo combinado e captura de carbono**. [s.l.] UNICAMP, 2015.

PETROBRAS. **Petrobras Activities**. Disponível em: <http://www.petrobras.com.br/pt/nossas-atividades/areas-de-atuacao/exploracao-e-producao-de-petroleo-e-gas/pre-sal/>. Acesso em: 10 out. 2014.

PIEROBON, L. et al. Multi-objective optimization of organic Rankine cycles for waste heat recovery: Application in an offshore platform. **Energy**, v. 58, p. 538–549, 2013.

PIEROBON, L. et al. Waste heat recovery technologies for offshore platforms. **Applied Energy**, v. 136, p. 228–241, 2014a.

PIEROBON, L. et al. Design methodology for fl exible energy conversion systems accounting for dynamic performance. **Energy**, v. 68, p. 667–679, 2014b.

PIEROBON, L.; HAGLIND, F. Design and optimization of air bottoming cycles for waste

heat recovery in off-shore platforms. **Applied Energy**, v. 118, p. 156–15, 2014.

PIERRI, E. et al. Challenges and opportunities for a European HVDC grid. **Renewable and Sustainable Energy Reviews**, v. 70, n. October 2016, p. 427–456, 2017.

PIMENTA, F.; KEMPTON, W.; GARVINE, R. Combining meteorological stations and satellite data to evaluate the offshore wind power resource of Southeastern Brazil. **Renewable Energy**, v. 33, n. 11, p. 2375–2387, 2008.

RIVERA-ALVAREZ, A.; COLEMAN, M. J.; ORDONEZ, J. C. Ship weight reduction and efficiency enhancement through combined power cycles. **Energy**, v. 93, p. 521–533, 2015.

ROOSEN, P.; UHLENBRUCK, S.; LUCAS, K. Pareto optimization of a combined cycle power system as a decision support tool for trading off investment vs. operating costs. **International Journal of Thermal Sciences**, v. 42, n. 6, p. 553–560, 2003.

ROVERE, E. L. LA; GROTTERA, C.; WILLS, W. Overcoming the financial barrier to a low emission development strategy in Brazil. **International Economics**, 2018.

ROVIRA, A. et al. Thermoeconomic optimisation of heat recovery steam generators of combined cycle gas turbine power plants considering off-design operation. **Energy Conversion and Management**, v. 52, n. 4, p. 1840–1849, 2011.

SARAVANAMUTTOO, H. et al. **Gas turbine theory**. 6th. ed. Dorset, UK: PEARSON Prentice Hall, 2009.

SEEG. **Emissões dos setores de energia, processos industriais e uso de produtos.** [s.l: s.n.].

SEVAN. **FPSO.** Disponível em: <https://sevanssp.com/sevan-brasil/>. Acesso em: 2 dez. 2018.

SIEMENS. **A Dependable Power Supply.** Disponível em: <https://www.siemens.com/press/en/presspicture/?press=/en/presspicture/2017/power-gas/2017-03-aeroderivative-gas-turbine/im2017030260pgen.htm>. Acesso em: 2 dez. 2018.

STODOLA, A. **Dampf- und Gasturbinen: Mit einem Anhang über die Aussichten der Wärmekraftmaschinen.**Berlin, GermanySpringer, , 1922.

SUSSKIND, H.; RASEMAN, C. J. **Power Plant Operating and Maintenance Costs.** Virginia: United States Atomic Energy Comission, 1970.

TALCYON. **FPSO.** Disponível em: <http://www.talcyon.com/industries/marine/>. Acesso em: 2 dez. 2018.

THE MATHWORKS INC. **MATLAB**Natick, Massachusetts, United States., 2018.

THERMOFLOW. **Thermoflex**, 2017.
TOFFOLO, A.; LAZZARETTO, A. Evolutionary algorithms for multi-objective energetic and

economic optimization in thermal system design. **Energy**, v. 27, n. 6, p. 549–567, 2002.

VALDÉS, M.; RAPÚN, J. L. Optimization of heat recovery steam generators for combined cycle gas turbine power plants. **Applied Thermal Engineering**, v. 21, p. 1149–1159, 2001.

VICTORY ENERGY. **GT-HRSG Combined Cycle / CHP**. Disponível em: <https://victoryenergy.com/enhanced-heat-recovery/gt-hrsg-power-utility/>. Acesso em: 2 dez. 2018.

VOLDSUND, M. et al. Exergy destruction and losses on four North Sea offshore platforms: A comparative study of the oil and gas processing plants. **Energy**, v. 74, p. 45–58, 2014.

WALNUM, H. T. et al. Modelling and simulation of CO2 (carbon dioxide) bottoming cycles for offshore oil and gas installations at design and off-design conditions. **Energy**, v. 59, p. 513–520, 2013.

WATSON, D. G. M. **Practical Ship Design**. Oxford: Elsevier, 1998.

WINDÉN, B. et al. An investigation into the logistical and economical benefits of using offshore thermal power in a future CCS scheme. **Energy Procedia**, v. 37, p. 2997–3004, 2013.

WINDÉN, B. et al. Investigation of offshore thermal power plant with carbon capture as an alternative to carbon dioxide transport. **Ocean Engineering**, v. 76, p. 152–162, 2014.